

İSTANBUL TECHNICAL UNIVERSITY ★ INSTITUTE OF SCIENCE AND TECHNOLOGY

AN INVESTIGATION ON IMC BASED FUZZY PID CONTROLLERS

**M.Sc. Thesis by
Doğan Onur YILMAZ**

Department : Chemical Engineering

Programme : Chemical Engineering

JUNE 2010

AN INVESTIGATION ON IMC BASED FUZZY PID CONTROLLERS

**M.Sc. Thesis by
Doğın Onur YILMAZ
(506081007)**

**Date of submission : 06 May 2010
Date of defence examination: 04 June 2010**

**Supervisor (Chairman) : Dr. Hikmet İSKENDER (ITU)
Members of the Examining Committee : Prof. Dr. İbrahim EKSİN (ITU)
Assis. Prof. Dr. Devrim B. KAYMAK
(ITU)**

JUNE 2010

İSTANBUL TEKNİK ÜNİVERSİTESİ ★ FEN BİLİMLERİ ENSTİTÜSÜ

**DAHİLİ MODEL KONTROL TEMELLİ BULANIK PID KONTROL
EDİCİLER ÜZERİNE BİR ARAŞTIRMA**

**YÜKSEK LİSANS TEZİ
Doğan Onur YILMAZ
(506081007)**

Tezin Enstitüye Verildiği Tarih : 06 Mayıs 2010

Tezin Savunulduğu Tarih : 04 Haziran 2010

**Tez Danışmanı : Dr. Hikmet İSKENDER (İTÜ)
Diğer Jüri Üyeleri : Prof. Dr. İbrahim EKSİN (İTÜ)
Yrd. Doç. Dr. Devrim B. KAYMAK (İTÜ)**

HAZİRAN 2010

FOREWORD

Firstly, I would like to forward my sincere thanks to Dr Hikmet İSKENDER and Prof Dr İbrahim EKSİN for their patient guidance, valuable support and helpful leading during the conduction of this thesis.

Secondly, I would like to present my grateful thanks to my father Mr Sinan YILMAZ, my mother Ms Seval YILMAZ and my brother Mr Ahmet Anıl YILMAZ for their inimitable sincere support and encouragements during all levels of this thesis.

Thirdly, I would like to send my very special thanks to Ms Elif KONUKSEVER for her unique moral support and care through the tough times of this study.

Lastly, it is a pleasure for me to send my sincere thanks to TÜBİTAK – BİDEB institution for their very valuable and generous scholarship support which has been a real encouraging power for conduction of this thesis study properly.

June 2010

Doğan Onur YILMAZ

Chemical Engineer

TABLE OF CONTENTS

	<u>Page</u>
FOREWORD.....	v
TABLE OF CONTENTS.....	vii
ABBREVIATIONS.....	ix
LIST OF TABLES.....	xi
LIST OF FIGURES.....	xiii
SUMMARY.....	xvii
ÖZET.....	xix
1. INTRODUCTION.....	1
2. DISTILLATION THEORY.....	3
2.1 Conventional Distillation.....	3
2.1.1 Types of distillation columns.....	3
2.1.2 Main components of distillation columns.....	4
2.2 Reactive Distillation.....	6
2.3 Reactive Distillation Process under Investigation.....	12
3. CONTROL THEORY.....	15
3.1 About PID Control.....	15
3.2 Proportional Control.....	16
3.3 Proportional-plus-Integral (PI) and Proportional-plus-Derivative Co.....	17
3.4 Proportional - Derivative - Integral (PID) Control.....	17
3.5 Ziegler – Nichols Method for Tuning PID Controllers.....	19
3.6 Internal Model Control (IMC) Strategy.....	20
3.6.1 General information about IMC.....	20
3.6.2 Practical design of IMC.....	21
3.7. Fuzzy Logic and Fuzzy PID Control.....	23
3.7.1 Introduction and what fuzzy logic control is.....	23
3.7.2 Fuzzy sets.....	24
3.7.3 Fuzzy rules and rule bases.....	24
3.7.4 Fuzzy membership functions.....	25
3.7.5 Fuzzy inference.....	26
3.7.6 Input and output scaling.....	29
3.7.7 Literature survey about fuzzy control.....	31
4. MODELING AND CONTROLLER DESIGN.....	33
4.1 Modeling.....	33
4.2 Controller Design.....	37
4.2.1 IMC PID controller design.....	37
4.2.2 IMC fuzzy PID controller design.....	38
5. SIMULATION: STRATEGIES FOR SELF TUNING FUZZY IMC PID CONTROLLER.....	43
5.1 Searching for Alternative Scaling Factors.....	43

5.2 Double Step Adjustment of Alpha (α).....	48
5.3 Overshoot Ratio Based Self Tuning Fuzzy IMC PID Controller.....	51
6. MULTI-REGION SELF TUNING FUZZY IMC PID CONTROLLERS.....	59
6.1 Six Region Self Tuning Fuzzy IMC PID Control Based on “R” Data.....	59
6.2 Three Hybridized Region Self Tuning Fuzzy IMC PID Control.....	69
6.3 Three Region Fuzzy Rule Based Self Tuning Fuzzy IMC PID Control.....	75
7. CONCLUSION AND SUGGESTIONS FOR FUTURE WORK.....	85
REFERENCES.....	87
APPENDIX – A.....	91
APPENDIX – B.....	101
APPENDIX – C.....	107
CURRICULUM VITAE.....	115

ABBREVIATIONS

P	:	Proportional
PI	:	Proportional Integral
PD	:	Proportional Derivative
PID	:	Proportional Integral Derivative
IMC	:	Internal Model Control
RD	:	Reactive Distillation
PLC	:	Programmable Logic Controller
GIS	:	Geographic Information Systems
FOPDT:		First Order Plus Dead Time
SOPDT:		Second Order Plus Dead Time
PB	:	Positive Big
ZR	:	Approximately Zero
NS	:	Negative Small
PM	:	Positive Medium
ISE	:	Integrated Square of Error
ITE	:	Integrated Time Weighted Error
ISAE	:	Integrated Square of Absolute Error
ISTE	:	Integrated Square of Time Weighted Error
OSR	:	Overshoot Ratio

LIST OF TABLES

	<u>Page</u>
Table 3.1: Ziegler - Nichols Chart for Defining Controller Parameters from System Data.....	20
Table 3.2: A Rule Base Table for an Error-Change of Error Type Fuzzy Control Strategy.....	25
Table 4.1: First Order Model Time Constants Representing Some Second Order Transfer Function Time Constants.....	38
Table 5.1: Error Index Results For Control Systems with Various α - β Combinations.....	47
Table 5.2: ITSE Error Indexes of Non-Self Tuning and Self Tuning Control Schemes for Primary and Alternative Process Models.....	50
Table 6.1: Scaling ranges and concerning control rules for six region self tuning Fuzzy IMC PID control.....	60
Table 6.2: Scaling ranges and concerning control rules for three hybridized region self tuning Fuzzy IMC PID control	71
Table 6.3: Comparative rise time and maximum overshoot results of non-self tuning and multi-region self tuning Fuzzy IMC PID controllers for various processes.....	84
Table 6.4: Comparative settling time and ITSE results of non-self tuning and multi-region self tuning Fuzzy IMC PID controllers for various processes.....	84

LIST OF FIGURES

	<u>Page</u>
Figure 2.1: Schematic demonstration of a typical single feed distillation column with two product streams.....	5
Figure 2.2: Processing alternatives for a typical $A + B \rightleftharpoons C + D$ reaction.....	7
Figure 2.3: The Eastman methyl acetate reactive distillation column.....	8
Figure 2.4: a) Flow diagram for conventional methyl acetate production process b) Reactive distillation unit proposed to replace the conventional process	8
Figure 2.5: Ideal reactive distillation column.....	10
Figure 2.6: One reactive tray in detail.....	10
Figure 2.7: Temperature profile among the reboiler of the reactive distillation column producing acetate esters.....	13
Figure 3.1: A feedback control loop with PID controller embedded, including disturbance and noise variables.....	16
Figure 3.2: Comparison of typical responses to a step change with P, PI and PID controls and with no control situation.....	18
Figure 3.3: Graphical demonstration for Ziegler Nichols tuning steps.....	19
Figure 3.4: Open loop control scheme.....	20
Figure 3.5: Typical IMC scheme.....	21
Figure 3.6: Modified configuration of IMC scheme.....	22
Figure 3.7: Simplification of IMC scheme.....	23
Figure 3.8: Membership grades of the days for the set of “weekend days” according to classical set and fuzzy set theories.....	24
Figure 3.9: Triangular and trapezoidal membership function curves.....	26
Figure 3.10: Operation of a fuzzy inference mechanism.....	27
Figure 3.11: Neighboring membership functions.....	28
Figure 3.12: Graphical representation of a fuzzy inference mechanism.....	30
Figure 3.13: Placement of scaling factors in fuzzy control scheme: a simple fuzzy PID control scheme.....	30
Figure 4.1: Response curves of FOPDT model and process.....	34
Figure 4.2: Process curve and three term SOPDT model curve.....	35
Figure 4.3: Responses of FOPDT and 3-term SOPDT models vs. system curve.....	36
Figure 4.4: Process curve vs. four parameter second order model response.....	36
Figure 4.5: Comparative graphic of three different model curves with respect to representation success.....	36
Figure 4.6: Closed loop control scheme with IMC PID controller.....	38
Figure 4.7: Fuzzy PID controller scheme.....	39
Figure 4.8: IMC Fuzzy PID control loop designed according to proposed Internal model control technique.....	40
Figure 4.9: Closed loop scheme for IMC Fuzzy PID controller with alternatively decoupled $\alpha - \beta$	41

Figure 4.10: Proposed Fuzzy IMC PID, classical IMC PID, and alternative Fuzzy IMC PID controllers integrated with identical processes.....	42
Figure 4.11: Comparative step response graphics of mentioned systems.....	42
Figure 4.12: Effort diagrams of designed controllers.....	42
Figure 5.1: Step responses for cases $\alpha=1, 5, 10$; $\beta=21.72$	43
Figure 5.2: Step responses for case $\alpha=15, 18, 21.72$; $\beta=21.72$	44
Figure 5.3: Step responses for cases $\alpha=1, 5, 10$; $\beta=10$	44
Figure 5.4: Step responses for cases $\alpha=15, 18, 21.72$; $\beta=10$	44
Figure 5.5: Step responses for cases $\alpha=1, 5, 10$; $\beta=1$	45
Figure 5.6: Step responses for cases $\alpha=15, 18, 21.72$; $\beta=1$	45
Figure 5.7: Step responses for cases $\alpha=10$; $\beta=1, 5, 10$	45
Figure 5.8: Step responses for cases $\alpha=10$; $\beta=15, 18, 21.72$	46
Figure 5.9: Block diagram showing classical Fuzzy IMC PID and double step self tuning schemes.....	49
Figure 5.10: Step responses of non self tuning and double step self tuning systems.....	49
Figure 5.11: Step responses of two control schemes for alternative process model.....	50
Figure 5.12: Step response of primary process model with overshoot based double step self tuning controller.....	52
Figure 5.13: Double step self tuning scheme for primary process model.....	53
Figure 5.14: Step responses for process in simulation 5.2.....	53
Figure 5.15: Step responses for process in simulation 5.3.....	54
Figure 5.16: Step responses for process in simulation 5.4.....	54
Figure 5.17: Step responses for process in simulation 5.5.....	54
Figure 5.18: Step responses for process in simulation 5.6.....	55
Figure 5.19: Step responses for process in simulation 5.7.....	55
Figure 5.20: Step responses for process in simulation 5.8.....	56
Figure 5.21: Step responses for process in simulation 5.9.....	56
Figure 5.22: Step responses for process in simulation 5.10.....	56
Figure 5.23: Step responses for process in simulation 5.11.....	57
Figure 6.1: Step responses for process in simulation 6.1.....	61
Figure 6.2: Step responses for process in simulation 6.2.....	61
Figure 6.3: Step responses for process in simulation 6.3.....	62
Figure 6.4: Step responses for process in simulation 6.4.....	62
Figure 6.5: Step responses for process in simulation 6.5.....	62
Figure 6.6: Step responses for process in simulation 6.6.....	63
Figure 6.7: Step responses for process in simulation 6.7.....	63
Figure 6.8: Step responses for process in simulation 6.8.....	64
Figure 6.9: Step responses for process in simulation 6.9.....	64
Figure 6.10: Step responses for process in simulation 6.10.....	65
Figure 6.11: Step responses for process in simulation 6.11.....	65
Figure 6.12: Step responses for process in simulation 6.12.....	65
Figure 6.13: Step responses for process in simulation 6.13.....	66
Figure 6.14: Step responses for process in simulation 6.14.....	66
Figure 6.15: Step responses for process in simulation 6.15.....	66
Figure 6.16: Step responses for process in simulation 6.16.....	67
Figure 6.17: Step responses for process in simulation 6.17.....	67
Figure 6.18: Step responses for process in simulation 6.18.....	68

Figure 6.19: Block diagram concerning to comparative control analysis for process block investigated in simulation 5.8.....	68
Figure 6.20: Hybridization devices designed for bands around rigid 0.33 and 0.67 section boundaries.....	71
Figure 6.21: Decision mechanisms of hybridization devices.....	72
Figure 6.22: Integration of hybridization device in to control scheme.....	72
Figure 6.23: Comparative step testing results for simulation 6.19.....	72
Figure 6.24: Comparative step testing results for simulation 6.20.....	73
Figure 6.25: Comparative step testing results for simulation 6.21.....	73
Figure 6.26: Comparative step testing results for simulation 6.22.....	73
Figure 6.27: Matlab window demonstrating membership functions for typical input.....	78
Figure 6.28: Matlab window demonstrating membership functions for typical output.....	79
Figure 6.29: Matlab window showing a typical rule base connecting input u with output alpha.....	79
Figure 6.30: Integration of fuzzy tuner into non-self tuning scheme.....	80
Figure 6.31: Comparative graphical representation of step responses generated by both the non-self tuning and three region fuzzy rule based self tuning Fuzzy IMC PID controllers.....	81
Figure 6.32: Comparative step testing results for simulation 6.23.....	82
Figure 6.33: Comparative step testing results for simulation 6.24.....	82
Figure 6.34: Comparative step testing results for simulation 6.25.....	82
Figure 6.35: Comparative step testing results for simulation 6.26.....	83
Figure A.1: Processing alternatives for a typical $A + B \rightleftharpoons C + D$ reaction.....	92
Figure A.2: Journal publications on reactive and catalytic distillation over last three decades.....	93
Figure A.3: Ammonia recovery in Solvay process.....	94
Figure A.4: a)Production of MTBE from MeOH and isobutene b)Production of ethylene glycol by hydration of ethylene oxide c)Cumene production from benzene and propene d)Production of propylene oxide from propylene chlorohydrin and lime.....	94
Figure A.5: The Eastman methyl acetate reactive distillation column.....	95
Figure A.6: a) Flow diagram for conventional methyl acetate production process b) Reactive distillation unit proposed to replace the conventional process.....	96
Figure A.7: Ideal reactive distillation column.....	97
Figure A.8: One reactive tray in detail.....	97
Figure A.9: Base case composition profiles (95% purities).....	98
Figure B.1: Block scheme and graphical results for model search B.1.....	102
Figure B.2: Block scheme and graphical results for model search B.2.....	102
Figure B.3: Block scheme and graphical results for model search B.3.....	103
Figure B.4: Block scheme and graphical results for model search B.4.....	103
Figure B.5: Block scheme and graphical results for model search B.5.....	104
Figure B.6: Block scheme and graphical results for model search B.6.....	104
Figure B.7: Block scheme and graphical results for model search B.7.....	105
Figure B.8: Block scheme and graphical results for model search B.8.....	105

Figure C.1: Block scheme of subsystem made up for calculating integrated time weighted square of error (ISTE) indexes.....	107
Figure C.2: Scheme used for comparison of non self tuning Fuzzy PID controller designed for primary reboiler process and its self tuning counterpart.....	108
Figure C.3: Scheme used for comparison study between a non self tuning Fuzzy IMC PID controller and a self tuning Fuzzy IMC PID controller.....	109
Figure C.4: Non-fuzzy self tuning device set; calculating $u = \text{error}/\text{input}$ ratio and making appropriate decisions according to changing value of “u” ratio.....	110
Figure C.5: Insight of action subsystems for if, else if and else cases.....	110
Figure C.6: Fuzzy self tuning device set.....	111
Figure C.7: Rule base editor window for “section x” control systems.....	111
Figure C.8: Rule base editor window for “section y” control systems.....	112
Figure C.9: Rule base editor window for “section z” control systems.....	112
Figure C.10: Fuzzy Inference System editor window for fuzzy Controller used in entire study.....	113
Figure C.11: Rule base editor window for fuzzy controller used in entire study.....	113
Figure C.12: Membership function editor window for fuzzy controller used in entire study.....	114

AN INVESTIGATION ON IMC BASED FUZZY PID CONTROLLERS

SUMMARY

In this study, certain self tuning algorithms and Multi-Region Self Tuning Method for Fuzzy IMC PID controllers have been proposed. As basis, recently proposed IMC based Fuzzy PID controller tuning technique is investigated. The performance of Fuzzy IMC PID controller has been compared with that of classical PID controller. For comparison, temperature response curve of reboiler of a reactive distillation column was modeled by using graphical method. Then step response analysis were conducted for both type of controllers on the model. Following this, some different process transfer functions were replaced with reboiler model in order to enlarge data field for comparison. Fuzzy IMC PID controller has demonstrated better results in general but seemed to need further improvement in controlling high order and high delay time processes. So, some self tuning strategies were investigated in order to obtain a self tuning algorithm experience for Fuzzy IMC PID controllers. As a result, self tuning rules have been prepared and these rules include necessary self tuning algorithms and coefficients for controlling various kinds of processes, whose time delay and time constant properties vary in a very large range, by using Self Tuning Fuzzy IMC PID controller. Simulation results showed that, proposed Multi-Region Self Tuning Fuzzy IMC PID controller provided better results for all kinds of processes compared to Non-self tuning Fuzzy IMC PID controller. Especially for very high time delay processes, Multi-Region Self Tuning Fuzzy IMC PID performance was far more successful than that of its non-self tuning counterpart.

DAHİLİ MODEL KONTROL TEMELLİ BULANIK PID KONTROL EDİCİLER ÜZERİNE BİR ARAŞTIRMA

ÖZET

Bu çalışmada, Dahili Model Kontrol Temelli Bulanık PID Kontrol Ediciler (DMKTBPID) için birtakım öz ayar kuralları ve Çok Bölgeli Öz Ayar Yöntemi önerilmiştir. Geliştirme işlemine temel olarak yakın geçmişte Bulanık PID kontrol ediciler için önerilmiş olan Dahili Model Kontrol yöntemi incelenmiştir. Bu kontrol stratejisinin performansı klasik PID kontrol edici ile kıyaslanmıştır. Kıyaslama için, öncelikle bir reaktif distilasyon kolonunun reboylarına ait sıcaklık grafiği modellenmiş ve bu model üzerinden basamak cevabı karşılaştırması yapılmıştır. Ardından, reboylar modeli birtakım farklı transfer fonksiyonları ile değiştirilerek kıyaslama için yeterli veri zenginliğine ulaşılması amaçlanmıştır. Bu çalışmalarda, DMKTBPID, klasik PID kontrol ediciye göre daha iyi sonuçlar vermiştir fakat bu kontrol edicinin yüksek mertebeli veya yüksek zaman gecikmeli sistemlerin kontrolü için birtakım geliştirmelere ihtiyaç duyduğu gözlenmiştir. Bunun için, DMKTBPID kontrol ediciler için birtakım öz ayar yöntemleri önerilmiş ve bu yolla bu kontrol ediciler için bir öz ayar algoritma tecrübesine erişilmesi amaçlanmıştır. Sonuç olarak birtakım öz ayar kuralları oluşturulmuştur ve bu kurallar, Öz Ayarlı DMKTBPID kontrol ediciler kullanılarak zaman sabiti ve zaman gecikmesi çok geniş menzillerde değişen farklı proseslerin başarıyla kontrol edilebilmesi için gerekli öz ayar algoritmaları ve katsayılarını içermektedir. Gerçekleştirilen bir dizi simülasyon çalışması sonucunda elde edilen sonuçlara göre, Çok Bölgeli Öz ayarlı DMKTBPID kontrol edicinin öz ayarsız klasik DMKTBPID kontrol ediciye göre çok daha iyi performans sergilediği sonucuna ulaşılmıştır. Özellikle çok yüksek zaman gecikmesine sahip proseslerin kontrolünde Çok Bölgeli Öz Ayarlı DMKTBPID kontrol edicinin uzak ara daha başarılı sonuçlar sağladığı gözlenmiştir.

1. INTRODUCTION

Classical P, PI, PD and PID type controllers are most commonly used ones in process industries today. Since their design strategies and online tuning methods have been developed in great proportions during historical progress, substitution of a classical controller in to any control scheme is treated to be the fastest and most convenient way of composing a successful control loop [1].

During the historical progress of control studies, classical controllers have been applied to many control systems and all these applications provided these controllers with large number of design techniques and tuning strategies. Thus, classical P, PI, PD and PID type controllers have generally been the most trusted solution to control any given process scheme.

On the other hand, it is known that, classical controllers owe their success to mathematical equations that are based on generalized relationships between process parameters and controller parameters. Thus, their performance is not generally appropriate for processes possessing nonlinear properties. On the other hand, high order systems and processes with large time delay are also not easy to be controlled properly by a classical controller in general [1].

In general, Fuzzy Logic Controllers show better results for high time delay and/or high order processes. One important disadvantage of fuzzy logic controllers against classical controller is that it is rather new concept compared to classical PID controller. Since the studies on fuzzy logic controllers are not as old as the ones on classical controllers, design and tuning strategies that are produced for fuzzy controllers are very few compared to classical controller design and tuning methods [1]. Recently proposed design strategy for fuzzy PID controllers based on IMC technique shows great potential for further improvement [1]. But, while it provides enhanced control performance for some sort of processes, it still has certain drawbacks for very high time delay processes and some high order processes.

In this study, a newly proposed IMC tuned Fuzzy PID controller and classical PID controller performances are compared for a variety of processes one of which is the process model generated for a real reboiler equipment of a reactive distillation column.

Following the examination of proposed controllers' performance, a variety of self tuning strategies for Fuzzy IMC PID controllers are developed in this study. As a result, self tuning algorithms have been prepared and these algorithms include necessary self tuning mechanisms that produce new coefficients for controlling various kinds of processes, whose time delay and time constant properties vary in a very large range, by using Self Tuning Fuzzy IMC PID controller. Several simulation studies were conducted and achieved results showed that, proposed Multi Region Self Tuning Fuzzy IMC PID controller provided better results for all kinds of processes compared to Non-self tuning Fuzzy IMC PID controller. Self tuning Fuzzy IMC PID performance was far more successful than that of its non-self tuning counterpart especially for very high time delay processes.

In this study; Chapter 2, gives brief information about conventional and reactive distillation technologies.

In Chapter 3, theoretical information about PI, PD, PID controllers, Ziegler Nichols tuning method and IMC technique can be found together with an overview of fuzzy logic and fuzzy control.

Chapter 4 involves detailed calculations about modeling studies and controller design studies.

Chapter 5 includes information about proposed self tuning strategies and simulation results obtained.

In Chapter 6, conclusions for the study and suggestions for the future work are presented.

2. DISTILLATION THEORY

2.1 Conventional Distillation

Distillation is based on the fact that the vapor of a boiling mixture will be richer in the components that have lower boiling points. Therefore, when this vapor is cooled and condensed, the condensate will contain more volatile components. At the same time, the original mixture will contain more of the less volatile material. Distillation columns are designed to achieve this separation efficiently. Although many people have a fair idea what “distillation” means, the important aspects that seem to be missed from the manufacturing point of view are that [2]:

- Distillation is the most common separation technique
- It consumes enormous amounts of energy, both in terms of cooling and heating requirements
- It can contribute to more than 50% of plant operating costs

The best way to reduce operating costs of existing units, is to improve their efficiency and operation via process optimization and control. To achieve this improvement, a thorough understanding of distillation principles and how distillation systems are designed is essential.

One way of classifying distillation column types is to look at how they are operated. Thus we have batch and continuous columns [2].

2.1.1 Types of distillation columns

a) Batch Columns

In batch operation, the feed to the column is introduced batch-wise. That is, the column is charged with a 'batch' and then the distillation process is carried out. When the desired task is achieved, a next batch of feed is introduced.

b) Continuous Columns

In contrast, continuous columns process a continuous feed stream. No interruptions occur unless there is a problem with the column or surrounding process units. They are capable of handling high throughputs and are the most common of the two types. We shall concentrate only on this class of columns.

Continuous columns can be further classified further as following:

According to the nature of the feed that they are processing

- Binary columns - feed contains only two components.
- Multi-component columns - feed contains more than two components.

According to the number of product streams they have

- Two product column – column has two product streams.
- Multi-product column - column has more than two product streams.

According to the extra feed exit location when it is used to help with the separation

- Extractive distillation - where the extra feed appears in the bottom product stream
- Azeotropic distillation - where the extra feed appears at the top product stream

According to the type of column internals

- Tray column - where trays of various designs are used to hold up the liquid to provide better contact between vapor and liquid, hence better separation
- Packed column - where instead of trays, 'packing' is used to enhance contact between vapor and liquid [2]

2.1.2 Main components of distillation columns

Distillation columns are made up of several components, each of which is used either to transfer heat energy or enhance material transfer. A typical distillation contains several major components [2]:

- A vertical shell where the separation of liquid components is carried out.
- Column internals such as trays/plates and/or packing which are used to enhance component separations.

- A reboiler to provide the necessary vaporization for the distillation process.
- A condenser to cool and condense the vapor leaving the top of the column.
- A reflux drum to hold the condensed vapor from the top of the column so that liquid (reflux) can be recycled back to the column.

The vertical shell houses the column internals and together with the condenser and reboiler, constitutes a distillation column. A schematic of a typical distillation unit with a single feed and two product streams is shown in Figure 2.1 [2].

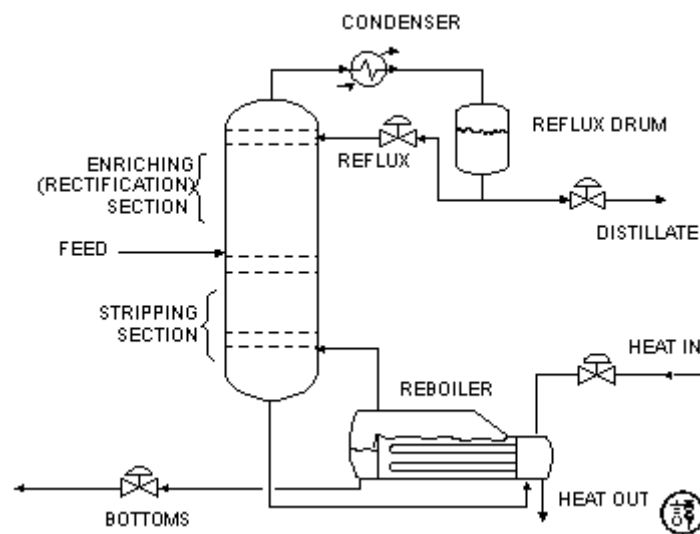


Figure 2.1: Schematic demonstration of a typical single feed distillation with two product streams [2].

The liquid mixture that is to be processed is known as the feed and this is introduced usually somewhere near the middle of the column to a tray known as the feed tray. The feed tray divides the column into a top (enriching or rectification) section and a bottom (stripping) section. The feed flows down the column where it is collected at the bottom in the reboiler. Heat is supplied to the reboiler to generate vapor. The source of heat input can be any suitable fluid, although in most chemical plants this is normally steam. In refineries, the heating source may be the output streams of other columns. The vapor raised in the reboiler is re-introduced into the unit at the bottom of the column. The liquid removed from the reboiler is known as the bottoms product or simply, bottoms. The vapor moves up the column, and as it

exits the top of the unit, it is cooled by a condenser. The condensed liquid is stored in a holding vessel known as the reflux drum. Some of this liquid is recycled back to the top of the column and this is called the reflux. The condensed liquid that is removed from the system is known as the distillate or top product. Thus, there are internal flows of vapor and liquid within the column as well as external flows of feeds and product streams, into and out of the column [2].

2.2 Reactive Distillation

The must of experiencing dramatic and suffering changes in lifestyle for the modern society is an inevitable truth which will sharply reduce per capita energy consumption in order to achieve a sustainable supply of energy [2]. The end of cheap energy era affected chemical industry in great proportions. As results of innovative studies which concentrate on decreasing costs and increasing profits, old chemical processes have been replaced by the ones that provide heat/energy, time and material savings. Economic and environmental conditions have encouraged industry to concentrate on technologies based on process “intensification”. This area of study which is subject to growing interest is defined as any chemical engineering development that provide the producers with chance of needing smaller inventories of chemical materials and maintaining higher energy efficiency. Reactive distillation is an excellent example of process intensification. It can provide an economically and environmentally attractive alternative to conventional multiunit flowsheets in some systems [3].

In chemical process industries, chemical reaction and purification of the desired products by distillation are generally conducted in separate sections. In a number of cases, the performance of this so called conventional process structure can be enhanced in great amounts by combination of reaction and distillation in a single multifunctional process unit. Reactive distillation (RD) is the globally known title given to this technology. “Catalytic distillation” could also be used for some cases in which heterogeneous catalyst particles are used in column which may improve reaction performance [4]. The process diagrams for both the conventional configuration and reactive distillation are given in Figure 2.2 [5]. This integration phenomenon has some important advantages. It can help chemical equilibrium limitations to be broken in some cases. Besides that, higher selectivities can be achieved. The heat of reaction can be integrated in order to be used for distillation

purposes. Auxiliary solvents can be avoided and azeotropic or closely boiling mixtures can be more easily separated than in non reactive columns. Increased process efficiency and reduction of investment and operational costs are natural results achieved by this approach. Some of these advantages are obtained by using reaction to improve separation performance; others are obtained by using separation to improve features of reaction environment [4].

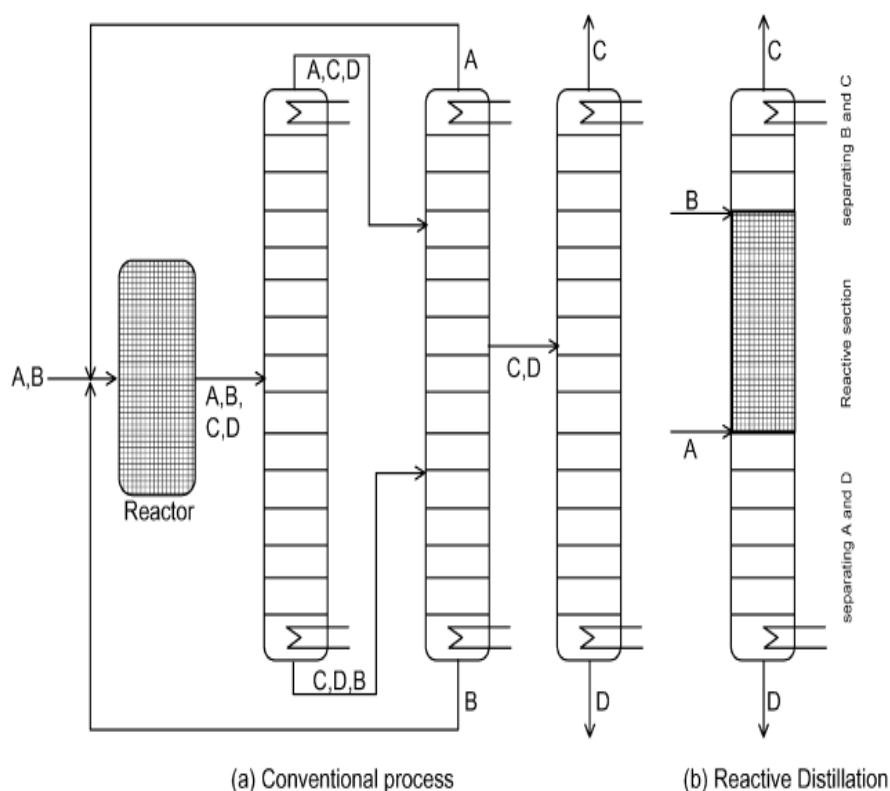


Figure 2.2: Processing alternatives for a typical $A + B \rightleftharpoons C + D$ reaction. a) Conventional reactor followed by a separator configuration b) Reactive distillation scheme [5]

Growing technology of reactive distillation which provided cost-effectiveness and compactness to the chemical plant, later kept finding great interest for production of many other chemicals. Along with esterifications and etherification, other reactions such as acetalization, hydrogenation, alkylation and hydration have been explored. Some of the objectives of existing and potential applications of reactive distillation are to: go beyond equilibrium limitation, maintain high selectivity towards a desired product, ensure energy integration, and perform difficult separations [4]. Figure 2.3 shows a photograph of Eastman methyl acetate reactive distillation column while

Figure 2.4 gives detailed demonstration about advantage of simplicity provided by reactive distillation.

Further general information and technical detail about reactive distillation could be briefly obtained from Appendix - A.

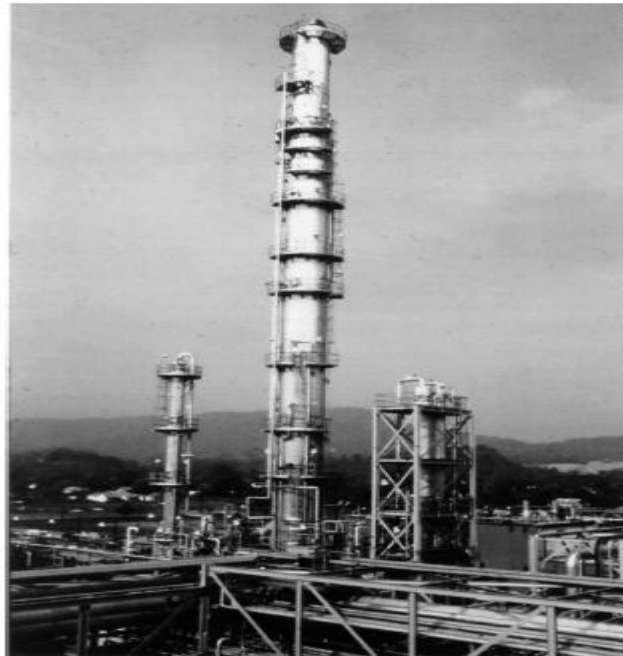


Figure 2.3: The Eastman methyl acetate reactive distillation column [3]

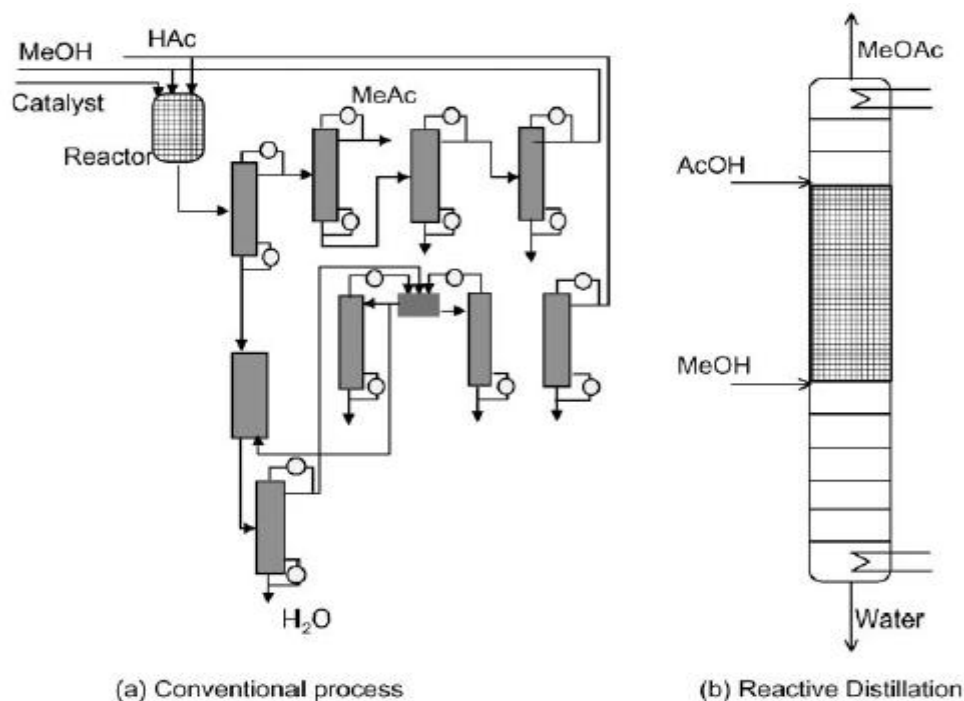


Figure 2.4: a) Flow diagram for conventional methyl acetate production process b) Reactive distillation unit proposed to replace the conventional process [5].

Advantages of reactive distillation come forward in those systems where certain chemical and phase equilibrium conditions exist. Because there are many types of reactions, there are many types of reactive distillation columns. Therefore, examination of the ideal classical situation can be appropriate to easily outline the basics. Taking into account the system in which the chemical reaction involves two reactants producing two products. The reversible reaction occurs in the liquid phase [3].



The products should be taken away from the reactants by distillation for reactive distillation to work properly. This needs the products to be lighter and/or heavier than the reactants. In terms of the relative volatilities that belong to the four components, an ideal case is when one product is the lightest and the other product is the heaviest, with the reactants having the intermediate boiling points [3].

$$\alpha_C > \alpha_A > \alpha_B > \alpha_D$$

Flowsheet of the concerning ideal reactive distillation column is given in Figure 2.5. In this situation, the lighter reactant A is fed into the lower section of the column but not at the very bottom. The heavier reactant B is fed into the upper section of the column but not at the very top. The middle of the column is the reactive section and contains N_{RX} trays. Figure 2.6 shows a single reactive tray on which the net reaction rate of the reversible reaction depends on the forward and backward specific reaction rates (k_F and k_B) and the liquid holdup (or amount of catalyst) on the tray (M_n). The vapor flowrates through the reaction section change from tray to tray because of the heat of the reaction [3].

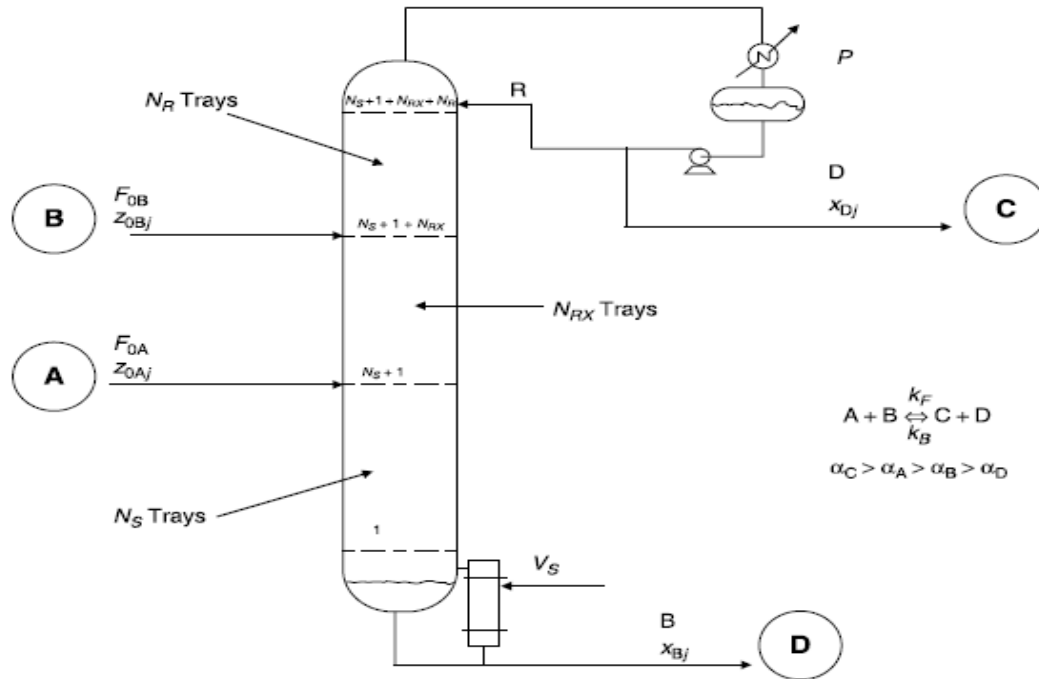


Figure 2.5: Ideal reactive distillation column [3]

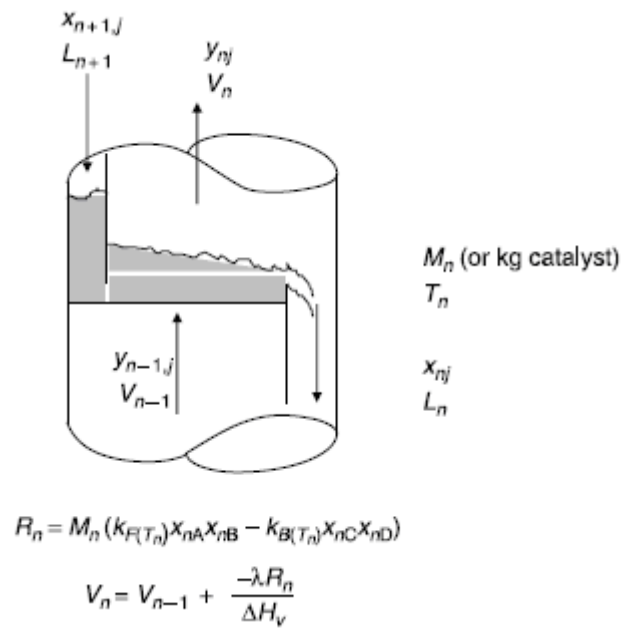


Figure 2.6: One reactive tray in detail [3]

As component A flows up the column, it reacts with B flowing down. Very light product C, which is swiftly removed in the vapor phase from the reaction zone, flows up the column. In same manner, very heavy product D is quickly taken away in the liquid phase and descends along the column [3].

The advantages of reactive distillation can be listed briefly as follows [5]:

- Simplifying or removing the separation system equipment can give possibility to important capital cost saving.
- Conversion of reactants can be pushed up to 100%, which will reduce recycle costs.
- Removing one of the products from the reaction mixture or decreasing the concentration of one of the reactants can lead to reduction of the rates of side reactions and therefore can improve selectivity for the desired products.
- Catalyst requirement for the same degree of conversion can be reduced.
- Reactive distillation is particularly advantageous when the reactor product is a mixture of species that can form several azeotropes with each other. Reactive distillation conditions can allow the azeotropes to be reacted away in a single vessel.
- By-product formation rate can be reduced.
- If the reaction is exothermic, the heat of reaction can be used to provide the heat of vaporization and reduce the reboiler duty.
- Avoidance of hot spots and runaways may be possible using liquid vaporization as thermal fly wheel [5].

Against the above-mentioned advantages of reactive distillation, there are several constraints and foreseen difficulties [5]:

- The reactants and products must have suitable volatility to maintain high concentrations of reactants and low concentrations of products in the reaction zone.
- If the residence time for the reaction is long, a large column size and large tray hold-ups will be needed. In such cases, it may be more economic to use a reactor-separator arrangement.
- It is difficult to design reactive distillation processes for very large flow rates since liquid distribution problems may occur in reactive distillation columns.
- The optimum conditions of temperature and pressure for distillation may be very distinct from those for reaction and vice versa [5].

2.3 Reactive Distillation Process Under Investigation

In this study, vapor phase temperature profile among the reboiler of a reactive distillation process is observed. The concerning reactive distillation process produces acetate esters from fusel alcohols. Feed stream of the reactive distillation column is fusel oil that is composed of 16% water, 17.12% ethyl alcohol, 1.86% n-propyl alcohol, 4.04% isobutyl alcohol, 60.99% isoamyl alcohol. This feed stream gives esterification reaction with glacial acetic acid. Since esterification reaction is an equilibrium reaction, one of the products water and ester compounds should be removed from product mixture. In process of producing acetates from fusel oil, removal of light esters such as propyl acetate and ethyl acetate together with the water coming from feed stream and reaction product stream is determined to be the best method [6].

The column used for this process is composed of 4 packing compartments. All of these compartments are 40 cm in length and 8 cm in diameter. Packing sections are filled with Rasching rings in order to enhance liquid-vapor contact surface. The feed stream is continuously pumped over the second compartment. The water stream composed of feed stream water content and reaction product water leaves the column by distillate stream together with light esters. Ester content of the distillate stream is fed back to system with reflux while water content is easily separated from light ester stream as bottom product of a secondary separation process and removed from the system [6].

The temperature of the reboiler of the column increases and decreases according to the amount of heating power exerted to the system. As a result of experimental studies, Tanrıverdi [6] obtained temperature vs. heat data of the reboiler system. The graphical representation of system response is given in Figure 2.7. Tanrıverdi and İskender [7] studied on the relevant process to analyze the performance of a double slope PID controller which introduced different proportional, derivative and integral gains for positive and negative step actions [7].

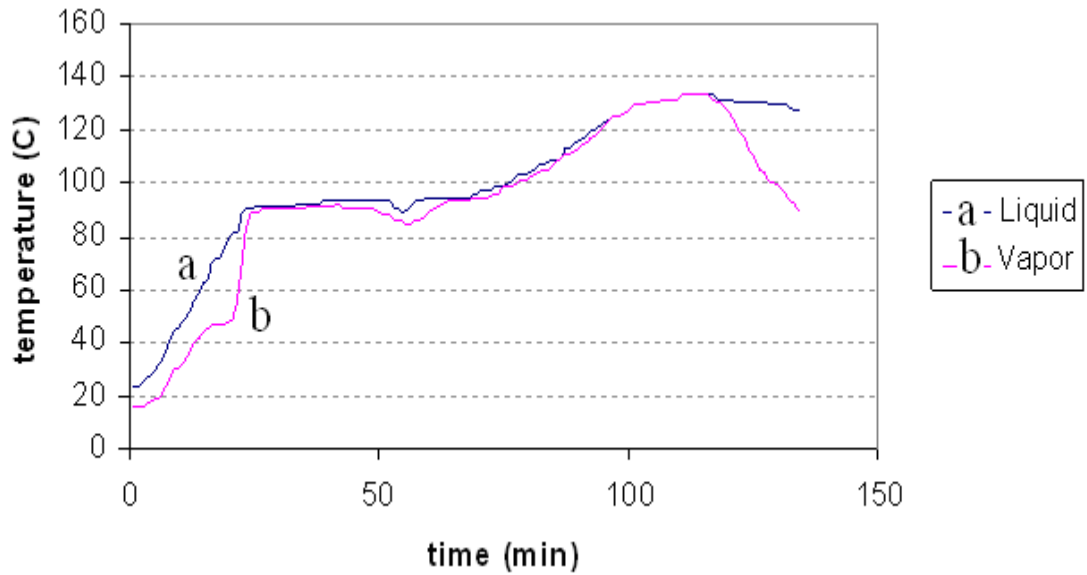


Figure 2.7: Temperature profile along the reboiler of the reactive distillation column producing acetate esters [6].

İskender and Tanrıverdi [8] also investigated the performance of a self tuning controller on same reboiler system. As a conclusion of their studies, it is particularly mentioned that, the temperature at the top of the reactive distillation column should be kept between 79 °C and 87 °C. Since the water content of distillate stream seems to disappear for temperatures less than 79 °C, the column flow regime is interrupted. On the other hand, the column temperature at the top should be kept less than 87 °C to prevent bottom product components from passing in to top product stream [8].

Cebeci [9] also performed a series of studies on the same reactive distillation reboiler process and made observations about performance of an IMC Based Dual Phase PID controller in controlling reboiler temperature. Dual phase PID controller concept introduces determination of two different sets of controller parameters for both the vapor and the liquid phases of the reboiler content [9].

In this study, performance of a new concept that couples Internal Model Control (IMC) design method with Fuzzy PID Controller will be investigated. An IMC Fuzzy PID Controller will be designed to control the temperature of the vapor phase of the concerning reboiler system. Furthermore, some self tuning strategies will be introduced into non-self tuning Fuzzy IMC PID controller scheme in order to evaluate a generalized set of self-tuning algorithms for Fuzzy IMC PID Controllers to be designed in the future.

3. CONTROL THEORY

3.1 About PID Control

“PID control” is the method of feedback control that uses the PID controller as the main tool. The basic structure of conventional feedback control systems is shown in Figure 3.1, using a block diagram representation. In this figure, the process is the object to be controlled. The purpose of control is to make the process variable y follow the set-point value r . To achieve this purpose, the manipulated variable u is changed at the command of the controller. As an example of processes, consider a heating tank in which some liquid is heated to a desired temperature by burning fuel gas. The process variable y is the temperature of the liquid, and the manipulated variable u is the flow of the fuel gas. The “disturbance” is any factor, other than the manipulated variable, that influences the process variable. PID control is one of the earlier control strategies. The PID controller was first placed on the market in 1939 and has remained the most widely used controller in process control until today [10]. Its early implementation was in pneumatic devices, followed by vacuum and solid state analog electronics, before arriving at today’s digital implementation of microprocessors. It has a simple control structure which was understood by plant operators and which they found relatively easy to tune. Since many control systems using PID control have proved satisfactory, it still has a wide range of applications in industrial control. According to a survey for process control systems conducted in 1989, more than 90 % of the control loops were of the PID type. PID control has been an active research topic for many years; see the monographs. Since many process plants controlled by PID controllers have similar dynamics it has been found possible to set satisfactory controller parameters from less plant information than a complete mathematical model. These techniques came about because of the desire to adjust controller parameters in situ with a minimum of effort, and also because of the possible difficulty and poor cost benefit of obtaining mathematical models [11].

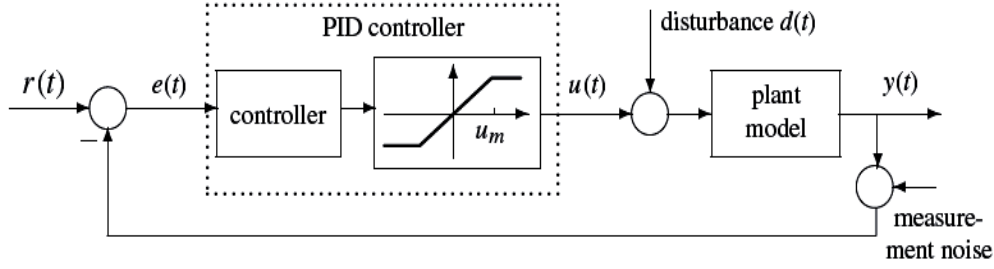


Figure 3.1: A feedback control loop with PID controller embedded, including disturbance and noise variables [11].

3.2 Proportional Control

A proportional controller moves its output proportional to the deviation in the controlled variable from set point:

$$u = K_c e + b = \frac{100}{P} e + b \quad (3.1)$$

$e = \pm(r - c)$, the sign selected to produce negative feedback. In some controllers, proportional gain “ K_c ” is expressed as a pure number; in others, it is set as $100/P$, where P is the proportional band in percent. The output bias b of the controller is also known as manual reset. The proportional controller is not a good regulator, because any change in output to a change in load results in a corresponding change in the controlled variable. To minimize the resulting offset, the bias should be set at the best estimate of the load and the proportional band set as low as possible. Processes requiring a proportional band of more than a few percent will control with unacceptable values of offset. Proportional control is most often used for liquid level where variations in the controlled variable carry no economic penalty, and where other control modes can easily destabilize the loop. It is actually recommended for controlling the level in a surge tank when manipulating the flow of feed to a critical downstream process. By setting the proportional band just under 100 percent, the level is allowed to vary over the full range of the tank capacity as inflow fluctuates, thereby minimizing the resulting rate of change of manipulated outflow. This technique is called averaging level control [12].

3.3 Proportional-plus-Integral (PI) and Proportional-plus-Derivative (PD) Control

Integral action eliminates the offset described above by moving the controller output at a rate proportional to the deviation from set point. Although available alone in an integral controller, it is most often combined with proportional action in a PI controller [12]:

$$u = \frac{100}{P} \left(e + \frac{1}{\tau_I} \int e dt \right) + C_0 \quad (3.2)$$

Above, τ_I is the integral time constant in minutes; in some controllers, it is introduced as integral gain or reset rate $1/\tau_I$ in repeats per minute. The last term in the equation is the constant of integration, the value the controller output has when integration begins. The PI controller is by far the most commonly used controller in the process industries [12].

On the other hand, PD controller couples proportional control with derivative action rather than integral action. In controller equation of PD, derivative term replaces integral term. Derivative action provides the controller with fast response but on the other hand, it can not deal with constant noise, as it gives excess response to high frequency set point changes.

3.4 Proportional - Derivative - Integral (PID) Control

The derivative mode moves the controller output as a function of the rate-of-change of the controlled variable, which adds phase lead to the controller, increasing its speed of response. It is normally combined with proportional and integral modes. The non-interacting form of the PID controller appears functionally as:

$$u = \frac{100}{P} \left(e + \frac{1}{\tau_I} \int e dt + \tau_D \frac{de}{dt} \right) + C_0 \quad (3.3)$$

Above, τ_D is the derivative time constant. Note that derivative action is applied to the controlled variable rather than to the deviation, as it should not be applied to the

set point; the selection of the sign for the derivative term must be consistent with the action of the controller [13].

In some analog PID controllers, the integral and derivative terms are combined serially rather than in parallel as done in the last equation. This results interaction between these modes, such that the effective values of the controller parameters differ from their set values as follows:

$$\tau_{I_{\text{eff}}} = \tau_I + \tau_D \quad (3.4)$$

$$\tau_{D_{\text{eff}}} = \frac{1}{1/\tau_D + 1/\tau_I} \quad (3.5)$$

$$K_c = \frac{100}{P} \left(1 + \frac{\tau_D}{\tau_I} \right) \quad (3.6)$$

The performance of the interacting controller is almost as good as the non-interacting controller on most processes, but the tuning rules differ because of the above relationships. With digital PID controllers, the non-interacting version is commonly used.

Noise on the controlled variable is amplified by derivative action, preventing its use in controlling flow and liquid level. Derivative action is recommended for control of temperature and composition, reducing the integrated error (IE) by a factor of two over PI control with no loss in robustness [13]. Figure 3.2 compares typical loop responses for P, PI, and PID controllers, along with the uncontrolled case [14]

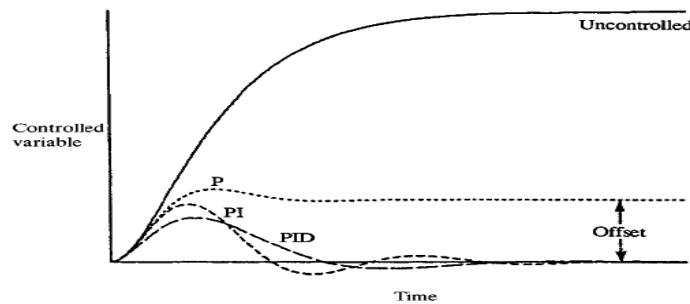


Figure 3.2: Comparison of typical responses to a step change with P, PI and PID controls and with no control situation [14].

3.5 Ziegler – Nichols Method for Tuning PID Controllers

- First, note whether the required proportional control gain is positive or negative. To do so, step the input u up (increased) a little, under manual control, to see if the resulting steady state value of the process output has also moved up (increased). If so, then the steady-state process gain is positive and the required Proportional control gain, K_c , has to be positive as well.
- Turn the controller to P-only mode, i.e. turn both the Integral and Derivative modes off.
- Turn the controller gain, K_c , up slowly (more positive if K_c was decided to be so in step 1, otherwise more negative if K_c was found to be negative in step 1) and observe the output response. Note that this requires changing K_c in step increments and waiting for a steady state in the output, before another change in K_c is implemented.
- When a value of K_c results in a sustained periodic oscillation in the output (or close to it), mark this critical value of K_c as K_u , the ultimate gain. Also, measure the period of oscillation, P_u , referred to as the ultimate period.
- Using the values of the ultimate gain, K_u , and the ultimate period, P_u , Ziegler and Nichols prescribes the values given in Table 3.1 for K_c , t_I and t_D , depending on which type of controller is desired [15].

Graphical expression of tuning procedure with Ziegler Nichols method is given in Figure 3.3.

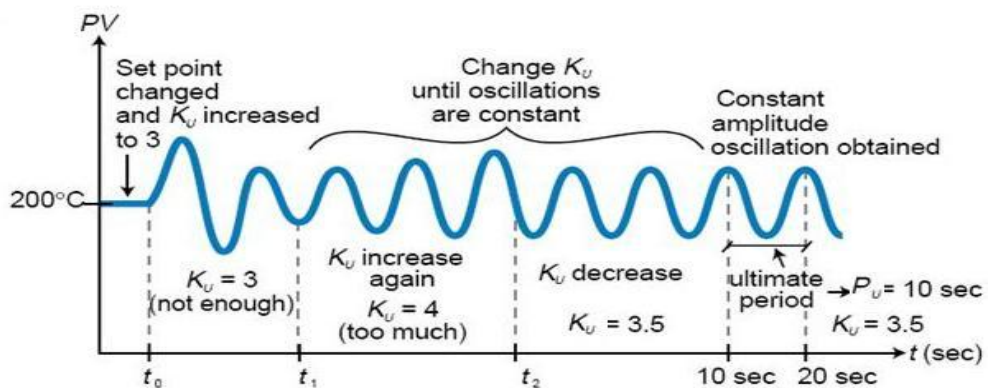


Figure 3.3: Graphical demonstration for Ziegler Nichols tuning steps [16].

Table 3.1: Ziegler - Nichols Chart for Defining Controller Parameters from System Data [15]

	K_c	τ_I	τ_D
P control	$K_u/2$		
PI control	$K_u/2.2$	$P_u/1.2$	
PID control	$K_u/1.7$	$P_u/2$	$P_u/8$

3.6 Internal Model Control (IMC) Strategy

3.6.1 General information about IMC

Internal Model Control bases on the Internal Model Principle, which states that, control can only be achieved if the controller somehow includes some representation of the process to be controlled. In fact, perfect control is treated to be possible if and only if the perfect model of a process is known in every detail. This situation would lead to the perfect control scheme given in Figure 3.4 [17].

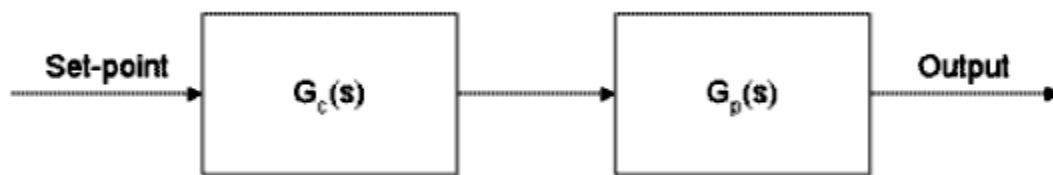


Figure 3.4: Open loop control scheme [17].

With the technical explanation, if; $G_c = 1/\check{G}_p$ condition is satisfied, perfect control could be achieved.

However, \check{G}_p process model doesn't generally match actual process G_p . This situation forms the basis for IMC control strategy, which has a potential to achieve perfect control. A typical IMC scheme is given in Figure 3.5.

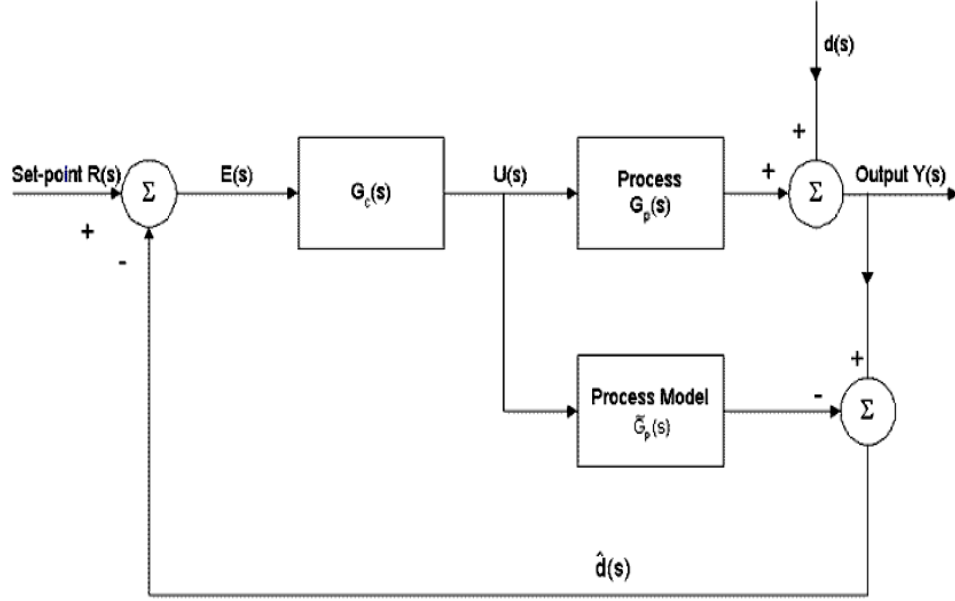


Figure 3.5: Typical IMC scheme [17].

In the scheme, $d(s)$ is unknown disturbance. Manipulated input $U(s)$ is fed to both the process and the model. The process output $Y(s)$ is compared with model output and resulting $\hat{d}(s)$ signal is fed back [17].

3.6.2 Practical design of IMC

Given a model of the process, first step is factoring \check{G}_p in to invertible and non-invertible parts.

$$\check{G}_p(s) = \check{G}_p^+(s) * \check{G}_p^-(s) \quad (3.7)$$

The non-invertible part \check{G}_p^- contains terms such as positive zeros or time delays, which will lead to instability or realisability problems if inverted.

Next step is setting $G_c = G_p^+(s)^{-1}$ and $G_{IMC}(s) = G_c(s) * G_f(s)$ where G_f is a filter transfer function of appropriate order.

As Figure 3.5 is modified to Figure 3.6 first, and then simplified to Figure 3.7, following equations leads to the appropriate transfer function for PID controller [17].

$$G_{PID}(s) = G_{IMC}(s) / (1 - G_{IMC}(s) * \check{G}_p(s)) \quad (3.8)$$

$$G_{PID}(s) = [\check{G}_p^+(s)^{-1} * G_f(s)] / [1 - \check{G}_p^-(s) * G_f(s)] \quad (3.9)$$

These equations generally lead to a PID controller transfer function as following, where A,B,C and D are constant numerical coefficients:

$$G_{PID}(s) = [A * S^2 + B * S + 1] / [C * S^2 + D * S] \quad (3.10)$$

This transfer function can be placed into control loop as PID controller block. On the other hand, with further mathematical identification of above transfer function, one can determine gain (K_c) and proportional, integral, derivative time constants of PID controller.

For instance; for a first order process transfer function and using a first order filter transfer function, PID parameters can be calculated according to following relations [18]:

$$p(s) = \frac{K_p e^{-Ts}}{(\tau s + 1)} \quad (3.11)$$

$$\tau_I = \tau + \frac{T^2}{2(\epsilon + T)}; K_c = \frac{\tau_I}{K_p(\epsilon + T)}; \tau_D = \frac{T^2(1 - \frac{T}{3\tau_I})}{2(\epsilon + T)} \quad (3.12)$$

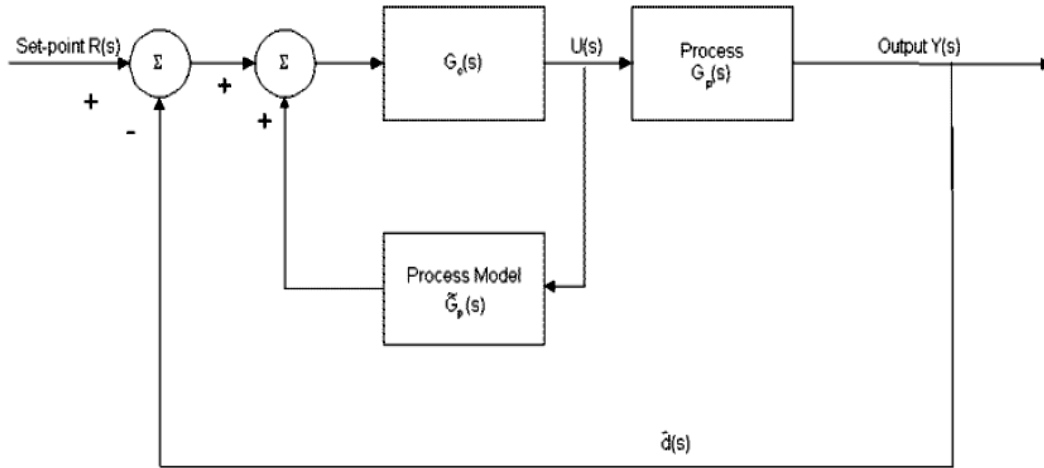


Figure 3.6: Modified configuration of IMC scheme [17].

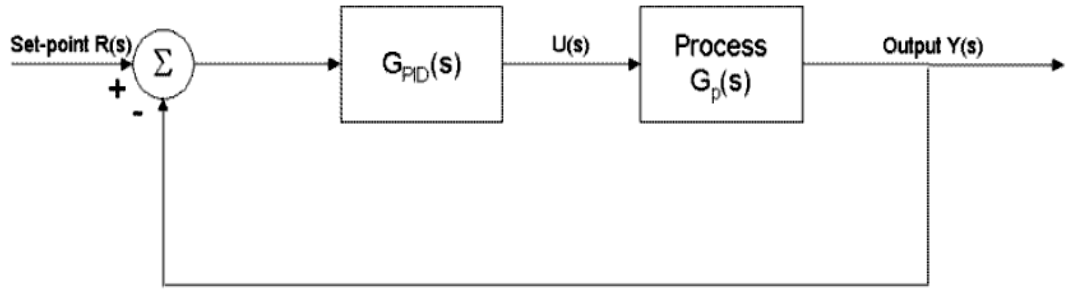


Figure 3.7: Simplification of IMC scheme. Process model \check{G}_p terms and G_c controller terms are integrated by a single G_{PID} block [17].

3.7 Fuzzy Logic and Fuzzy PID Control

3.7.1 Introduction and what fuzzy logic control is

Traditionally, computers make rigid “yes” or “no” decisions, by means of decision rules based on two valued logic: true /false, yes/no or 1 / 0. An example is an air conditioner with thermostat control that recognizes just two states: above the desired temperature or below the desired temperature. On the other hand, fuzzy logic allows a graduation from “true” to “false”. A fuzzy air conditioner may recognize “warm” and “cold” room temperatures. The rules behind this are less precise [19]. For example;

“If the room temperature is warm and slightly increasing, then increase the cooling.”

Many classes or sets have fuzzy rather than sharp boundaries, and this is the mathematical basis of fuzzy logic. The set of “warm” temperature measurements is one example of a fuzzy set.

The core of a fuzzy controller is a collection of “verbal” or “linguistic” rules of the “if – then” form. The rules can bring the reasoning used by computers closer to that of human beings.

In the example of the fuzzy air conditioner, the controller works on the basis of a temperature measurement. The room temperature is just a number, and more information is necessary to decide whether the room is warm. Therefore; the designer must incorporate a human’s perception of warm room temperatures.

Straight forward implementation is to evaluate beforehand all possible temperature measurements. For example; on a scale from “0 to 1”, “warm” corresponds to “1” and “not warm” corresponds to “0” [19].

For a temperature interval from 15 to 27 °C;

Measurements (°C)	15	17	19	21	23	25	27
Grade	0	0.1	0.3	0.5	0.7	0.9	1

3.7.2 Fuzzy sets

Fuzzy logic and fuzzy control begins with the concept of a fuzzy set. A fuzzy set is a set without a crisp, clearly defined boundary. It can contain elements with only a partial degree of membership.

To understand what a fuzzy set is, the example about the days of the week and their contribution to the set of “weekdays” could be given.

According to the thinking based on classical sets, one can say that, the days which can be called as weekdays are Monday, Tuesday, Wednesday, Thursday and Friday while Saturday and Sunday should be named as weekend days. On the other hand, getting fuzzy sets as the basis for classifying these days, one can say that, Friday is a little more likely to be a weekend day compared to Tuesday or Wednesday. So its membership grade to the set of weekend days is some value between 0 and 1 where the grades for Saturday and Sunday are 1. Figure 3.8 shows this difference between the philosophies of classical sets and fuzzy sets [20].

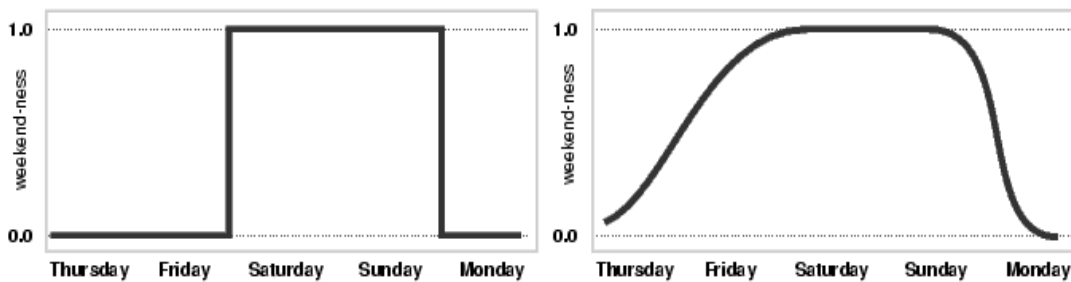


Figure 3.8: Membership grades of the days for the set of “weekend days” according to classical set and fuzzy set theories [20].

3.7.3 Fuzzy rules and rule bases

Fuzzy rules are the statements that receive the inputs of the controllers, generate the appropriate decision according to them and define the control action to be performed. The most common definition of this process could be demonstrated by giving a rule base table as an example. A rule base that simply takes the measurement error and

the rate of change of error as input and decides for the control action is shown in Table 3.2. The translations for shortcuts could be done as; NB means Negative Big, or PS means Positive Small and ZE means Zero and so on for the other ones.

For example, according to this table; if the error from the set point is very large positive and it is still increasing rapidly; the rule base takes it as: error is PB and change of error is PB. So, the decision that follows this realization will be PB. In other words for example, if the temperature of the reactor is much smaller than the desired value and it is still decreasing rapidly, then the heating vapor stream rate should be very high. The fuzzy rules work on if then statements such as the prior example.

If error is NS and change of error is PS then control output is ZE.

It means that; if the temperature is a little higher than the set point and it is slightly decreasing then there is no need to perform any spectacular control action.

Table 3.2: A rule base table for an error-change of error type fuzzy control strategy [21]

$\Delta e / e$	NB	NM	NS	ZE	PS	PM	PB
NB	NB	NB	NB	NM	NS	NS	ZE
NM	NB	NM	NM	NM	NS	ZE	PS
NS	NB	NM	NS	NS	ZE	PS	PM
ZE	NB	NM	NS	ZE	PS	PM	PB
PS	NM	NS	ZE	PS	PS	PM	PB
PM	NS	ZE	PS	PM	PM	PM	PB
PB	ZE	PS	PS	PM	PB	PB	PB

3.7.4 Fuzzy membership functions

A membership function is a curve that defines how each point in the input space is mapped to a membership value between 0 and 1. The input space is sometimes referred to as the universe of discourse [20].

The simplest membership functions are formed using straight lines. Of these, the simplest is the triangular membership function. It is simply defined by three points. Another common type of membership functions is trapezoidal shape membership functions. This type has a flat top that smoothes the membership recognition for the

data defined near to the center of the shape. Figure 3.9 shows triangular and trapezoidal type membership function curves.

The work held by membership functions is to classify the input data by partially introducing it to the several definitions. For example, there exists a temperature interval from 150°C to 250°C. The input signal is received such that, the measured temperature is 200°C. The membership of this temperature value for the set of moderate is 1 over 1. On the other hand it also has partial membership in cold and hot temperature sets, for example 0.4 (Some value between 0 and 1).

Another example could be given for set point control cases. For example if the temperature of a reactor is desired to be kept constant at 170°C and the reference temperature for the controller is set as 170°C. During operation, the temperature is measured as 175°C. The error will be +5°C. This corresponds to positive error. It also has some membership values for PB, PM, PS, ZE, NS, NM, NB sets. The membership of +5°C error for PM is 0.8 while its membership for PB is 0.1, for PS 0.3, for ZE 0.1 while for NS, NM and NB it is 0. This means that controller accepts this error as positive medium as a general definition but it also doesn't ignore its contribution to the other relevant neighbor fuzzy sets. On the other hand, for the same controller -45°C error would be accepted as totally NB error and coupled with 1 over 1 membership grade for that set while its membership for other sets would be defined as 0.

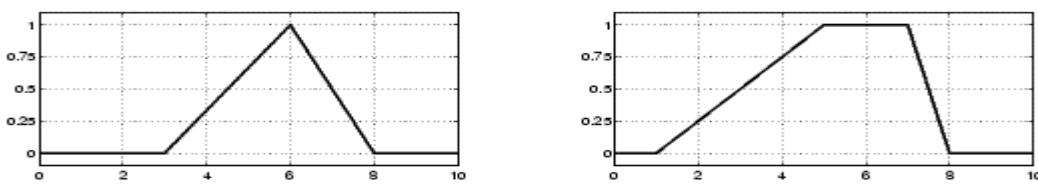


Figure 3.9: Triangular and trapezoidal membership function curves [20]

3.7.5 Fuzzy inference

Inference mechanism is one of the key steps for the decision making process of a fuzzy controller. Inference is the conjunction maintained by the controller between input signals and the generated output. An inference mechanism contains membership functions and fuzzy rules in order to produce an output by means of manipulating inputs that may be more than one. The operation of inference mechanism can be divided in to three steps [21]:

- Fuzzification
- Fuzzy processing of the inputs and output generation
- Defuzzification

These steps are shown graphically in Figure 3.10. The first step fuzzification involves processing of the crisp input values. Crisp input is generally a numerical value that can not be defined by linguistic terms. For example; “error=0.3” is a scaled crisp input. Fuzzification block receives crisp input and makes it fuzzy according to its input membership functions. For example; if input membership functions for input “error” being small medium and big as shown in Figure 3.11.

When the crisp input 0.3 is recognized, the membership grade of this value for fuzzy sets “small”, “medium” and “big” are determined by fuzzification block. In this example, that are 0.25, 0.5 and 0, respectively. As a result of fuzzification, input “0.3” is processed both as a small input and a medium input in appropriate biases.

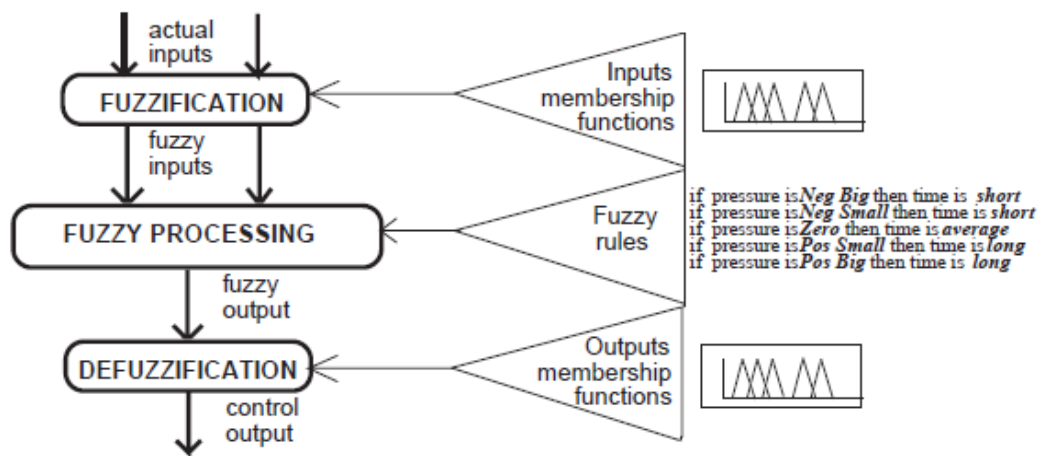


Figure 3.10: Operation of a fuzzy inference mechanism [21]

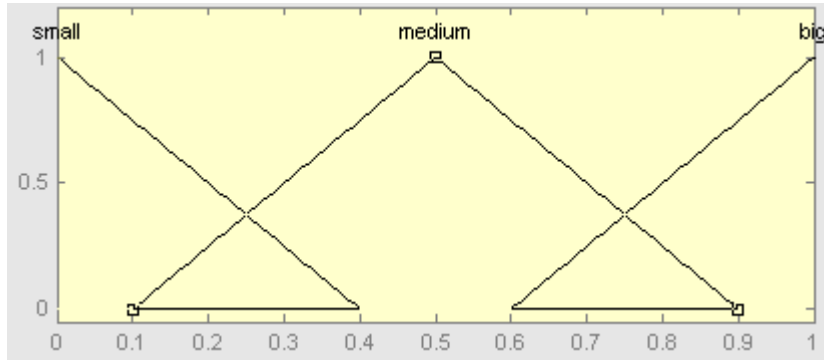


Figure 3.11: Neighboring membership functions

The second step fuzzy processing involves the use of fuzzy rules that are mentioned earlier in this study. The fuzzified inputs are processed according to their membership grades defined by fuzzification block. For example; if we consider a rule base that is in the following shape;

Rule 1: If input 1 is small and input 2 is small then output is small large

Rule 2: If input 1 is small and input 2 is medium then output is small medium

Rule 3: If input 1 is small and input 2 is big then output is medium

Rule 4: If input 1 is big and input 2 is big then output is big large

and so on.

This rule base will take the membership grades for each classification such as input 1 is small, input 1 is medium or input 1 is big and will place it in the corresponding rule. It will then process all inputs (only two in this example) together with the selected “and / activation operation” mechanism which is generally a mathematical multiplication operation or the logical minimum operator. For example, for rule 1; the membership of input 1 is 0.25 and the membership of another input is 0.8. Inference “and” operation will multiply these grades in order to produce a rule output that only defines the action performed by that specific rule. The output of the rule in this example according to the minimum operator will be: $\min(0.25, 0.8) = 0.25$. This rule output is then introduced to the output scaling factor corresponding to the rule. In this example, the output membership function for rule 1 is small large. The grade for which the output satisfies this membership function is calculated in same manner that is used in input fuzzification.

After the activation mechanism, the next part of the inference comes which is called accumulation operation. The accumulation operation involves gathering of all the rule outputs that are received from each individual rule. The outputs of all rules are processed according to the selected accumulation operator which is generally selected as mathematical summation or logical maximum operators. For each of the possible output values ranged from 0 to 1, the maximum of the rule output membership results are collected. In our example, the satisfaction of small large, small medium, medium and big large memberships that correspond to rules 1, 2, 3 and 4 respectively are defined for the whole output range and the maximum value for each point is evaluated.

The last step defuzzification involves creation of a crisp output from the graphical fuzzy output definition that is achieved by accumulation operation. There are several methods for defuzzification in literature the most common of which are center of gravity, mean of maxima and bisector of area methods. The graphical representation of inference mechanism for an example from help page of MATLAB software program is given in Figure 3.12.

3.7.6 Input and output scaling

Input and output scaling is a very important feature for fuzzy controller mechanism since it determines the quality of input feed to the inference mechanism and correct reading of the output. Input and output scaling factors of a fuzzy controller could be demonstrated as gain blocks placed before and after the inference core of the fuzzy controller. Figure 3.13 shows the general placement of the scaling blocks in a control scheme that determines the output control signal by means of evaluating “error” and “change of error input” signals.

fuzzy controllers in literature examples are generally placed after the inference mechanism. Placing it on to output control signal, the integration of all observed control signals can be evaluated. So; “beta” gain factor here is becoming the integral gain element the output of which is directly fed to integrator. Finally, “alfa” is the regular proportional output scaling factor. Fuzzy controller gain parameters for specific control systems are generally determined by means of first defining the parameters of a conventional controller which successfully manages the desired control action for the same system. Once the parameter of the conventional controller is determined, stochastic assignment of fuzzy controller scaling (gain) factors can be done by using heuristic tables.

3.7.7 Literature survey about fuzzy control

Moreover to the basic information above about Fuzzy Logic Control and Fuzzy PID control schemes, further knowledge about fuzzy control theories can be achieved from the literature. Since Fuzzy logic control has been one of the recent most popular areas in control engineering field, there outstanding numbers of studies conducted on improving the performances gained from fuzzy controllers. Some of these studies will be mentioned in this part only to provide deeper guidance in to the subject.

Erenoğlu et. Al. [22] studied on an intelligent hybrid fuzzy PID controller which is practically a hybrid combination of a conventional PID and a fuzzy PID controller. With selection of appropriate gain factors, hybrid controller achieved improved results in transient and steady state responses.

Woo et al. [23] studied on a Fuzzy controller scheme with self tuning scaling factors. Using a function tuner method which tunes derivative and integral gain coefficients with two different functions depending on error value, they achieved shorter settling time and restrained system behavior with much less oscillations.

Güzelkaya, Eksin and Yeşil [24] studied on self tuning of Fuzzy PID controller coefficients via relative rate observer. Relative rate observer scheme provides control loop with the ability of making decision based on two inputs: error and system response speed. Working according to second time derivative of the error, relative rate observer regulates integral and derivative gain coefficients.

Karasakal et. al. [25] studied on implementation of relative rate observer based self tuning fuzzy PID controller on PLC.

Mudi and Pal [26] proposed a robust self tuning scheme for PI and PD type fuzzy controllers. Proposed scheme manipulates integral and derivative gain coefficients of the controller according to the error value. Its main idea is based on the fact that; in transient response, gains should be tuned to speed up the system response and in steady state response, gains have to be tuned to provide robustness.

Li and Tso [27] proposed a mathematical analysis for designing and tuning of Fuzzy PID control, in order to achieve a simpler design procedure.

Duan, Li and Deng [1] proposed an Internal Model Control (IMC) based tuning method for definition of appropriate scaling factors for Fuzzy PID controllers. Their studies on this scheme provided basis for this study. The method proposed by their study will be explained in detail during following parts of this study.

Furthermore, this study is based on the aim of improving the performance of the proposed scheme proposed in [1] and providing a generalized algorithm for defining most appropriate scaling factors of Fuzzy IMC PID controllers implemented on a variety of processes.

4. MODELING AND CONTROLLER DESIGN

4.1 Modeling

On the first step of studies, some calculations has been made in order to find several models that will be suitable for the process response curve of which had been under investigation. Concerned process curve was given in Figure 2.7.

Modeling studies began with generation and testing of a first order model with time delay and comparison of responses that belong to the model and the real process. On this path, the studies are firstly conducted by taking the vapor phase curve as the basis. The time where the system response reached 63% of its largest value is noted. The magnitude of the response at this time is also imported from the graph. These values are 26.25 minutes and 89.67°C, respectively. After that, these two values are substituted in to Equation 4.1 in order to calculate time constant that represents the system. In this equation, t is time, $s(t)$ is response, K is ultimate output gain (133.33 °C), T is time constant and L is the system delay time which was formerly determined to be 2 minutes.

$$s(t) = K(1 - e^{-(t-L)/T}) \quad (4.1)$$

As the result of calculations, first order time constant of the process has been found to be 21.72 minutes. With the given gain (K) of 0.187 °C.minute/ kcal, which was previously found in recent studies, the first order transfer function with dead time (FOPDT) is created as shown in Equation 4.2.

$$P(S) = 0.187 * e^{-2S} / (21.72S + 1) \quad (4.2)$$

Step response of FOPDT model is shown with in Figure 4.1. Comparison between the model and process responses yield that, first order model doesn't actually represent this system. Its response is by too far from the actual curve.

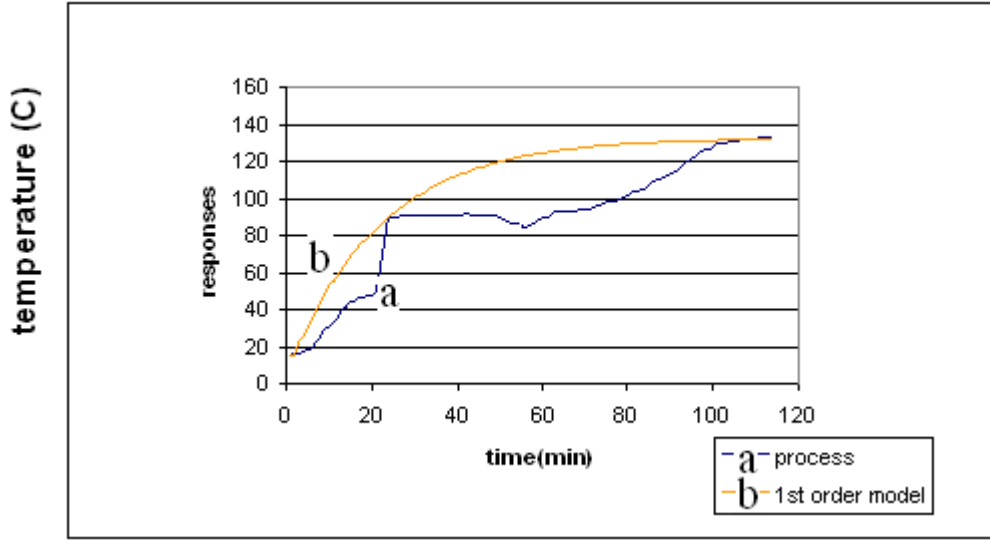


Figure 4.1: Response curves of FOPDT model and process

After FOPDT model, the next model to be generated and investigated was three term second order with dead time process model. The time period to be selected as basis for calculating time constant are selected properly in order to represent the system curve at its most critical points. In other words, classical 63% of response rule has not been used in this particular study. On this way, system response at $t=43$ minutes is imported from graph and it was 90.67°C . These two values are substituted in to Equation 4.3.

$$s(t) = K * \{ 1 - [1 + ((t-L)/T)] * [e^{-(t-L)/T}] \} \quad (4.3)$$

From Equation 4.3, the time constant of second order transfer function is determined to be 17.46 minutes. Transfer function of three-term second order model with dead time is given in Equation 4.4.

$$P(S) = 0.187 * e^{-2S} / (17.46S + 1)^2 \quad (4.4)$$

Step response of three term second order model is given with graph in Figure 4.2. Figure 4.3 also gives the comparative view of two model curves and process curve. It is obvious that, second order model gives better result and represents the system curve much more realistic compared to the first order model.

The third step of modeling studies was creating a four parameter second order model for the process and investigating its representation abilities. In order to determine two different time constants for the second order transfer function, the times where the step response of the process reaches 33% and 67% of its maximum

value are noted. The magnitudes of the response at these times are also read from the graphic. These are; $t_1=23$ min., $t_2=85$ min., $s(t_1)=74.67$ °C, $s(t_2)=106.67$ °C, respectively. These values are substituted in to Equation 4.5 in appropriate order.

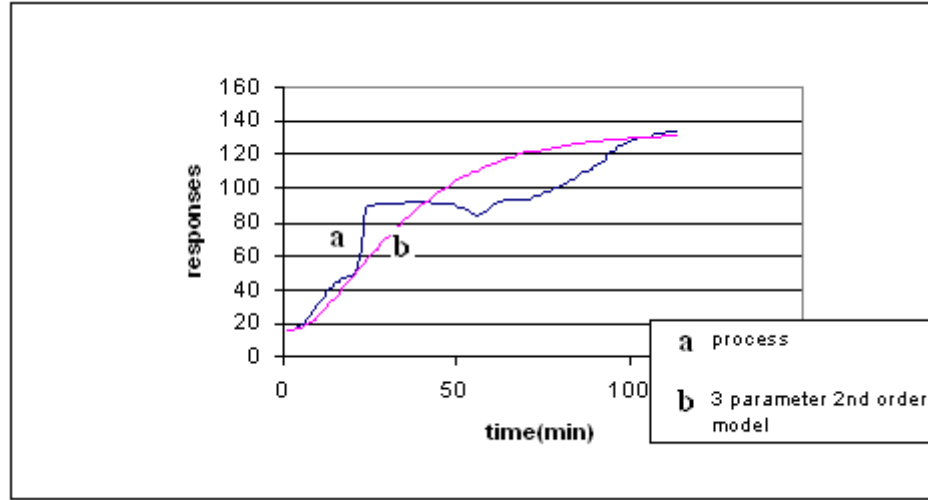


Figure 4.2: Process curve and three term SOPD model curve

In Equation 4.5, $s(t_1)$ is solved for t_1 and $s(t_2)$ is for t_2 . T_1 and T_2 values that prove both equations true are determined to be the time constants of four parameter model. Approximate results of the calculations show that time constants of the model could be selected as: $T_1=6$ and $T_2=21$. Transfer function of four parameter second order model is given in Equation 4.6.

$$s(t) = K * \{ 1 + [T_2 * e^{-(t-L)/T_2} - T_1 * e^{-(t-L)/T_1}] / (T_1 - T_2) \} \quad (4.5)$$

$$P(S) = 0.187 * e^{-2S} / [(6S+1)*(21S+1)] \quad (4.6)$$

Step response of four parameter model is examined. Its performance is observed to be better than FOPDT model but not as successful as three parameter second order model. The comparative graphics concerning this model are given in Figure 4.4 and Figure 4.5.

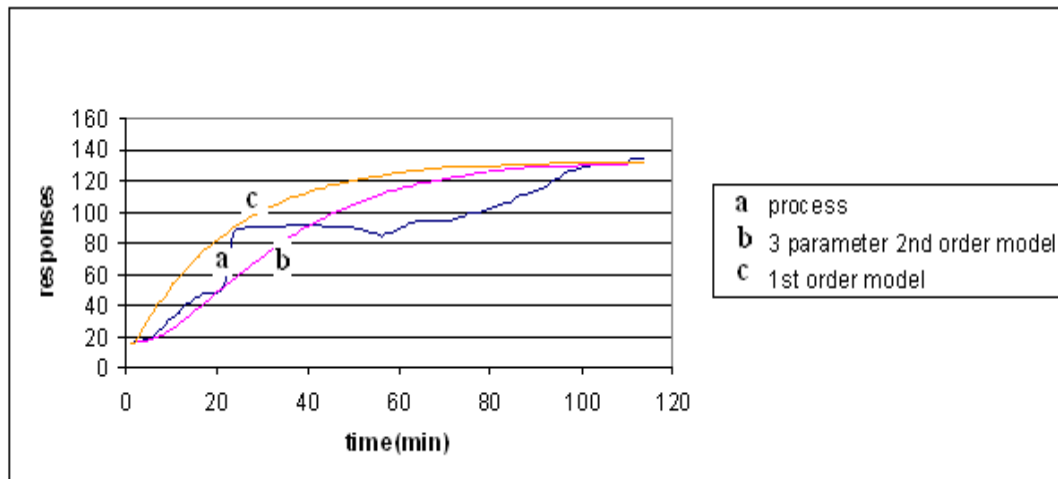


Figure 4.3: Responses of FOPDT and 3-term SOPDT models vs. system curve

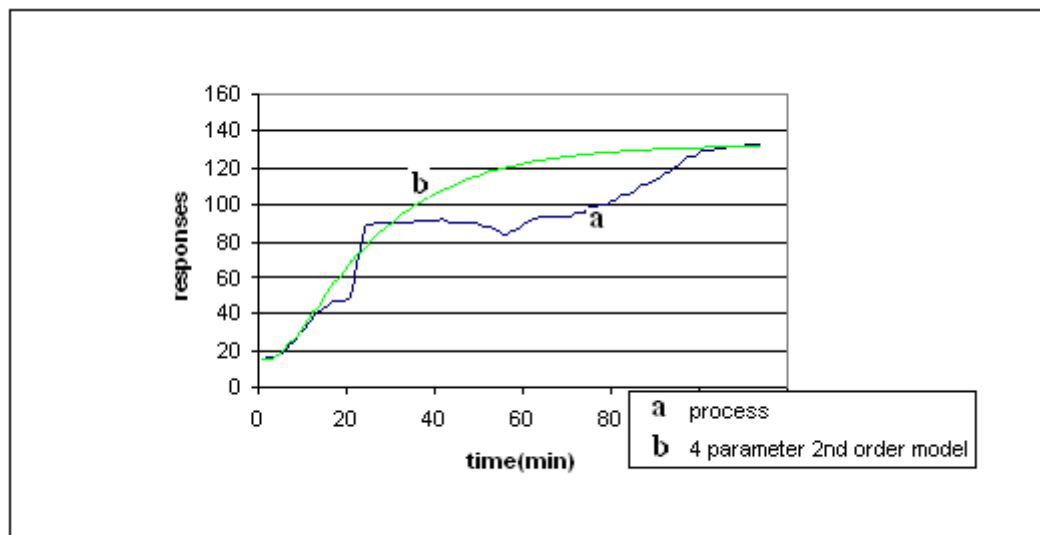


Figure 4.4: Process curve vs. four parameter second order model response

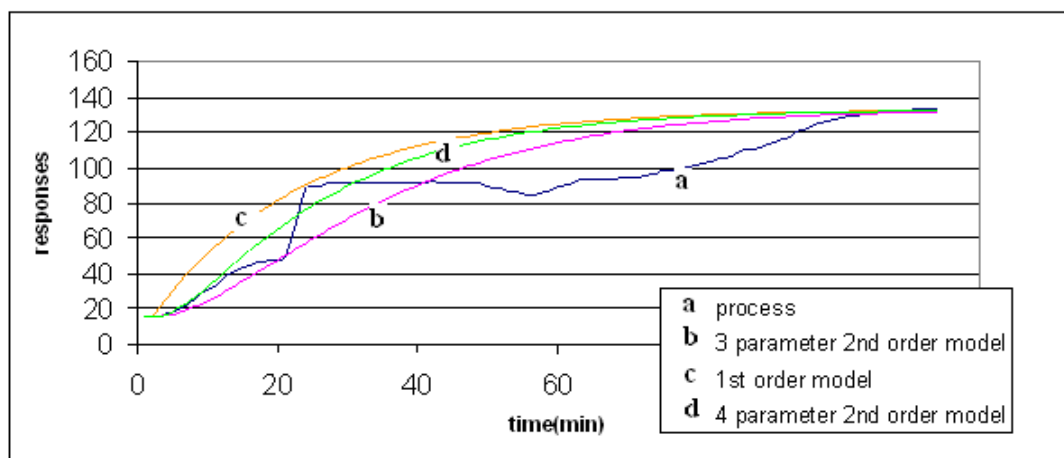


Figure 4.5: Comparative graphic of three different model curves with respect to representation success

4.2 Controller Design

The second step of the studies was designing various types of controllers in order to compare the performances of some specific alternatives.

4.2.1 IMC PID controller design

A PID type classical controller is designed with internal model control technique. Design calculations are conducted based on the first order model of the process in order to examine the resulting control performances at presence of a modeling error.

The delay term is approximated according to First Order Pade Approximation and the transfer function turned in to the form given in Equation 4.7.

$$P(S) = 0.187 * [(1-S)/(1+S)] / (21.72S + 1) \quad (4.7)$$

Filter transfer function is determined to be $f(S)$ and given in Equation 4.8.

$$f(S) = 1 / (t_f S + 1) \quad (4.8)$$

where t_f is filter time constant equal to 10.86 minutes that is half of process time constant.

By using Equations 4.9 to 4.13, transfer function of PID controller is determined as given in Equation 4.14.

$$P(S) = P^+(S) * P^-(S) \quad (4.9)$$

$$P^+(S) = (1-S)/(1+S) \quad (4.10)$$

$$P^-(S) = 0.187 / (21.72S + 1) \quad (4.11)$$

$$C(S) = f(S) / P^-(S) \quad (4.12)$$

$$C_{IMC}(S) = C(S) / [1 - C(S)*P(S)] \quad (4.13)$$

$$C_{IMC}(S) = [21.72 S^2 + 22.72S + 1] / [2.03S^2 + 2.40S] \quad (4.14)$$

The simulation of control environment is done by using MATLAB / Simulink program. The control loop that is created for this control study is given in Figure 4.6. The process block is characterized based on three parameter second order model of the real process equation of which was given previously in Equation 4.4.

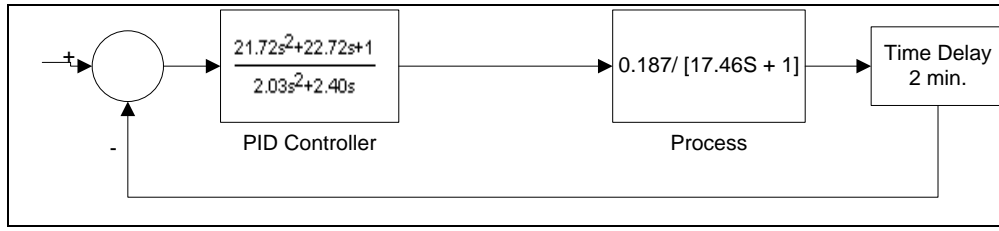


Figure 4.6: Closed loop control scheme with IMC PID controller

4.2.2 IMC fuzzy PID controller design

During these study, all non-self regulating and self regulating fuzzy IMC PID controllers are designed according to the first order models of relating second order processes. So, as it is seen above, “T” time constant values that are used in controller designs and self tuning rule preparation should always be understood as time constant of first order models rather than the ones of second order processes. This information is also valid for following sections of this study unless any other directive is introduced.

In Table 4.1, various second order transfer function time constants are given together with the first order model time constants representing themselves. Detailed information about studies conducted to provide these first order models can be obtained from Appendix - B.

Table 4.1: First order model time constants representing some second order transfer function time constants.

Second order process time constant	First order model time constant
25	38
5	8
2	3
30	49
3	5
10	16
15	24
4	7
17	21

Designing Fuzzy PID controllers by internal model control technique is a recently proposed idea [1]. According to this, input and output gain scales of Fuzzy controller are determined according to various equations major of which is composed of process parameters. These equations are given in Equations 4.15 to 4.20. In these equations; T: first order model time constant, L: delay time, t_c : filter time constant, K: process gain. In Figure 4.7, Fuzzy PID controller scheme and location of concerning scaling gains are shown.

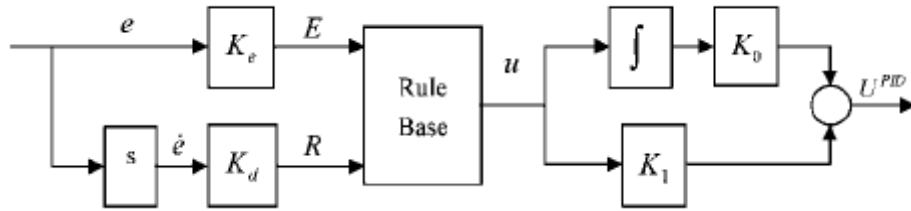


Figure 4.7: Fuzzy PID controller scheme [1].

$$K_e = 1 \quad (4.15)$$

$$K_d = K_e * \alpha \quad (4.16)$$

$$K_0 = (A/B) * \{1 / [K * K_e * (t_c + (L/2))]\} \quad (4.17)$$

$$K_1 = K_0 * \beta \quad (4.18)$$

$$\alpha = \min(L/2, T) \quad (4.19)$$

$$\beta = \max(L/2, T) \quad (4.20)$$

IMC Fuzzy PID controller design study for present process is made according to these proposed equations [1]. Again, the first order model is used as basis of controller design, since it is necessary to make performance comparison between fuzzy and classical IMC PID controllers. Related closed loop control scheme is given in Figure 4.8.

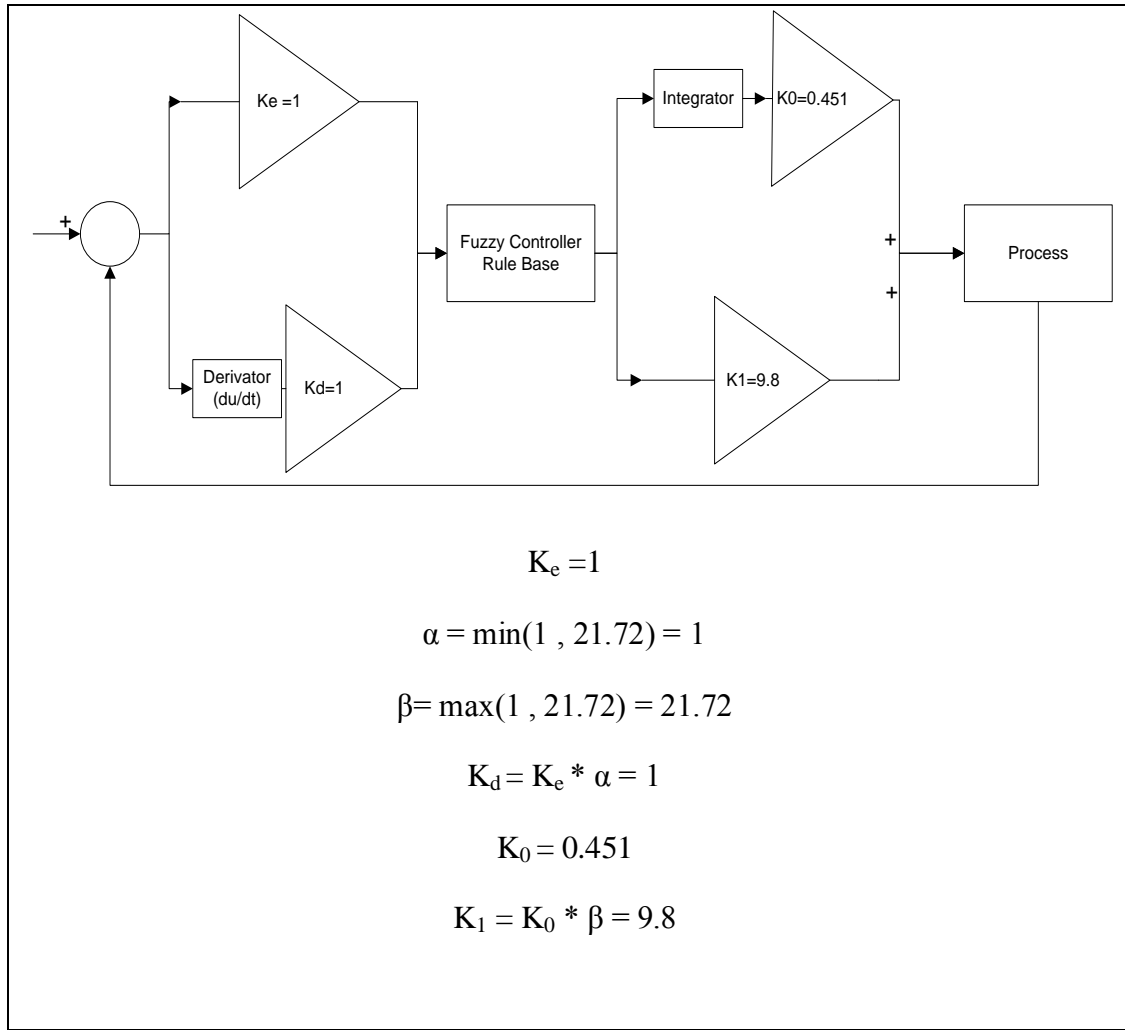


Figure 4.8: IMC Fuzzy PID control loop designed according to proposed internal model control technique.

The way to decouple α and β is mainly based on the desired control characteristics. As α gets smaller, the system response gets faster but this may end up with increasing overshoot. On the other hand, as α gets larger, system response becomes more sluggish but this can provide control action with a more certain settling performance [1].

To make a fair comparison between these two decoupling choices, one more controller with maximum α and minimum β is also investigated in this section. Figure 4.9 shows the closed loop created for this alternative controller.

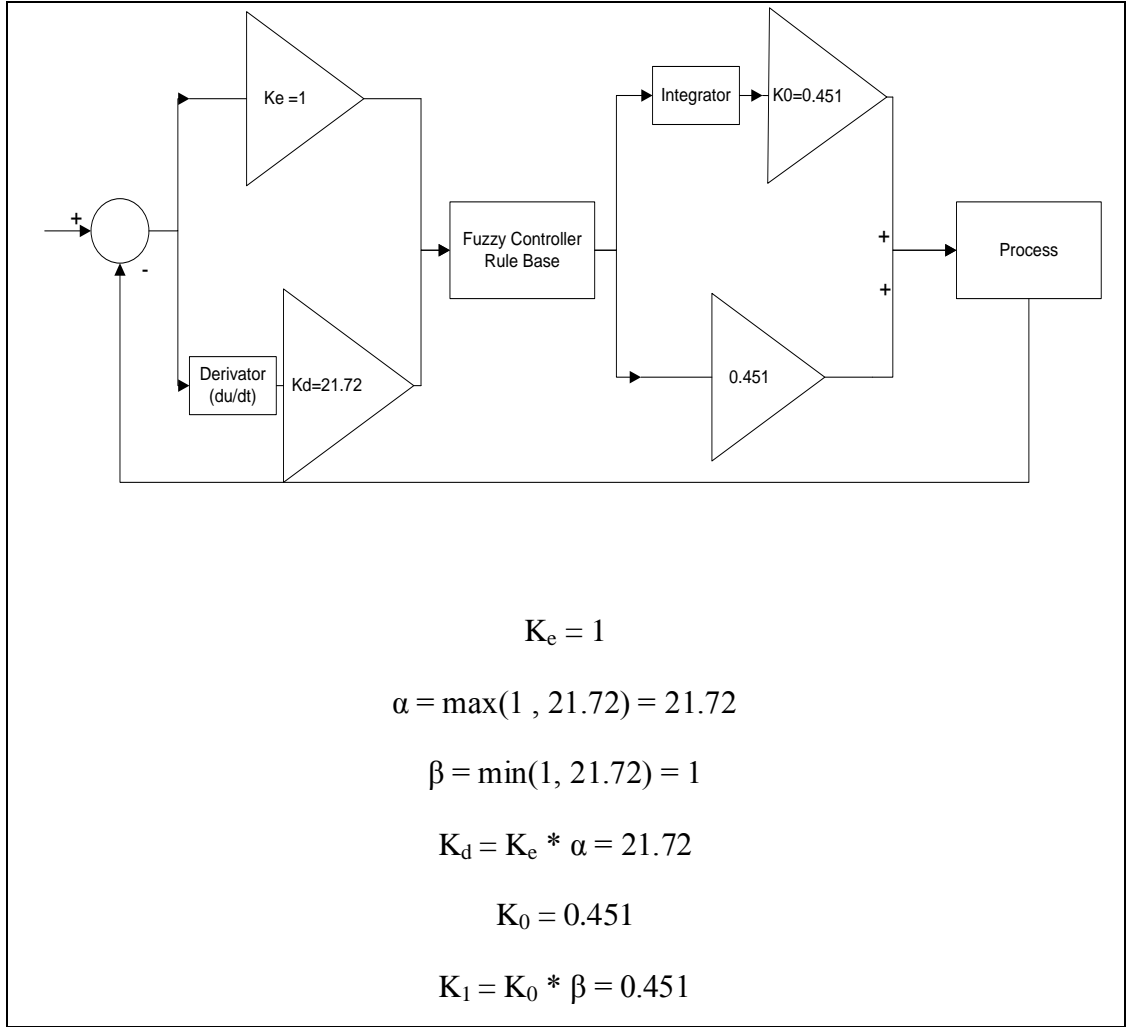


Figure 4.9: Closed loop scheme for IMC Fuzzy PID controller with alternatively decoupled $\alpha - \beta$.

The controllers that are designed in this study are integrated with same process in order to investigate their performances and make proper comparison. The diagram that includes all three control schemes is given in Figure 4.10.

Step response of each system is observed. The proposed IMC Fuzzy PID controller and classical IMC PID controller resulted in very similar performances while the fuzzy controller with larger α and smaller β maintained larger rise time but smaller overshoot and settling time. Step responses and controller efforts concerning all three loops are shown in Figure 4.11 and 4.12, respectively.

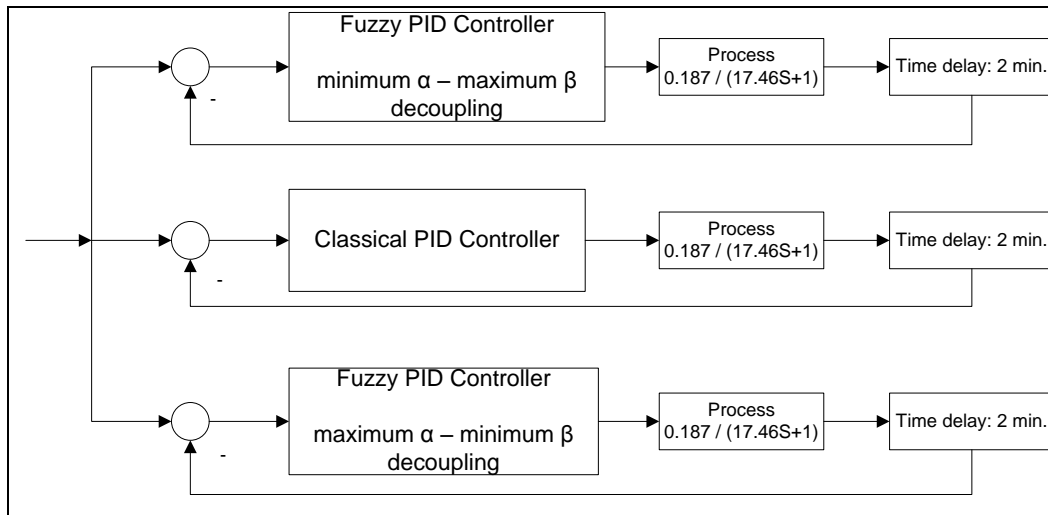


Figure 4.10: Proposed Fuzzy IMC PID, classical IMC PID, and alternative Fuzzy IMC PID controllers integrated with identical processes.

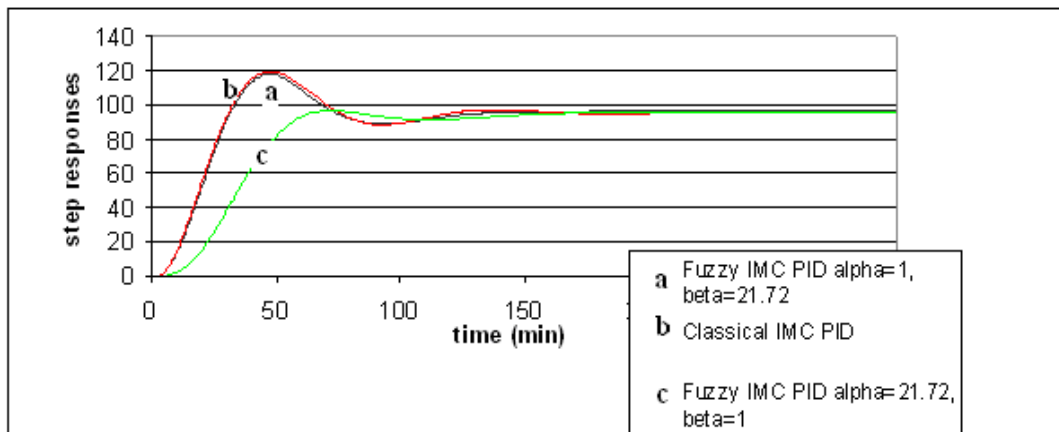


Figure 4.11: Comparative step response graphics of mentioned systems.

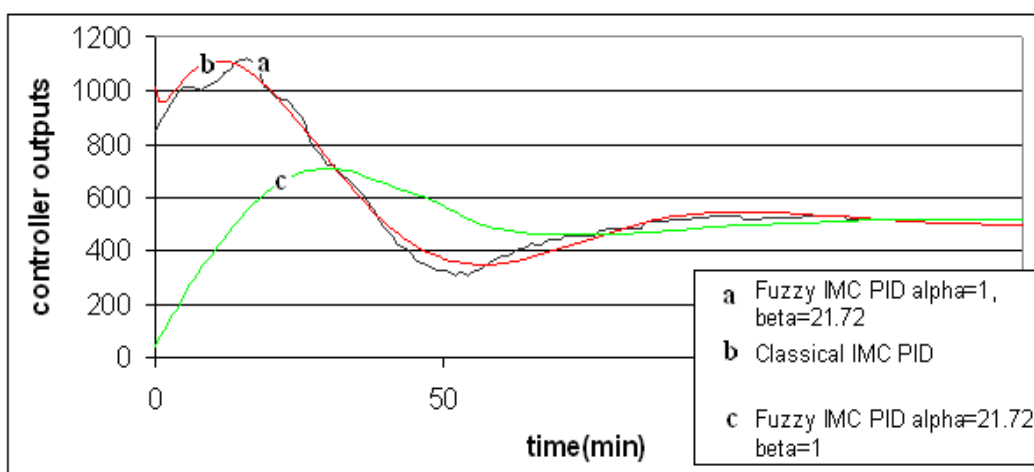


Figure 4.12: Effort diagrams of designed controllers (heating power in terms of kW).

5. SIMULATION: STRATEGIES FOR SELF TUNING FUZZY IMC PID CONTROLLER

5.1 Searching For Alternative Scaling Factors

As it is seen in previous section, smaller α and larger β selection makes the system response faster but causes some overshoot while larger α and smaller β provides more sluggish response but smaller settling time with much less overshoot. Starting off from this situation, one may think that it may be possible to find an intermediate answer which may include characteristics of both above. In order to achieve the best possible result, a series of trials all of that concerns to different α - β combinations are conducted for the process under investigation. The step responses for all the variations that are examined are given in Figures 5.1 to 5.8.

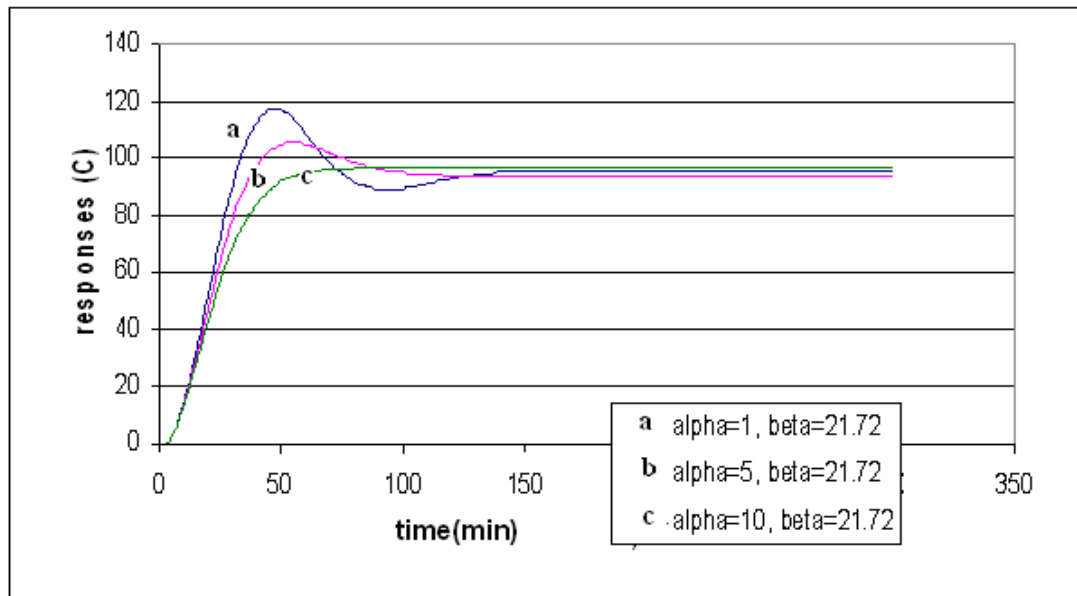


Figure 5.1: Step responses for cases $\alpha=1, 5, 10$; $\beta=21.72$

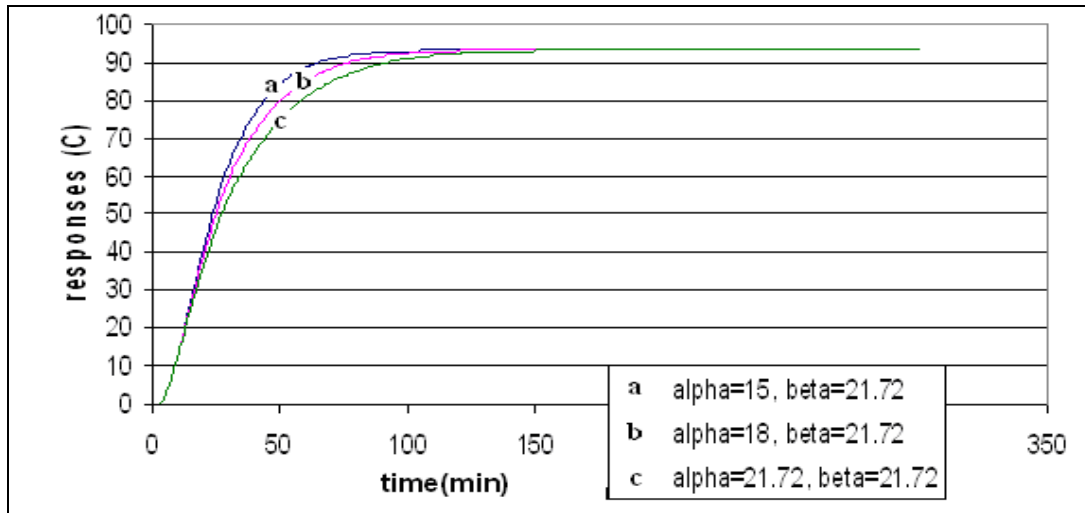


Figure 5.2: Step responses for case $\alpha= 15, 18, 21.72$; $\beta=21.72$

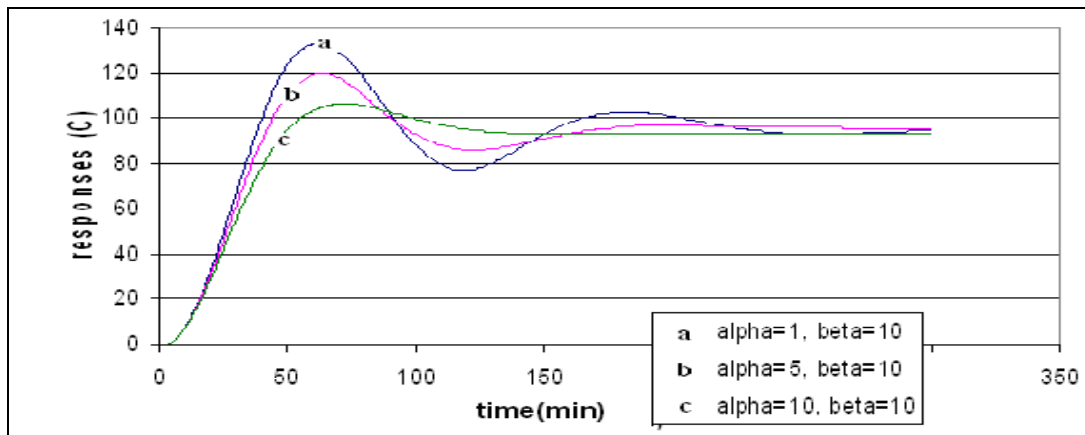


Figure 5.3: Step responses for cases $\alpha= 1, 5, 10$; $\beta= 10$

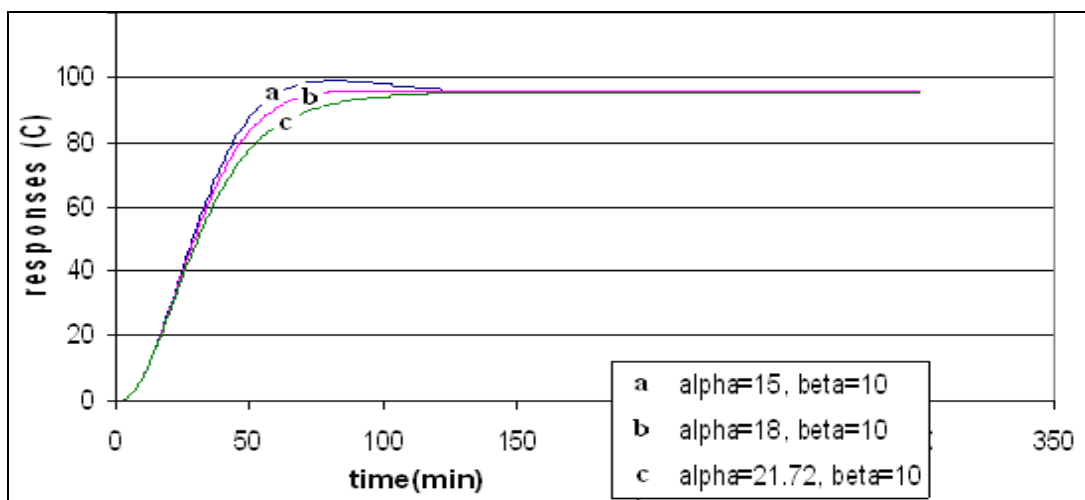


Figure 5.4: Step responses for cases $\alpha= 15, 18, 21.72$; $\beta= 10$

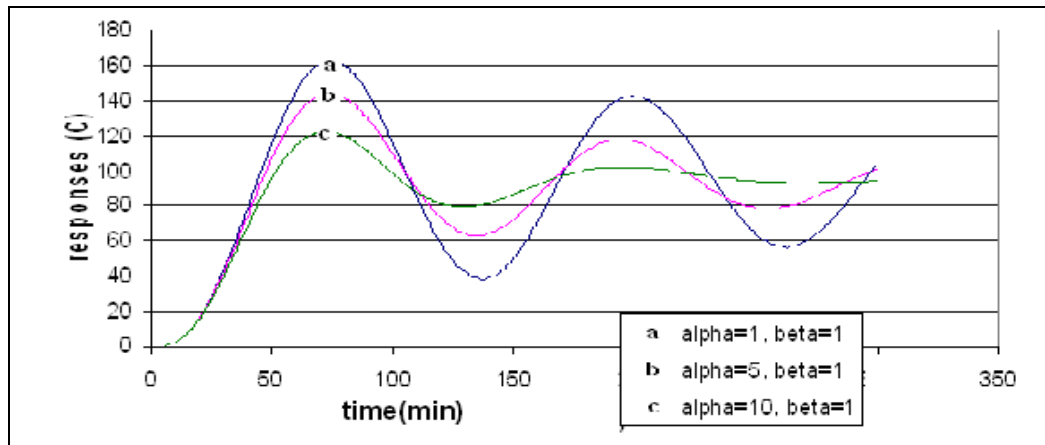


Figure 5.5: Step responses for cases $\alpha=1, 5, 10$; $\beta=1$

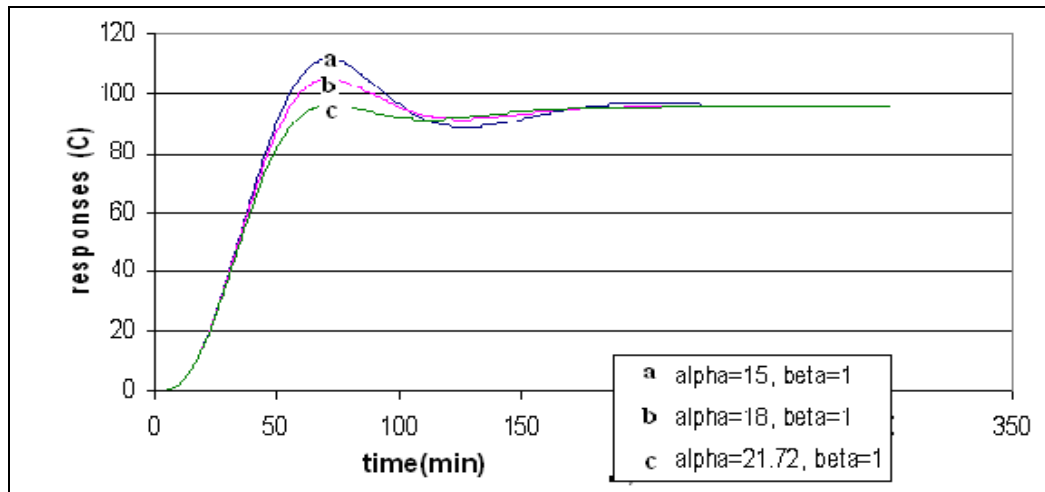


Figure 5.6: Step responses for cases $\alpha=15, 18, 21.72$; $\beta=1$

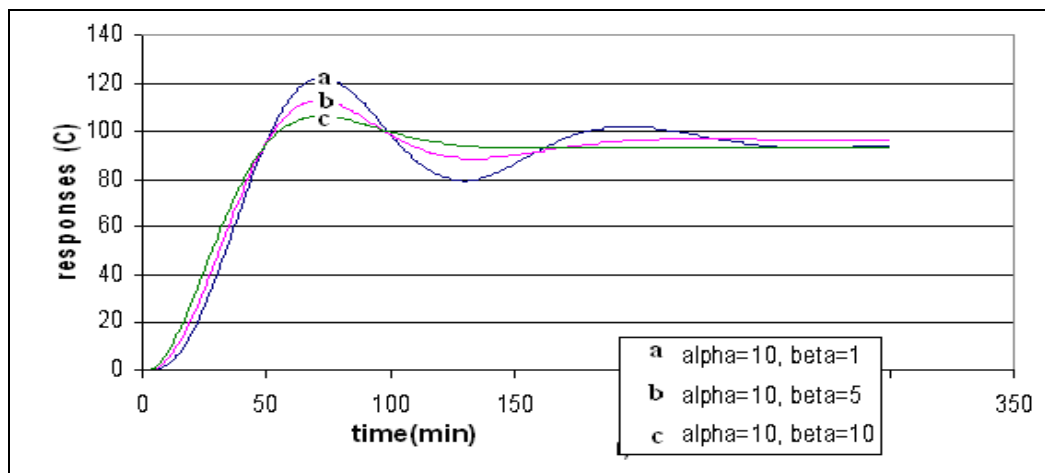


Figure 5.7: Step responses for cases $\alpha=10$; $\beta=1, 5, 10$

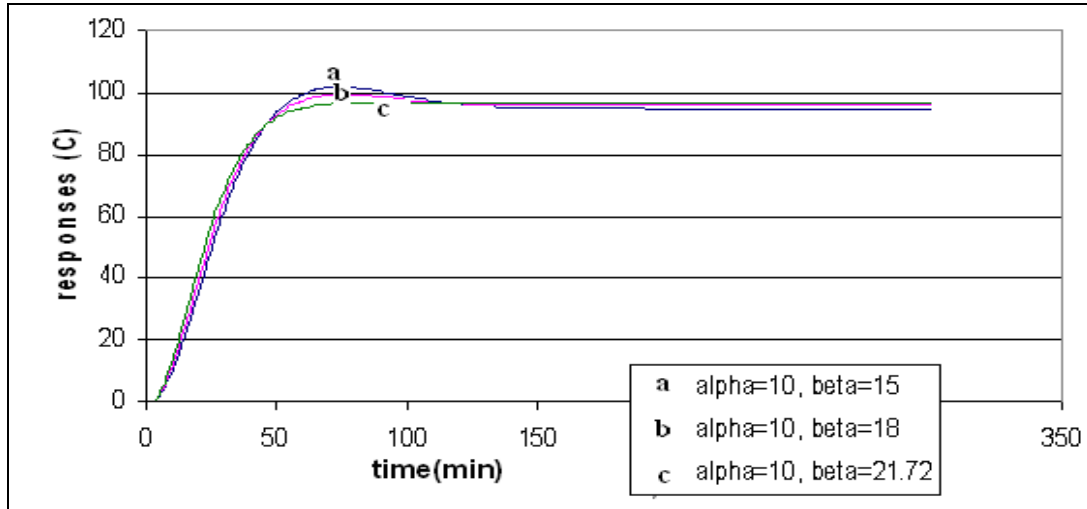


Figure 5.8: Step responses for cases $\alpha=10$; $\beta=15, 18, 21.72$

According to step response graphics, when the α (α) is increased gradually and β (β) is kept constant, system response is getting slower at the beginning but it shows less overshoot and a better settling. The same α values are coupled with different β values in Figures 5.1 to 5.6 and it is observed that, the same behavior is kept with slightly increasing overshoot tendency with decreasing β values. The overshoot is witnessed to reach its maximum for $\alpha = \beta = 1$.

On the other hand, when β is increased gradually and α is kept constant, the results are observed to be like the ones in Figures 5.7 and 5.8. In the increasing β cases, the constancy of α value keeps transient part of the response in unity. For 6 different β values, the first response behaviors are very close to each other but after the response reaches to the set point for the first time (after rise time) the systems with smaller β values show much larger overshoots.

It is important here to mention that, while the increments or decreasing of α value affects the rise time in great proportions and slightly affects the overshoot behavior, the changes in β causes nearly zero effect for rise time though it very strongly manipulates overshoot amplitudes.

To make a proper selection between all these alternatively coupled $\alpha - \beta$ sets, it is important to watch the responses with partial priorities. For the transient part of response, the faster rise time is the most important aspect to be satisfied. So the configuration with $\alpha=1$ and $\beta=21.72$ seems to be the best choice since it shows the smallest rise time among all others. On the other hand, for the steady state part of the response, best settling and smallest overshoot is vital. So the configuration with $\alpha=10$

and $\beta=21.72$ that shows best settling performance with no overshoot could be named as the best candidate for concerning situation.

On the other hand, error indexes show that, the configuration with $\alpha=5$ and $\beta=21.72$ gives the most appropriate results according to ISE and ISTE and ITAE calculations. Although $\alpha=15$, $\beta=10$ configuration gives smallest ITAE result, overall examination of all three index results mention the success of $\alpha=5$ - $\beta=21.72$ configuration. Error index results are given in Table 5.1.

Table 5.1: Error index results for control systems with various α - β combinations.

Alpha (α)	Beta (β)	ISE (10^5)	ISTE (10^6)	ITAE (10^4)
1,00	21,72	1,423	1,726	9,460
5,00	21,72	1,418	1,501	8,809
10,00	21,72	1,496	1,675	10,360
15,00	21,72	1,595	2,028	12,650
18,00	21,72	1,684	2,347	13,720
21,72	21,72	1,822	2,884	15,570
1,00	10,00	2,208	5,894	28,650
5,00	10,00	1,942	3,414	17,060
10,00	10,00	1,900	2,722	14,060
15,00	10,00	1,918	2,551	6,708
18,00	10,00	1,961	2,710	9,617
21,72	10,00	2,048	3,037	8,913

In the previous section, transient and steady state responses of various combinations were compared and the most appropriate configurations were chosen. In this section,

the configurations with best performances are desired to be combined by a self tuning strategy in order to achieve the best possible overall system response. With the other words, the transient performance of $\alpha=1 - \beta=21.72$ system and steady state performance of $\alpha=10$ or $5 - \beta=21.72$ system is planned to be combined to make system response rise fast and also settle well.

5.2 Double Step Adjustment Of Alpha (α)

In order to create global rules that will be true for various processes with different parameters such as time constant and delay time, the selection of boundaries between different control equations and parameters of these equations must be generalized based on system parameters.

In this section, the value of alpha (α) will become partially independent of specific functions and totally become dependent only on process parameters. The strategy for this section is defined with following rules:

If	(error/input) = u > 0.37,	then	$\alpha = \min (T, L/2)$
Else if	u > 0.01,	then	$\alpha = 0.5 * \max(T, L/2)$
Else		then	$\alpha = \max(T, L/2)$

As it is seen from above equations, the limiting error values 0.37 and 0.01 are still arbitrary but selection of α values are based on system parameters. While some parts of this selection could be treated as global, the boundary values defining function ranges and “0.5 of the max” rule can not be accepted global since they could be changed independent of system properties. In the following part, two different comparative control schemes with two different process parameters will be examined to show effectiveness of mentioned control strategy.

First comparison is conducted for primary process with given transfer function:

$$P(S) = [0.187 / (17.46S + 1)^2] * e^{-2s} \quad (\text{from Eq. 4.4})$$

Block diagram of whole simulation is given in Figure 5.9.

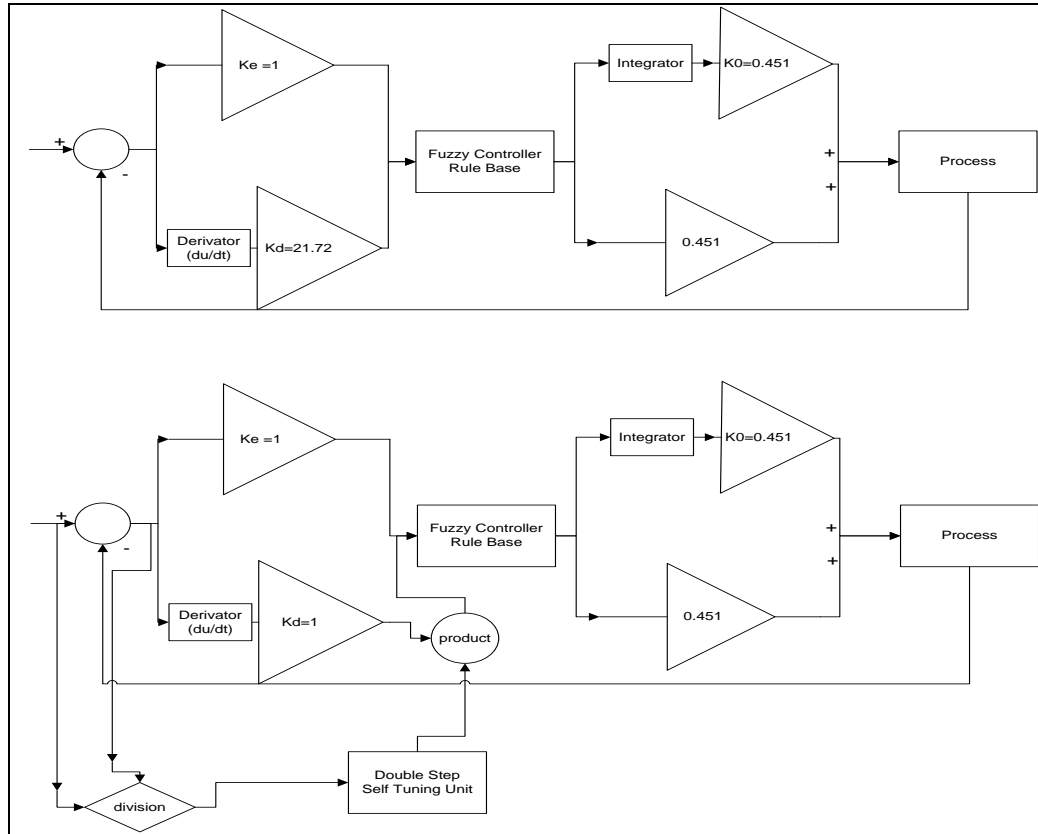


Figure 5.9: Block diagram showing classical Fuzzy IMC PID and double step self tuning schemes.

The step responses are given in Figure 5.10.

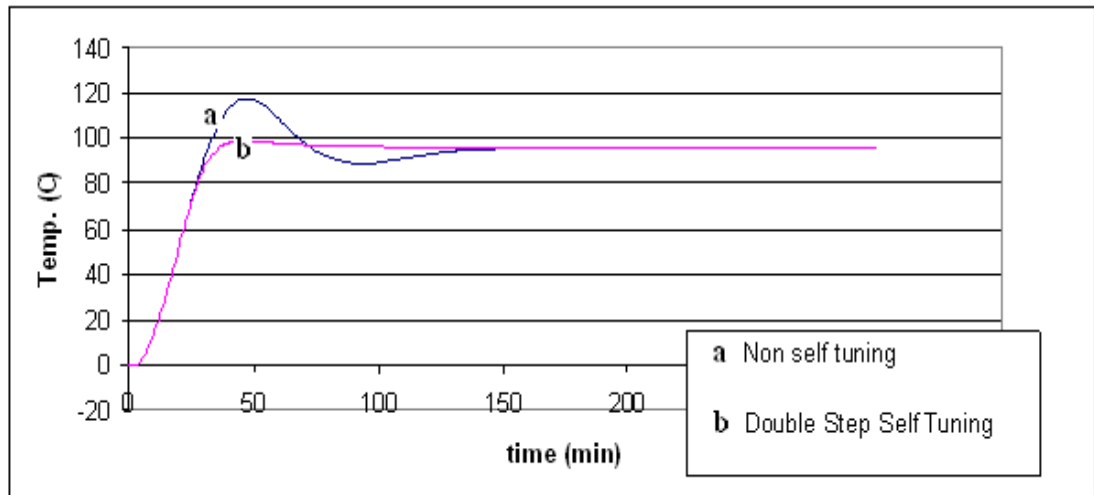


Figure 5.10: Step responses of non self tuning and double step self tuning systems.

Second comparison study is conducted for an alternative process with following transfer function:

$$P(S)= 0.0708/ (120S + 1)^2 * e^{-18S} \quad (5.1)$$

Step responses for this study are given in Figure 5.11.

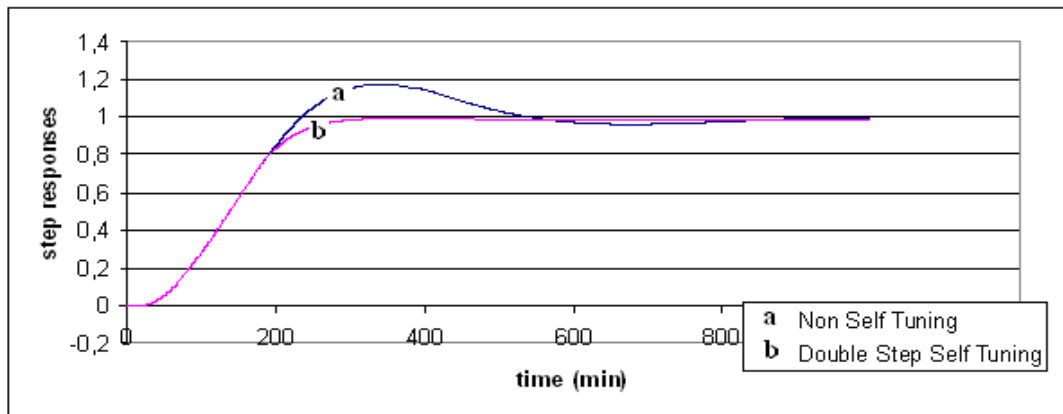


Figure 5.11: Step responses of two control schemes for alternative process model.

The performance comparison is made by calculating Integrated Time Weighted Square of Error index and results are given in Table 5.2.

Table 5.2: ITSE error indexes of non-self tuning and self tuning control schemes for primary and alternative process models.

ISTE	Scheme 1 non self tuning	Scheme 2 self tuning
Primary process model	$1.726 * 10^6$	$1.208 * 10^6$
Alternative process model	8377	6844

As it is obviously seen from step responses and error tables, double step self tuning Fuzzy IMC PID controller scheme gives better results compared to its non-self tuning type for time constant dominant second order systems.

On the other hand, these results yet can not be generalized for all kinds of processes since characteristic reactions of delay dominant processes or higher or lower order process can not be foreseen yet.

5.3 Overshoot Ratio Based Self Tuning Fuzzy IMC PID Controller

The control strategy that will be explained in this section is different from the one mentioned in Section 5.2 with its property of being far more independent of arbitrary constants and boundary values.

In this strategy; control action can be divided in to 2 steps:

On the first step, process to be controlled is connected to non-self regulating controller and system is run for once. The step response of this scheme is examined and the first overshoot peak value is sampled. This value is divided with input signal value and OSR ratio is obtained:

$\text{OSR} = \text{overshoot} / \text{input}$
--

On the second step, OSR ratio is used in order to produce self tuning rules and boundaries as follows:

If	error / input (u) > $\sqrt{\text{OSR}}$	then	$\alpha = \min (L/2, T)$
Else if	u > $(\text{OSR})^2$	then	$\alpha = \sqrt{\text{OSR}} * \max (L/2, T)$
Else		then	$\alpha = \max (L/2, T)$

The idea behind this configuration is to define the boundary value of u at which α will be increased from a minimum level to a higher one according to the response of non self tuning system. According to this, systems with higher response times and larger overshoots will be introduced with an earlier adjustment of α while the systems that give smaller overshoot, which corresponds to a faster response, will be controlled by a later adjustment of α . In other words, for faster responding systems, tuning action will be fired in ranges respectively closer to the set point compared to those defined for slower ones.

Simulation studies are made in order to examine the effectiveness of this strategy. Among these, the processes with different time constant values and time delay

properties are used to understand the operation limits of the control rules associated with this strategy.

- Simulation 5.1: $P(S) = [0.187 / (17.46S + 1)^2] * e^{-2S}$ (Primary process model)

Step response of non self tuning controller for this process was given in Figure 4.11.

It is seen from that graph that, OSR for this loop can be calculated as:

$$OSR = (118 - 95) / 95$$

$$OSR = 0.242$$

$$\sqrt{OSR} = 0.492$$

$$(OSR)^2 = 0.0586$$

The step response graphic of proposed self tuning controller is given in Figure 5.12.

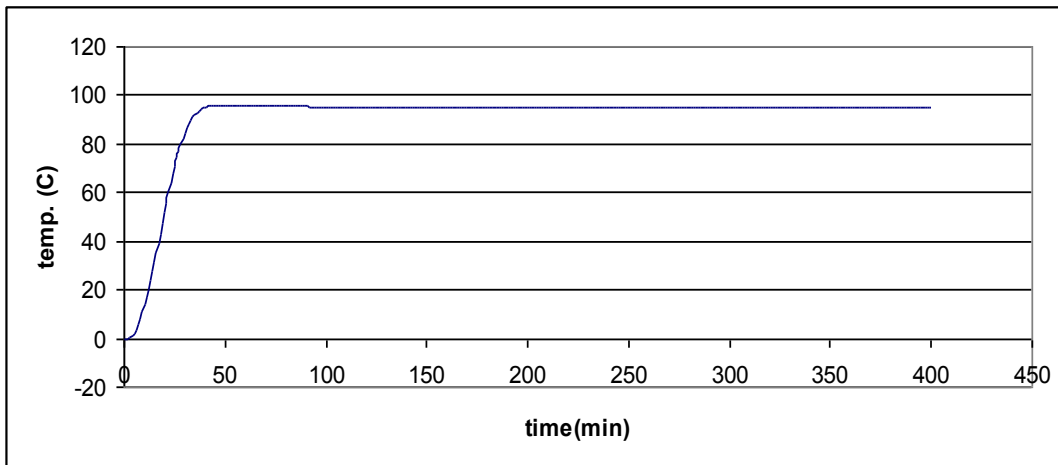


Figure 5.12: Step response of primary process model with overshoot based double step self tuning controller.

Figure 5.13 shows block diagram of overshoot based double step self regulating control scheme for primary process model.

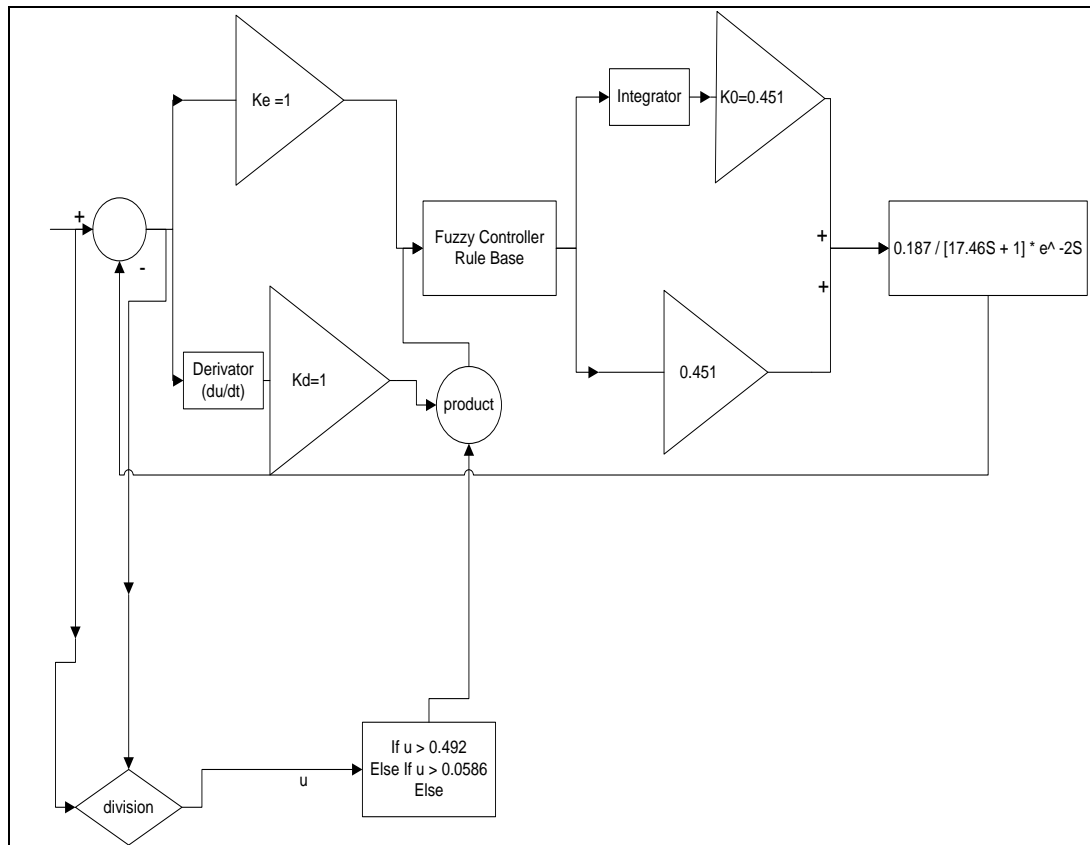


Figure 5.13: Double step self tuning scheme for primary process model.

The comparative results of step tests conducted on various processes are shown in Figures 5.14 - 5.23.

- Simulation 5.2: $P(S) = [3 / (2S + 1)^2] * e^{-0.1S}$

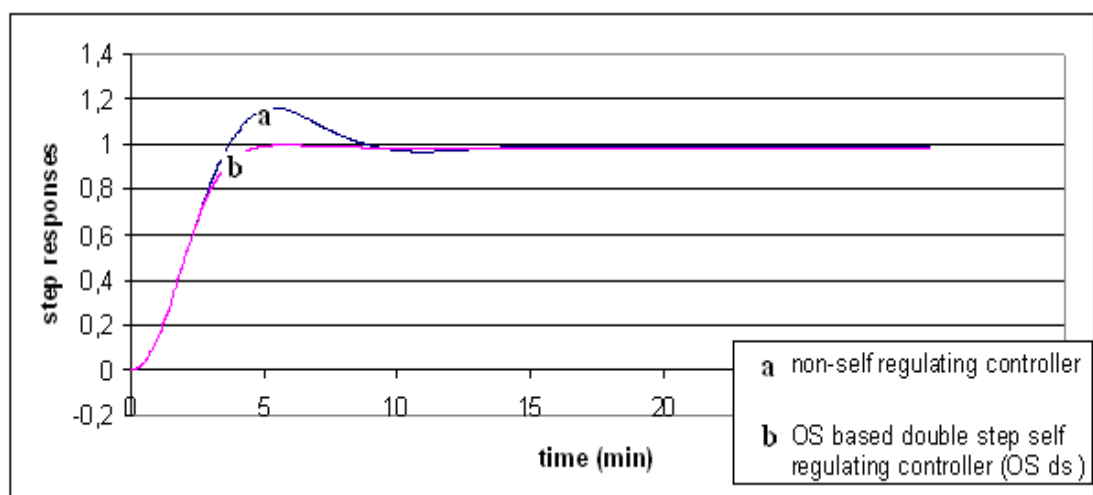


Figure 5.14: Step responses for process in simulation 5.2.

- Simulation 5.3: $P(S) = [0.0708 / (120S + 1)^2] * e^{-18S}$

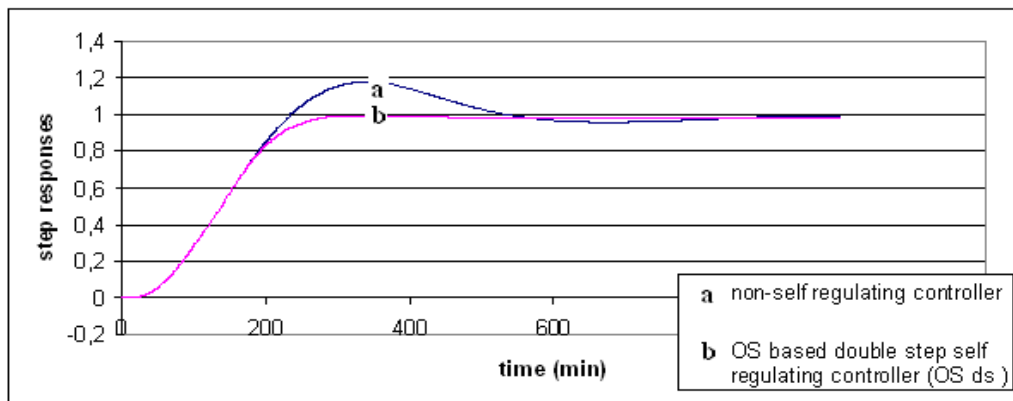


Figure 5.15: Step responses for process in simulation 5.3.

- Simulation 5.4: $P(S) = [3 / (5S + 1)^2] * e^{-2S}$

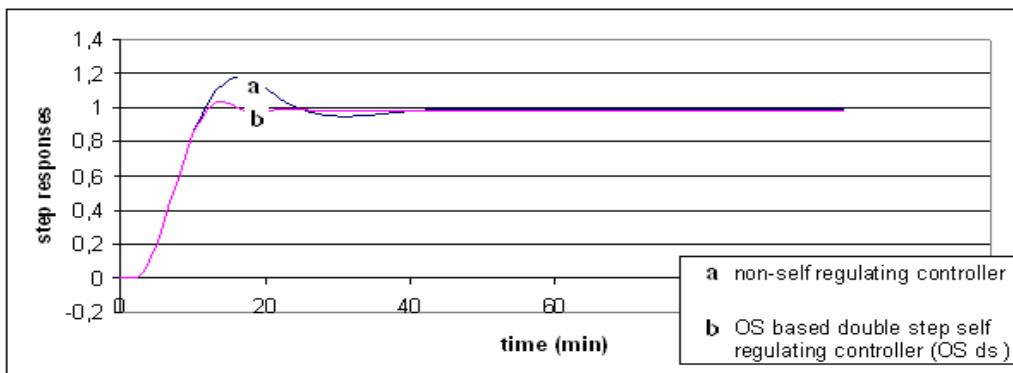


Figure 5.16: Step responses for process in simulation 5.4.

- Simulation 5.5: $P(S) = [1 / (25S + 1)^2] * e^{-14S}$

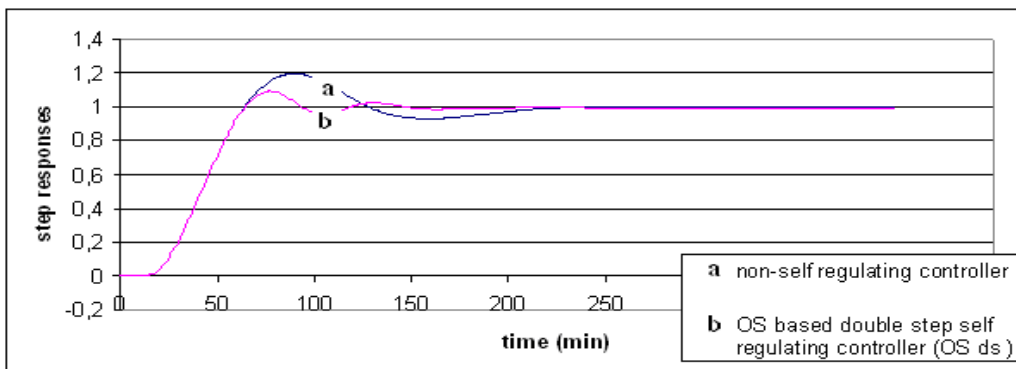


Figure 5.17: Step responses for process in simulation 5.5.

- Simulation 5.6: $P(S) = [1 / (25S + 1)^2] * e^{-19S}$

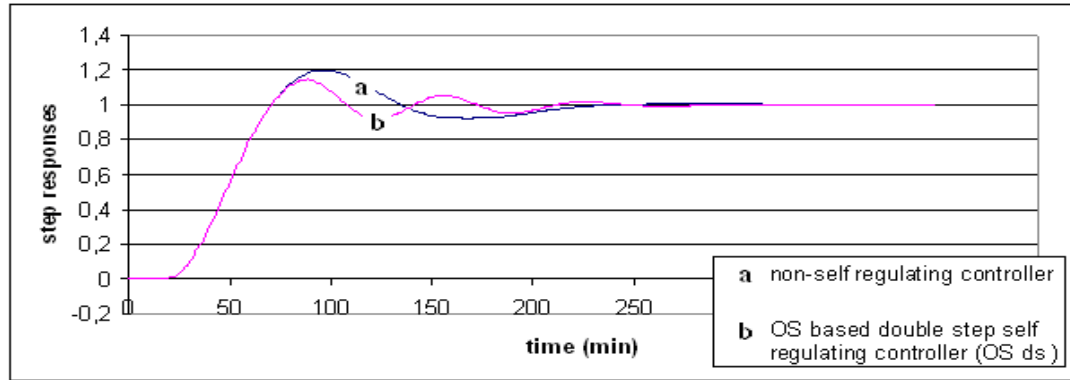


Figure 5.18: Step responses for process in simulation 5.6.

As it could be seen from the graphic results in Figures 5.14 – 5.21, proposed self tuning rules are successful for a specific range of process parameters. On the other hand, especially the results in Figures 5.22 and 5.23 show that, for some processes the proposed strategy shows negative effect on control performance.

The limiting case, beyond which the proposed OSR based double step self tuning control scheme can not perform well is then defined as follows:

OSR based double step self tuning control scheme performs well and enhances control performance if:

$$R=[L/(L+T)] < 0.33 \quad (5.2)$$

- Simulation 5.7: $P(S) = [0.4 / (15S + 1)^2] * e^{-14S}$

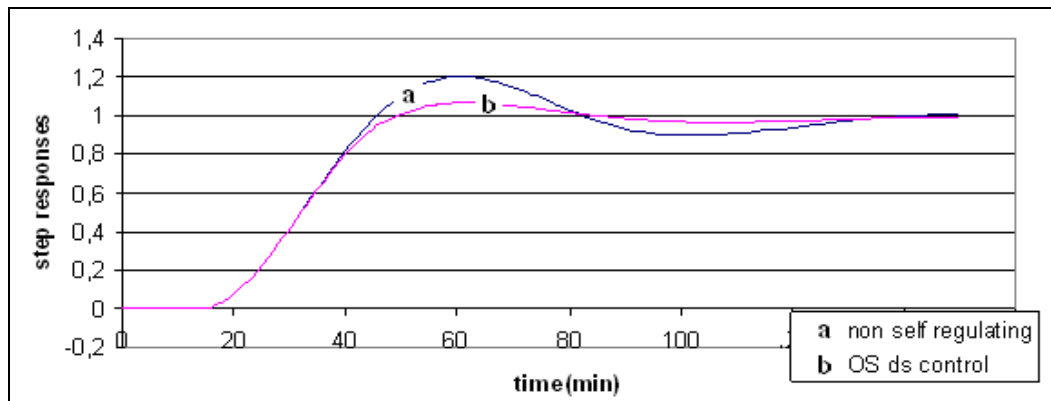


Figure 5.19: Step responses for process in simulation 5.7.

- Simulation 5.8: $P(S) = [1 / (25S + 1)^2] * e^{-20S}$

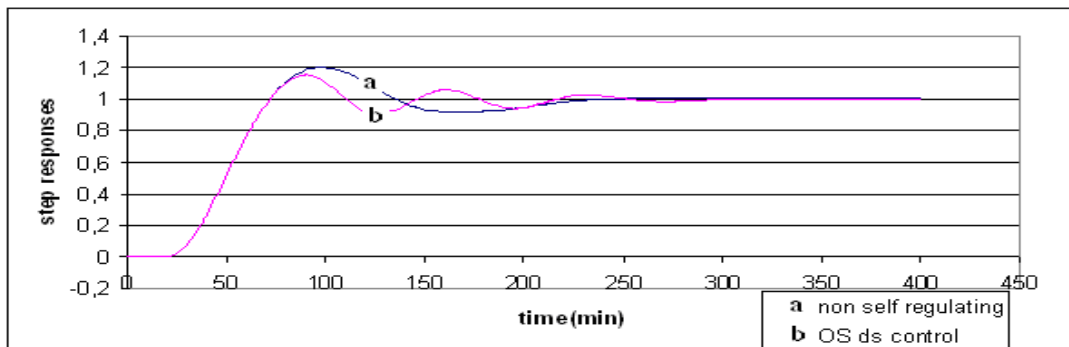


Figure 5.20: Step responses for process in simulation 5.8.

- Simulation 5.9: $P(S) = [1 / (25S + 1)^2] * e^{-25S}$

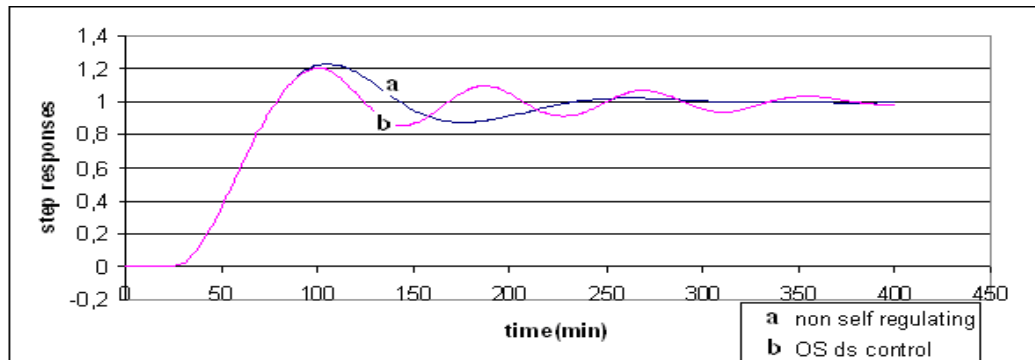


Figure 5.21: Step responses for process in simulation 5.9.

- Simulation 5.10: $P(S) = [5 / (10S + 1)^2] * e^{-20S}$

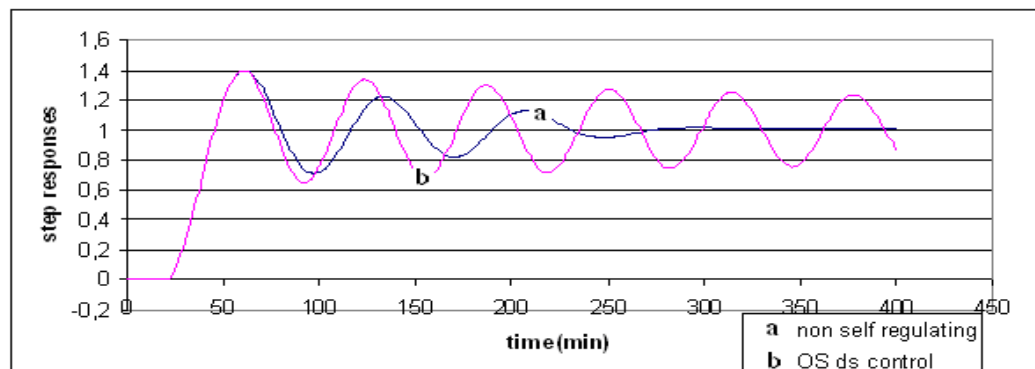


Figure 5.22: Step responses for process in simulation 5.10.

- Simulation 5.11: $P(S) = [3 / (5S + 1)^2] * e^{-6S}$

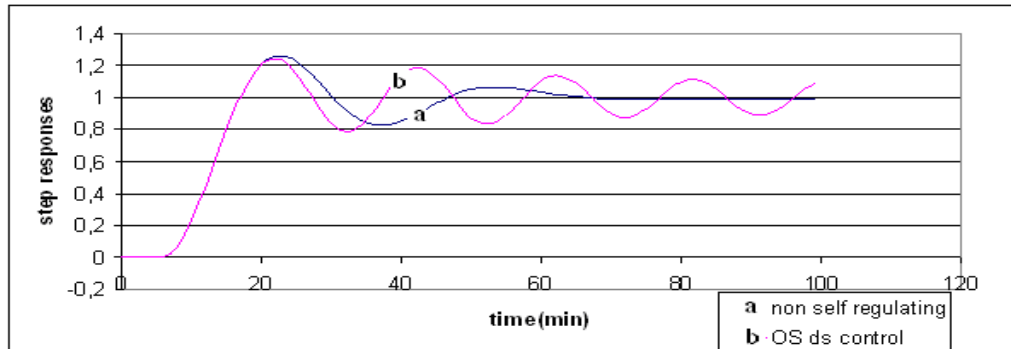


Figure 5.23: Step responses for process in simulation 5.11.

Where; L is time delay of process and T is first order model time constant representing second order process. (For detail, investigate on Table 4.1.)

If ratio “ R ” goes beyond the mentioned boundary 0.33, then the advantage introduced by OSR based self tuning controller gets weaker gradually and as R goes beyond 0.5~0.6, self tuning controller begins to show very unacceptable effect and corrupts overall system performance as it is seen in Figures 5.22 and 5.23.

6. MULTI-REGION SELF TUNING FUZZY IMC PID CONTROLLERS

6.1 Six Region Self Tuning Fuzzy IMC PID Control Based On “R” Data

The control strategy proposed in Section 5.3 takes the overshoot data of non-self tuning controller as basis and conducts calculations and decision makings according to the ratio of overshoot to input value. With its property of being totally independent of arbitrary coefficients and boundary values, it could be regarded as a kind of improvement over other previous control strategies.

On the other hand, since this technique requires reading of non-self regulating controller data, it is somehow dependent to another control scheme from its very foundation. This naturally makes this strategy be regarded as a half-manual / half automatic one because it still needs the observation and decision making of control operator.

In order to maintain some more improvement, it will be necessary to make the whole procedure independent of any other control scheme operation and resulting data. Thus, another strategy will be proposed in this section. This strategy is about reading directly the parameters of the process that will be controlled rather than overshoot data of non-self regulating control data.

The basic idea under this technique is reading time constant (T) and delay time (L) values associated with relevant process and calculating the characteristic ratio of “ $R=L/(L+T)$ ”. After this step, procedure includes deciding in to which range the value of R corresponds to and use specific functions that are already set up for each individual range. The important point here is; all of these functions have a common property of having “ $R=L/(L+T)$ ” data as the only independent variable. The procedure of this control strategy is more briefly given at the following list.

- Read process data.
- Learn about numerical values of T: time constant and L: delay time.

- Calculate the ratio $R=L/(L+T)$.
- Learn the range to which the “R” corresponds.
- Use matching functions and decision boundaries for self tuning of alpha (α).

Table 6.1: Scaling ranges and concerning control rules for six region self tuning Fuzzy IMC PID control

Scaling Ranges for $R=L/(L+T)$

	0,1	0,33	0,40	0,67	
	a	b	c	d	e
Case a	<div>If $u > \sqrt{R}$ then $\alpha = \min (L/2,T)$ Else if $u > R$ then $\alpha = \sqrt{R} * \max(L/2,T)$ Else then $\alpha = \max (L/2,T)$</div>				
Case b	<div>$k=0,33-R$ If $u > \sqrt{k}$ then $\alpha = \min (L/2,T)$ Else if $u > k$ then $\alpha = \sqrt{k} * \max(L/2,T)$ Else then $\alpha = \max (L/2,T)$</div>				
Case c	<div>$t=0,67-R$ If $u > \sqrt{t}$ then $\alpha = \min (L/2,T)$ Else then $\alpha = \sqrt{t} * \max (L/2,T)$</div>				
Case d	<div>$p=1-R$ If $u > \sqrt{p}$ then $\alpha = \max (L/2,T) / \sqrt{p}$ Else then $\alpha = \min (L/2,T) * \sqrt{p}$</div>				
Case e	<div>$\alpha = 0,67 * [L/2=T]$</div>				

The idea based on which the algorithms of this strategy developed is same with that of the previous one that works based on overshoot data. Since “R” value gets bigger gradually by dominance of time delay over time constant, it is fair to mention that, as the time constant “T” loses its effectiveness over system, “R” gets larger. So, the tuning action of alpha (α) should be fired in rather closer ranges to the set point as the value of “R” gets larger because it points to another relational phenomenon that system time constant becomes less effective over the general behavior and system response grows faster. So, tuning alpha in closer ranges to the set point will be more reasonable since it will avoid over damping without causing overshoot also. Besides

that, all this theory is applicable for the opposing cases in which the time constant gets more effective and “R” gets smaller.

The list of ranges and corresponding functions, boundaries together with relating control rules are given in Table 6.1.

For each individual range for R value, numerous simulation studies are made with processes having different T, L and R parameters. Comparative graphical step testing results of each of these studies are given in Figures 6.1 – 6.18.

- Simulation 6.1 (Primary Process Model): $P(S) = [0.187 / (17.46S + 1)^2] * e^{-2s}$
T=21.72, R=0.0843

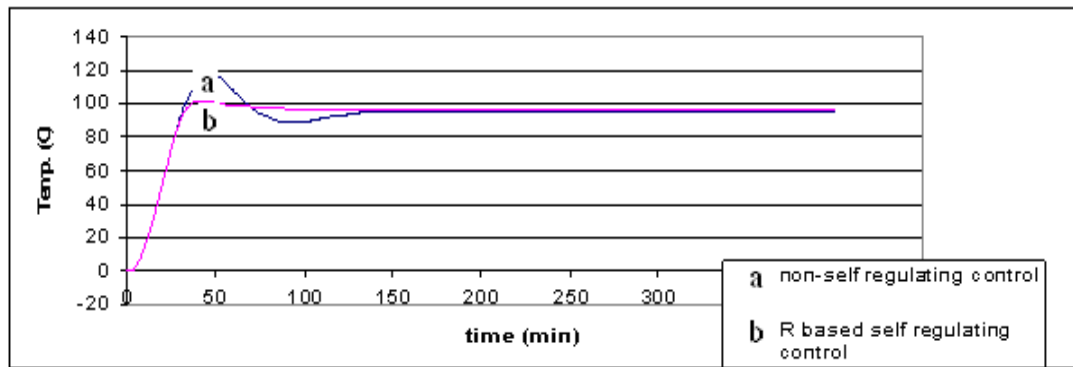


Figure 6.1: Step responses for process in simulation 6.1.

- Simulation 6.2: $P(S) = [3 / (2S + 1)^2] * e^{-0.1s}$
T=3, R=0.0323

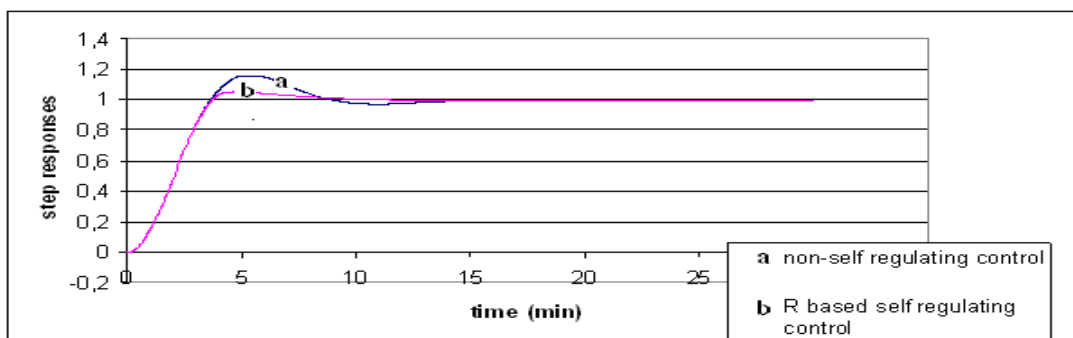


Figure 6.2: Step responses for process in simulation 6.2.

- Simulation 6.3: $P(S) = [0.0708 / (120S + 1)^2] * e^{-18s}$

T=180, R=0.091

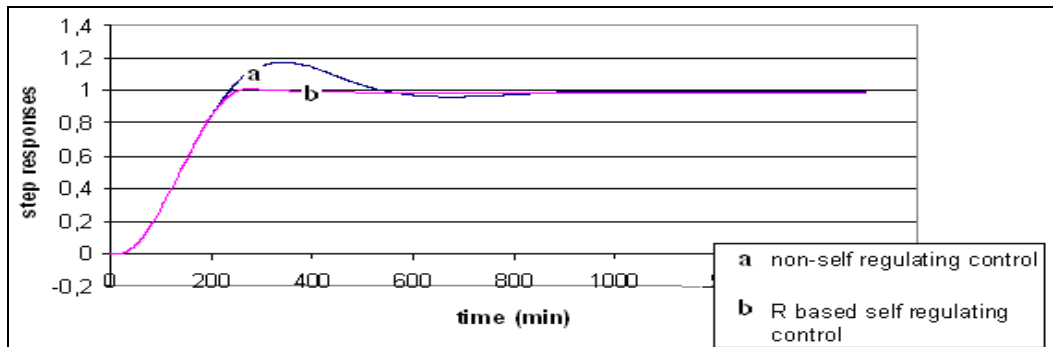


Figure 6.3: Step responses for process in simulation 6.3.

- Simulation 6.4: $P(S) = [3 / (5S + 1)^2] * e^{-2s}$

T=8, R=0.2

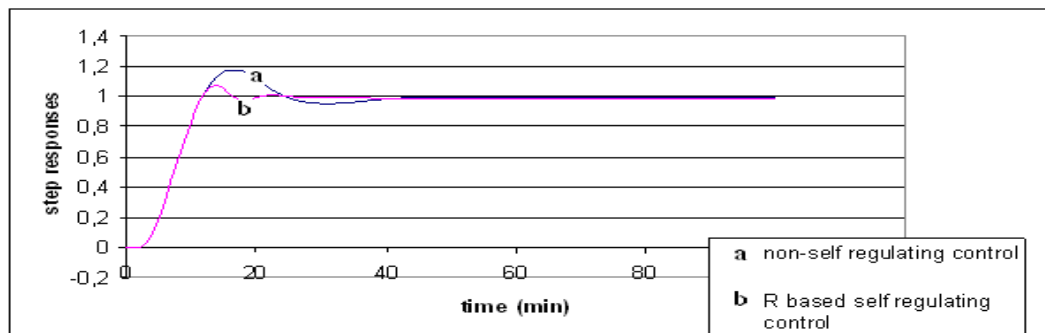


Figure 6.4: Step responses for process in simulation 6.4.

- Simulation 6.5: $P(S) = [1 / (25S + 1)^2] * e^{-14s}$

T=38, R=0.269

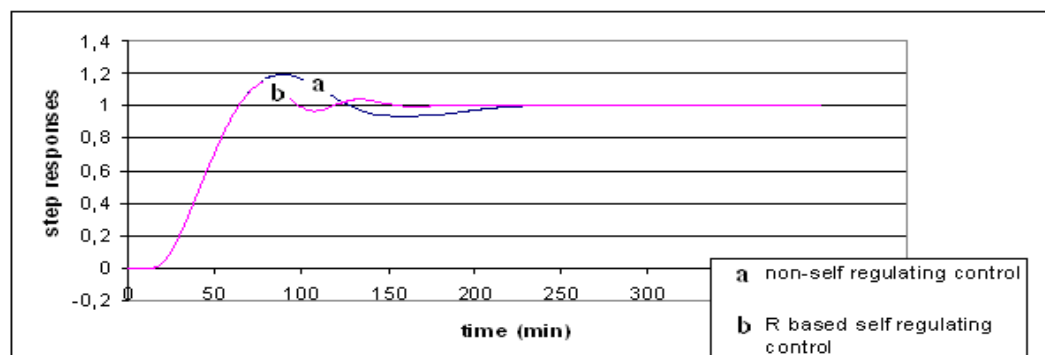


Figure 6.5: Step responses for process in simulation 6.5.

As it is seen from the graphical results in Figures 6.1 – 6.18; proposed self tuning control scheme improves control performance for processes that show overshoot with non-self regulating controller and make them approach to ideal step responses. On the other hand, it settles down the systems that show continuous oscillatory response.

Proposed Multi Region Self Tuning Fuzzy IMC PID control scheme introduces improvement in control of processes, T - L domination bias of which show variety in a wide range.

- Simulation 6.6: $P(S) = [1 / (25S + 1)^2] * e^{-19s}$

T=38, R=0.333

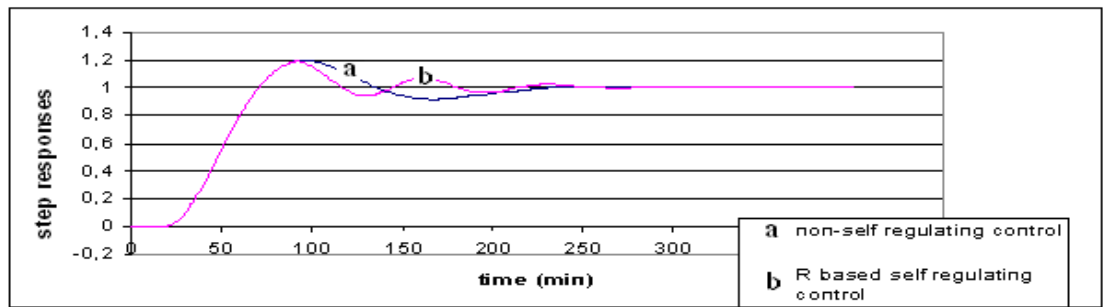


Figure 6.6: Step responses for process in simulation 6.6.

- Simulation 6.7: $P(S) = [0.4 / (15S + 1)^2] * e^{-14s}$

T=24, R=0.368

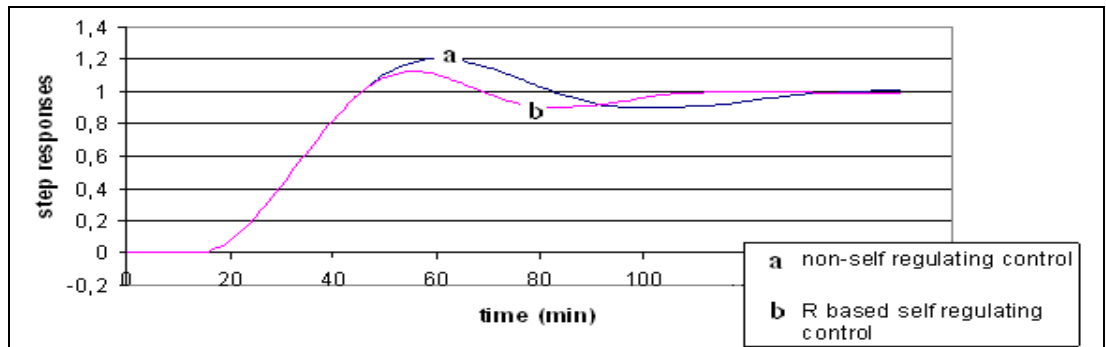


Figure 6.7: Step responses for process in simulation 6.7.

The behaviors of processes that are classified in each section vary in very different styles from each other. While the processes included by a, b and c sections are well controlled by starting from minimum and gradually increasing alpha values as the response goes to set point, the processes with higher “R” ratios demanded a different strategy. So, for section d, a different strategy is generated which provides

very high alpha scale at response zones far from steady state, and diminishes alpha sharply as error approaches to zero because section d processes show oscillatory response to the controllers with large alpha values around steady state. There are also some correction constants in Table 6.1. These are k, t and p. These correction constants are introduced in order to provide consistency to the rules in between the upper and lower boundaries of sections. Their absence was causing impossibility for the rules, which were directly based on “R” ratio, in defining a whole section.

- Simulation 6.8: $P(S) = [1 / (25S + 1)^2] * e^{-20s}$

T=38, R=0.345

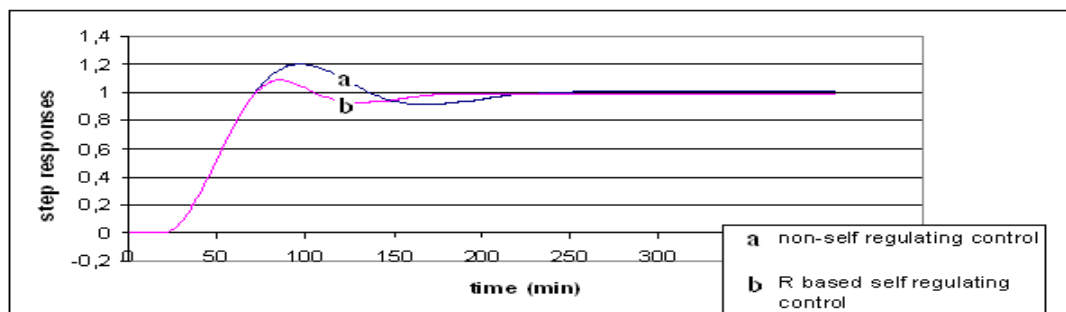


Figure 6.8: Step responses for process in simulation 6.8.

- Simulation 6.9: $P(S) = [1 / (25S + 1)^2] * e^{-25s}$

T=38, R=0.397

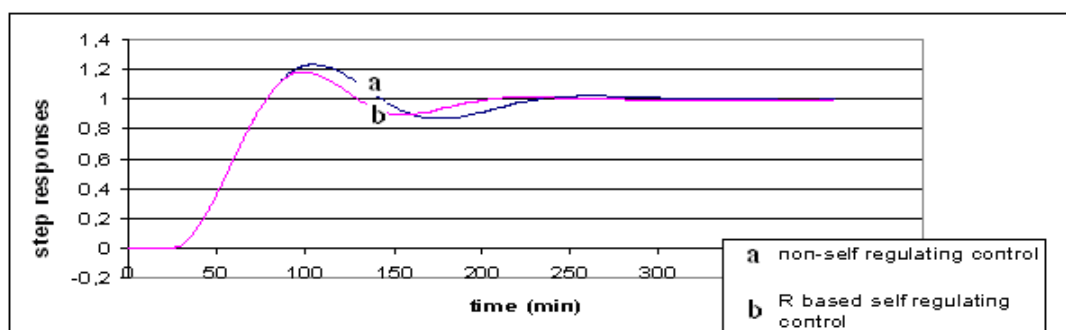


Figure 6.9: Step responses for process in simulation 6.9.

- Simulation 6.10: $P(S) = [3 / (30S + 1)^2] * e^{-26s}$

T=49.4, R=0.345

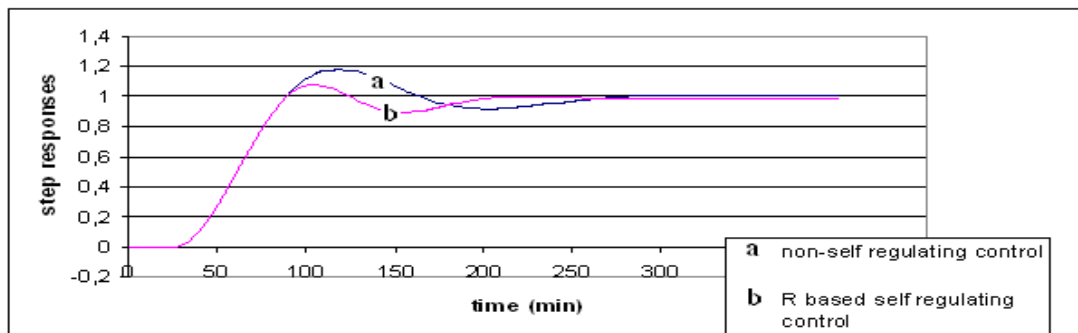


Figure 6.10: Step responses for process in simulation 6.10.

- Simulation 6.11: $P(S) = [5 / (10S + 1)^2] * e^{-20s}$

T=16, R=0.556

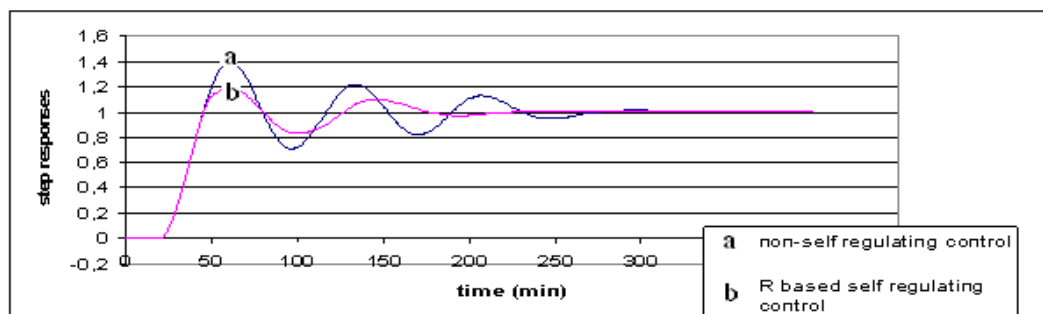


Figure 6.11: Step responses for process in simulation 6.11.

- Simulation 6.12: $P(S) = [5 / (10S + 1)^2] * e^{-25s}$

T=16, R=0.61

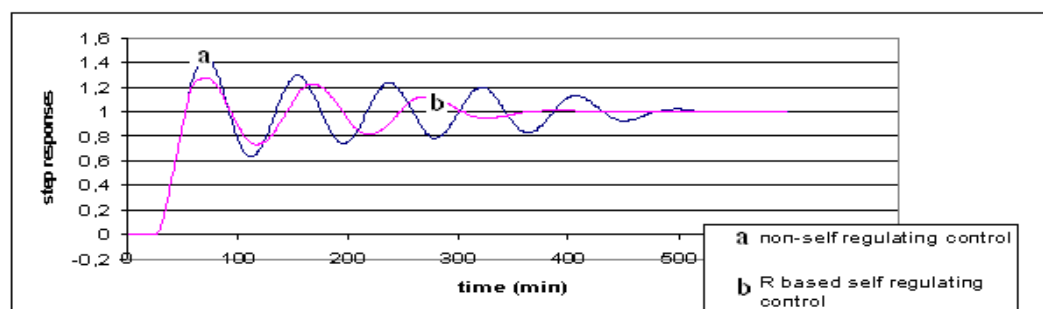


Figure 6.12: Step responses for process in simulation 6.12.

- Simulation 6.13: $P(S) = [6 / (15S + 1)^2] * e^{-44s}$

T=24, R=0.65

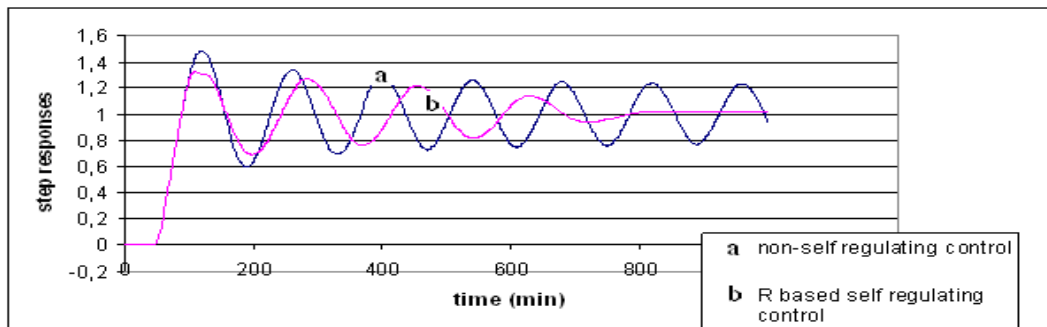


Figure 6.13: Step responses for process in simulation 6.13.

- Simulation 6.14: $P(S) = [3 / (5S + 1)^2] * e^{-7s}$

T=8, R=0.467

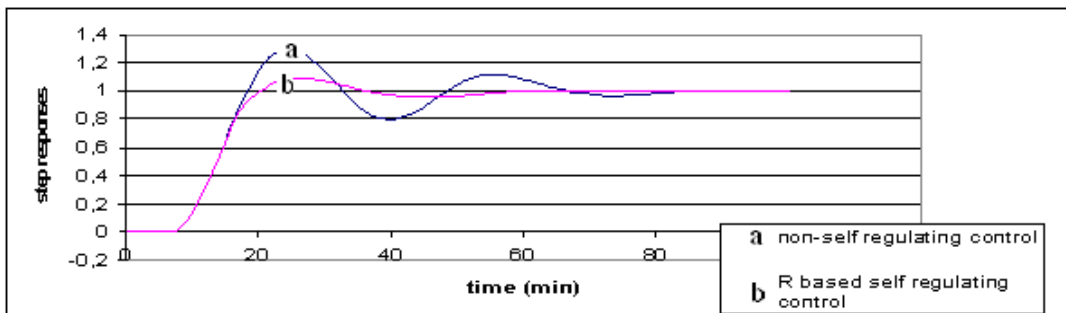


Figure 6.14: Step responses for process in simulation 6.14.

- Simulation 6.15: $P(S) = [3 / (5S + 1)^2] * e^{-6s}$

T=8, R=0.429

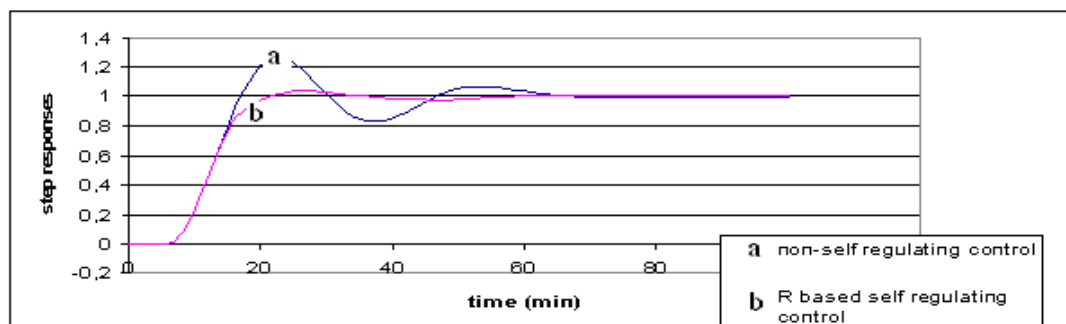


Figure 6.15: Step responses for process in simulation 6.15.

For instance, block diagram concerning to one these comparative analyses is given in Figure 6.19. This block diagram is the one set up for Simulation 5.8, results of which was given in Figure 5.20.

The idea behind the rules mentioned in Table 6.1 are derived from numerous simulation studies, overall analysis of which gave the opportunity to make some generalizations along the whole 0-1 range of “R” ratio. It is important to note that, these are empirical rules that are generated according to personal experience gained from hundreds of simulation studies.

- Simulation 6.16: $P(S) = [3 / (2S + 1)^2] * e^{-6s}$

$$T=3, R=0.667$$

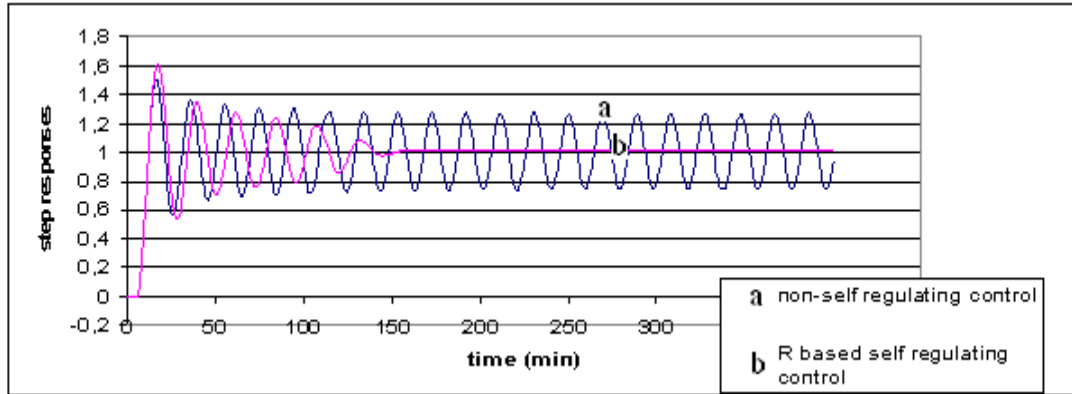


Figure 6.16: Step responses for process in simulation 6.16.

- Simulation 6.17: $P(S) = [3 / (3S + 1)^2] * e^{-10s}$

$$T=5, R=0.667$$

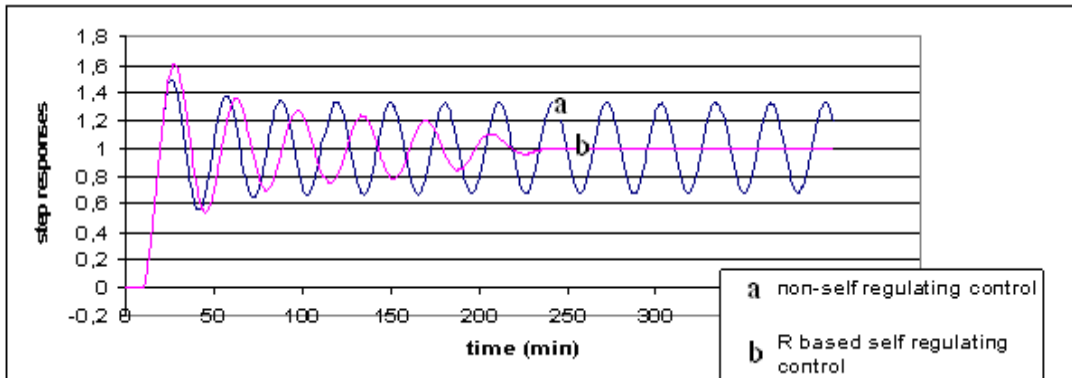


Figure 6.17: Step responses for process in simulation 6.17.

- Simulation 6.18: $P(S) = [5 / (10S + 1)^2] * e^{-32s}$

T=16, R=0.667

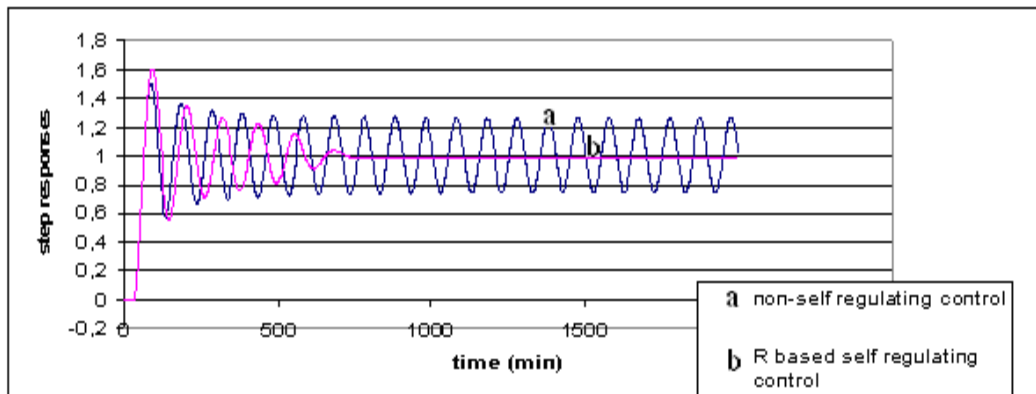


Figure 6.18: Step responses for process in simulation 6.18.

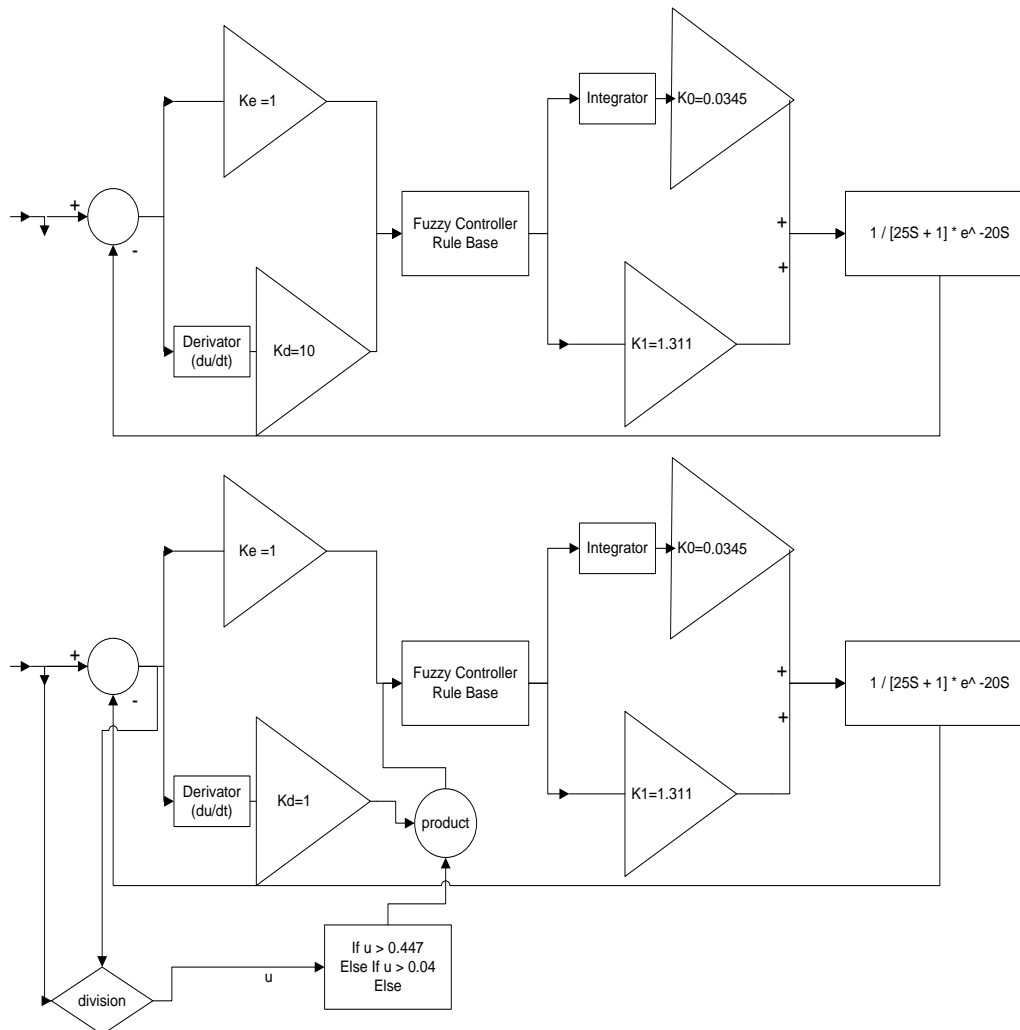


Figure 6.19: Block diagram concerning to comparative control analysis for process block investigated in Simulation 5.8.

6.2 Three Hybridized Region Self Tuning Fuzzy IMC PID Control

The method which was introduced in previous section (Sec. 6.1) provides exact control rules and self tuning boundaries for very specific ranges of “R” ratio. On the other hand, since the boundaries of six sections that are mentioned briefly on table given in Section 6.1 are very unevenly distributed, their simplicity and applicability may cause question marks in operators mind.

So, in order to prevent those effects caused by the strategy mentioned in previous section, the next aim of the studies were defined as trying to simplify scaling ranges and dividing the whole 0-1 range in to three equal parts. Getting this done, the same process models with other sections are used in order to maintain a successful comparison between controller performances. As result for the conducted simulation studies, another table has been prepared in which 0-1 range for “R” ratio is divided in to three equal sections and rules are re generated in order to have generalized algorithms for enhanced ranges.

Procedure for the strategy is almost same with the previous one since the general idea behind these two are nearly identical. So, general path that should be followed in order to use these self tuning algorithms properly is given below one more time in order to maintain familiarity.

- Read process data.
- Learn about numerical values of T: time constant and L: delay time.
- Calculate the ratio $R=L/(L+T)$.
- Learn the range to which the “R” corresponds.
- Use matching functions and decision boundaries for self tuning of alpha (α).

Besides providing a simplified range for “R” range, the studies conducted for this part also created solution to another problem associated with the whole history and base of this study. As it could easily be seen from the simulation results given in all previous parts, as the “R” ratio goes up to higher values, the ability of control techniques are becoming inadequate. Because, the increasing “R” means increasing effectiveness of time delay “L” over time constant “T”. These kinds of systems are

called delay dominant systems and their successful control is much more difficult compared to the time dominant systems that introduce relatively small “R” ratios.

In order to solve the control problem for delay dominant systems, in this part, diminishing of integral gain coefficient of fuzzy logic controller is suggested. While the simulation results for non-self regulating Fuzzy IMC PID controller on these systems show constantly oscillating behavior, the newly proposed method in this section maintains reasonable system responses. The simplified sectioning of “R” and proposed rules for newly formed sections including the ones for highly delay dominant systems ($R > 0.67$) are given in Table 6.2.

In addition to providing a much simpler sectioning for range of “R” and suggesting solution to controlling highly delay dominant systems, this study also contains fuzzy (hybridized) rule base changing property. This property is based on the problem that, rule bases are changing very sharply at the section boundaries which are at $R = 0.33$ and $R = 0.67$. For example; control of a process with $R = 0.32$ is conducted with “case x” rules totally, while a process with $R = 0.34$ is controlled by “case y” rules. So in order to prevent this unreasonable sharp rule base change, in this section, control schemes are redesigned and provided with hybridization devices. Which take 0.23-0.43 and 0.56-0.76 ranges as hybridization bands around sharp section boundaries and control the processes that fall in to these bands with hybridized rules biased between two concerning rule bases. For example, a process with $R = 0.72$ is controlled by a hybridized controller that is biased fairly between “case y” and “case z” rules. Such that, this kind of a controller for this example process takes 20% of total response from controller working according to case y rules and 80% of it from the controller working according to case z rules and sums these two. So, according to the place of “R” in between two band boundaries 0.56 and 0.76, a hybrid response is created. Detailed demonstration of hybridization device and a typical hybrid control scheme block diagram are given in Figures 6.20 to 6.22.

Table 6.2: Scaling ranges and concerning control rules for three hybridized region self tuning Fuzzy IMC PID control

Simplified Sections for $R=L/(L+T)$ Ratio and Proposed Self Tuning Rules			
<div style="text-align: center;"> $0 \text{-----} 0.33 \text{-----} 0.67 \text{-----} 1$ $x \qquad \qquad \qquad y \qquad \qquad \qquad z$ </div>			
Case x	$R=L/(L+T)$	$u=\text{error} / \text{input}$	
If $u > \sqrt{R}$ Else if $u > 0.0001$ (very small value near "0") Else	then then then	$\alpha = \min (L/2, T)$ $\alpha = \sqrt{R} * \max (L/2, T)$ $\alpha = \max (L/2, T)$	
Case y	$t=1-R$		
If $u > \sqrt{0.63}$ Else	then then	$\alpha = \max (L/2, T) / \sqrt{t}$ $\alpha = \min (L/2, T) * \sqrt{t}$	
Case z			
<div style="text-align: center;"> *** $\alpha = \beta = \min (L/2, T)$ [In any case] </div>			
*** Beta coefficient for systems in case z is calculated according to minimum of $(L/2, T)$ rather than maximum which is the general case in all simulations in this study.			
*** Integral coefficient K_D of fuzzy controller for this section systems are calculated taking %67 excess of time delay L as basis rather than L itself while using equation 17. Purpose of this correction is to diminish the integral coefficient in order to prevent oscillatory response associated with these systems.			

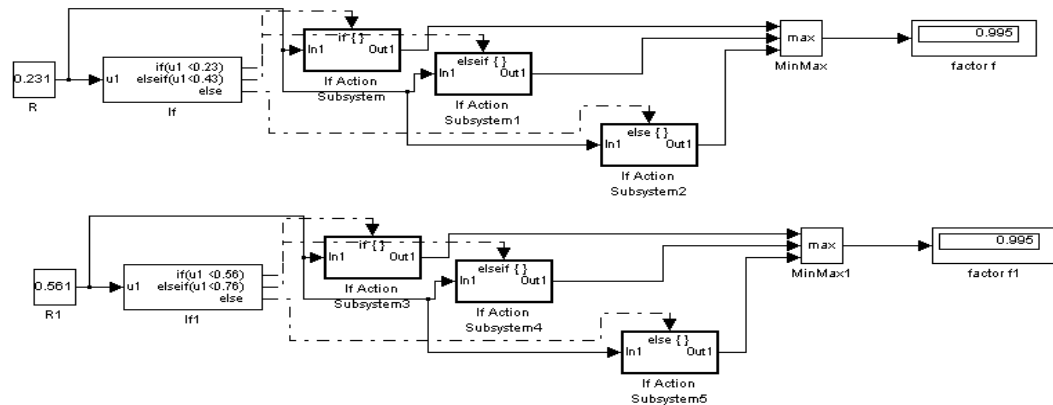


Figure 6.20: Hybridization devices designed for bands around rigid 0.33 and 0.67 section boundaries.

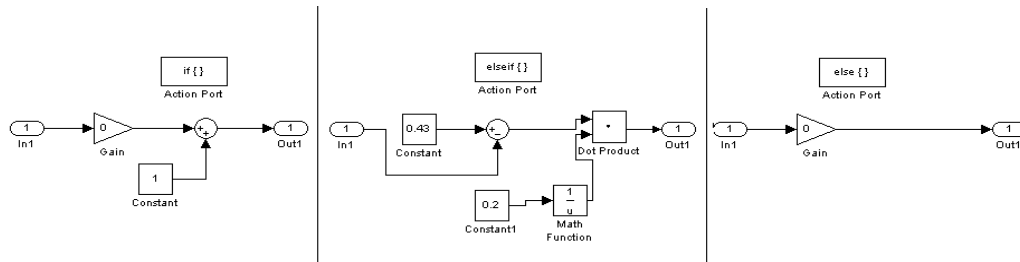


Figure 6.21: Decision mechanisms of hybridization devices. When input R is smaller than 0.23, than pure result “1” is produced, If input is between 0.23 and 0.43, than hybridized output is produced. If input R is larger than 0.43, than pure 0 output is produced

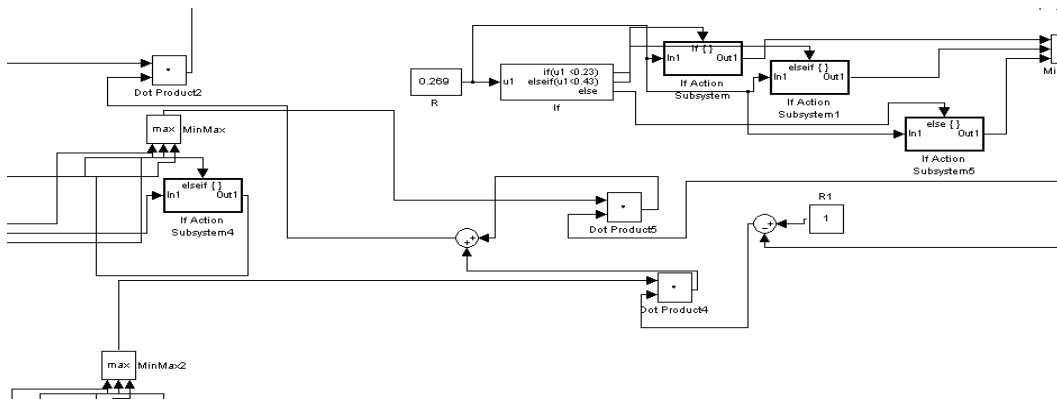


Figure 6.22: Integration of hybridization device in to control scheme. The main output of the device is multiplied by the control action of first controller while the secondary controller action is multiplied by output subtracted from 1.

Step testing results of some control study simulations are given in Figures 6.23 to 6.26.

- Simulation 6.19: $P(S) = [1 / (25S + 1)^2] * e^{-14s}$

T=38, R=0.269

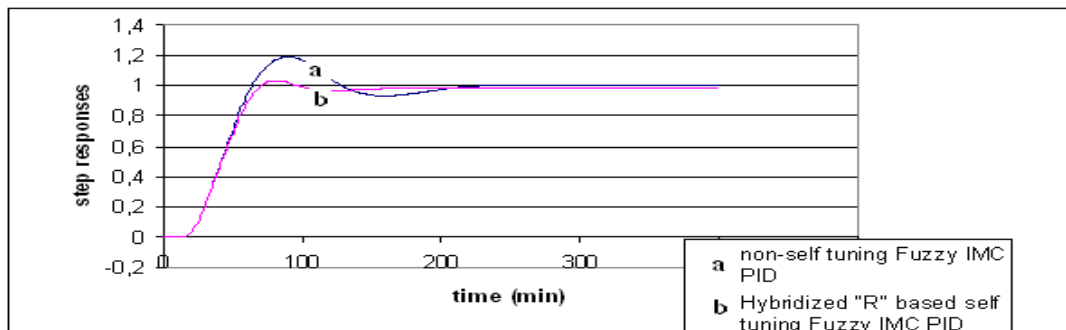


Figure 6.23: Comparative step testing results for simulation 6.19.

- Simulation 6.20: $P(S) = [1 / (25S + 1)^2] * e^{-25s}$

T=38, R=0.397

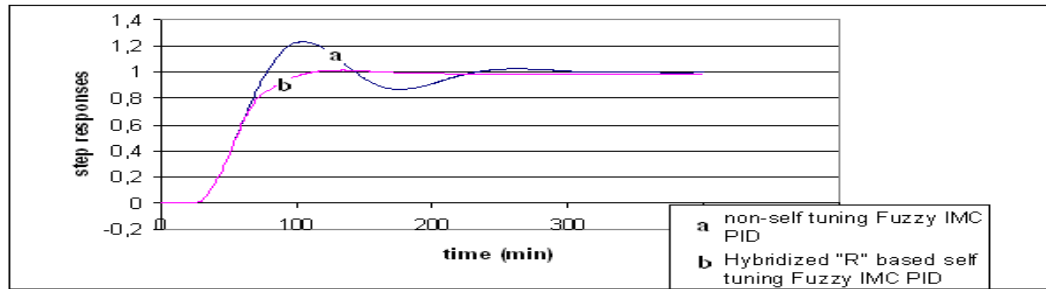


Figure 6.24: Comparative step testing results for simulation 6.20.

- Simulation 6.21: $P(S) = [6 / (15S + 1)^2] * e^{-44s}$

T=24, R=0.65

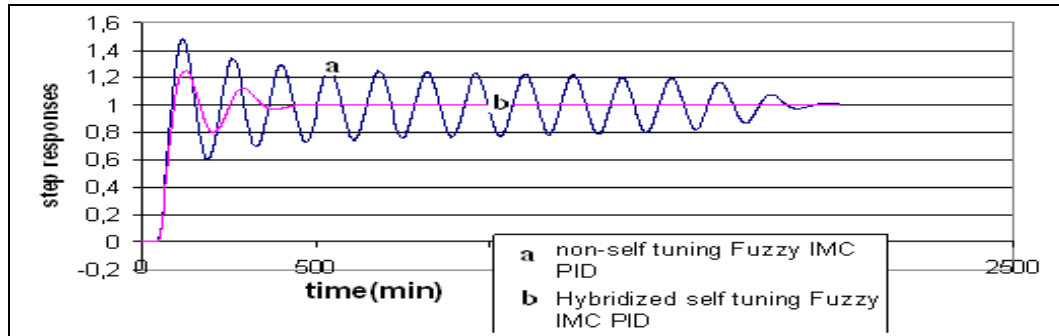


Figure 6.25: Comparative step testing results for simulation 6.21.

- Simulation 6.22: $P(S) = [5 / (3S + 1)^2] * e^{-75s}$

T=5, R=0.938

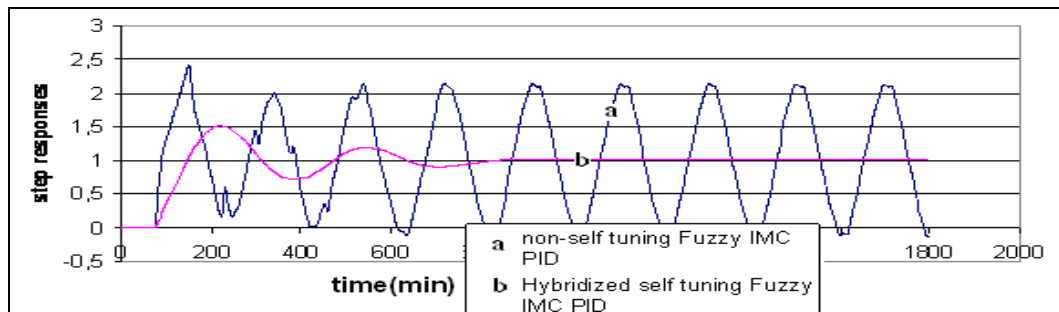


Figure 6.26: Comparative step testing results for simulation 6.22.

The results that are given in Figures 6.23 to 6.26 are from only few of very numerous studies all of which proves that, hybridized self tuning strategy based on given self tuning rules and hybridization idea enhances performance of non-self tuning Fuzzy IMC PID controller in great proportions.

According to the Figures 6.23 – 6.26; it could easily be said that, step responses of control scheme concerning to recently proposed multi region self tuning strategy is much more successful than those of the non-self tuning controller.

The idea behind the rules in sections x and y are very simple in fact. Although these rules may seem very confusing at first sight, all of them refer to reasonable explanations.

First, “case x” rules are designed according to the following idea: When the system response is far from steady state, the controller action speed should be kept very fast. So value of alpha coefficient should be at minimum in order to prevent sluggish response. As the response approaches to steady state gradually, value of alpha is increased to an intermediate value and kept there until response gets very close to steady state. Finally, when error gets very small and response almost reaches the steady state, alpha is increased to its possible maximum.

Second, “case y” rules are first designed in same way with “case x” rules. However, processes that are represented by “section y” did not respond well to this strategy. Following studies showed that, “case y” processes needed to be controlled with much larger alpha values far from the steady state and alpha should be decreased rapidly as system response approaches to set point. So alpha is first kept at values higher than the maximum of range limited by min-max of $(L/2, T)$ by dividing the $\max(L/2, T)$ by $\sqrt{(1-R)}$. Then the second rule that deals with steady state is defined to produce a much smaller alpha value because processes in “section y” ($0.67R > 0.33$) gave very oscillatory responses to control attempts with high alpha values near steady state. So, the overall rule base for section y is defined according to these concerns.

On the other hand, the step response of the process given in Figure 6.26 points to a much more important issue. The Fuzzy IMC PID controller that is designed according to the standard calculations, that are mentioned in Fuzzy IMC PID controller design section, performs very poor for the processes with very high “R” ratios. Those processes behavior of which is majorly dominated by “time delay L” parameter need some special concern in order to be controlled properly. So, as it was mentioned before in Table 6.2, calculation of “integral scaling gain K0” according to the Equation 4.17 is corrected by replacing “variable L” with “ $L*1.67$ ” and calculating K0 according to 67% excess of original time delay L value. This correction maintains achieving a rather smaller K0 value which also leads to a smaller K1 gain with β

factor held constant. So as a result, diminishing integral scaling gains enforces the controller performance for processes with very large time delay. On the other hand, same strategy does not work for processes with smaller time delays because those systems already show a reasonably damped response. Decreasing integral coefficient causes those systems to show over damped responses.

6.3 Three Region Fuzzy Rule Based Self Tuning Fuzzy IMC PID Control

In previous few sections, the main purpose of the studies have generally been self tuning of alpha scaling factor of Fuzzy IMC PID controllers by empirical rules that included specific equations and boundaries. The very first studies concerned on adjusting alpha according to value of error that gradually approaches to zero by using simple functions. Following studies examined the effectiveness of multi stage self tuning strategies. The further ones inspected features of conducting self tuning by using only process properties such as time delay, time constant and overshoot data. Finally last sections concluded with a simple sectioning of R range and providing control actions by concerning simple experimental rules and hybridized rule base selections.

At this stage of the study, the main concern of this section is providing the current control strategy with a level further fuzziness. In fact, by being based on a fuzzy logic controller that is self tuned by if-then rules according to error value and in addition, determining the necessary rules by fuzzy (hybrid) transitions between rule bases, current level of control scheme is already contains a few layers of fuzziness. Next layer of fuzziness that is thought to be added to these is about fuzzifying if-then rules that determine the value of alpha.

Although the rules that were finally mentioned in previous section gave a simple overview of process behaviors and provided improvement in control performances of Fuzzy IMC PID controller, their boundaries such as “if $u > 0.63$ clause” may go under further simplification in order to give possibility to much easier design of controllers.

In fuzzifying the concerning rules and replacing strict rule bases by fuzzy decision making mechanisms, there are some important key issues which can be described briefly like following:

- Take three section partitioning of R range as basis and divide in same manner as sections x, y and z.
- Since all these rules are based on minimum and maximum values of (L/2,T) couple, they are process based and change with the process. So calculate the concerning minimum and maximum limits and store them for rules base design.
- For each section (x, y, z), create a fuzzy rule base that work on one input and one output variable.
- Each of the fuzzy input and output ranges shall contain five membership functions that shall be named as: very small, small, medium, large and very large. Five membership functions provide required distinction of minimum and maximum values in fuzzy understanding scheme.
- Input ranges shall be set between 0 and 1 since the minimum and maximum values of input $u = \text{error}/\text{input}$ are 0 and 1 respectively.
- Output ranges shall be carefully set according to minimum and maximum values of alpha that could be inferred by coupling the process data and rules given in previous x, y, z section based algorithm.
- Once all steps mentioned above are satisfied, self tuning mechanisms based on strict if-then rules can now be replaced by relational fuzzy logic tuners.

For each three section, a separate characteristic fuzzy rule base is defined and these rule bases are given in following:

- Section x - Rule Base
($u = \text{error} / \text{input}$)
- If u is very large, then alpha is very small.
- If u is large, then alpha is very small.
- If u is medium, then alpha is very small.
- If u is small, then alpha is small.
- If u is very small, then alpha is very large.

These rules can be better understood if one observes the numerical rules that were generated for section x in previous section. According to both for section x, when the system response is very far from the set point, alpha scaling factor is kept at minimum level in order to provide fast response. This manner is kept constant until the system response penetrates in to a range close to steady state. When error gets small enough, alpha is slightly increased to degree “small” and when response reaches set point, output alpha is set to very large immediately in order to provide robustness around set point and avoid overshoot.

- Section y – Rule Base
- If u is very large, then alpha is very large.
- If u is large, then alpha is very large.
- If u is medium, then alpha is very small.
- If u is small, then alpha is very small.
- If u is very small, then alpha is very small.

Taking in to account the behavior of processes that are classified in section y, rule base for this section is inevitably different from that for section x. The successful control of these processes could be made by setting alpha to high values for large error zones and decreasing it immediately as response approaches set point. Experimental step response studies showed that, processes of this class returned undamped oscillatory behavior for large alpha values near steady state. Minimum and maximum boundaries of output membership functions for this section are out of boundaries determined by $\min (L/2, T)$ – $\max (L/2, T)$ range which was the base for section x rules. Detailed understanding of these boundaries can be obtained from the rules given in previous part about simple three section self tuning of alpha with a hybridization device.

- Section z – Rule Base
- If u is very large, then alpha is very small.
- If u is large, then alpha is very small.
- If u is medium, then alpha is very small.
- If u is small, then alpha is very small.

- If u is very small, then α is very small.

Rule base for this section is simply based on keeping α at its minimum level independent of any variable. As a result, output action is kept constant at “very small” degree in each case.

Besides α , beta (β) scaling factor, which conducts the relationship between K_0 and K_1 gain factors, is also kept at $\min(L/2, T)$ value only for this section. In sections x and y , beta factor is always set to be equal to $\max(L/2, T)$ as default.

Calculation of K_1 gain is also made by taking 67% excess of time delay (L) as basis for it was also made the same way for section z in previous three section based study.

In order to provide familiarity with the studies conducted for this part, the detailed structure of fuzzy logic tuners performed by Matlab software program including rule bases and membership functions are given in Figures 6.27 – 6.29.

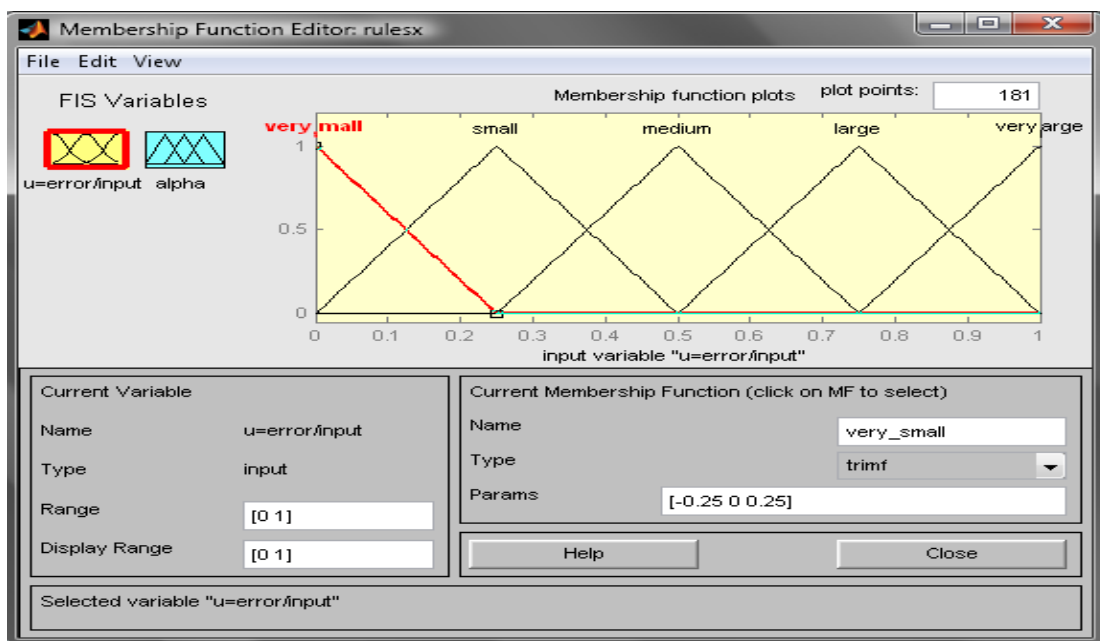


Figure 6.27: Matlab window demonstrating membership functions for typical input ($u=\text{error/system input}$) variable.

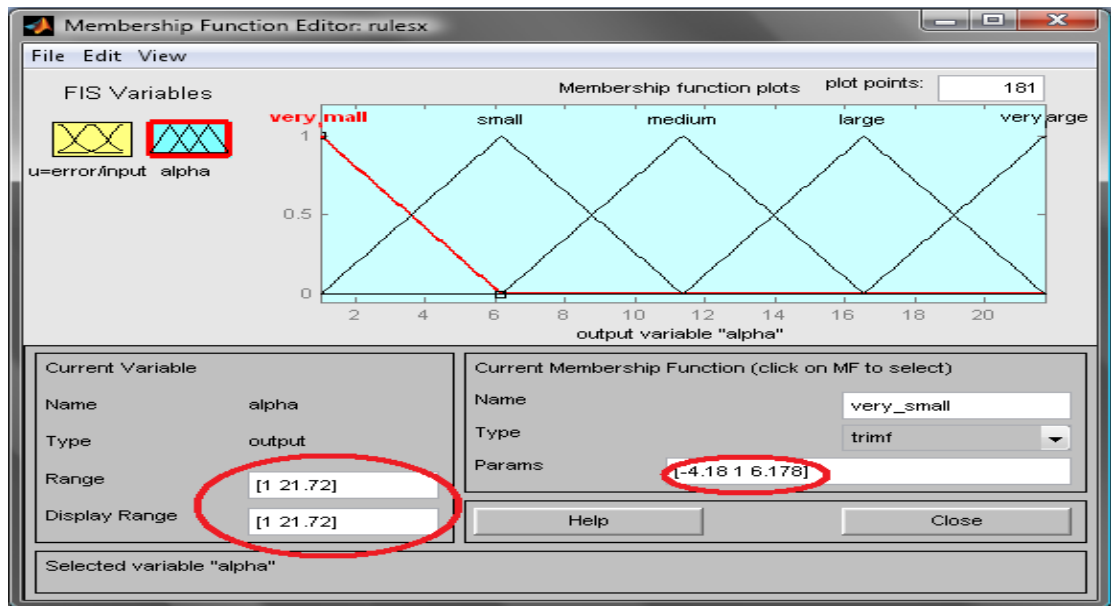


Figure 6.28: Matlab window demonstrating membership functions for typical output α variable. Note that, lower and upper limits of whole range is determined by $\min(L/2, T)$ and $\max(L/2, T)$ parameters of process model.

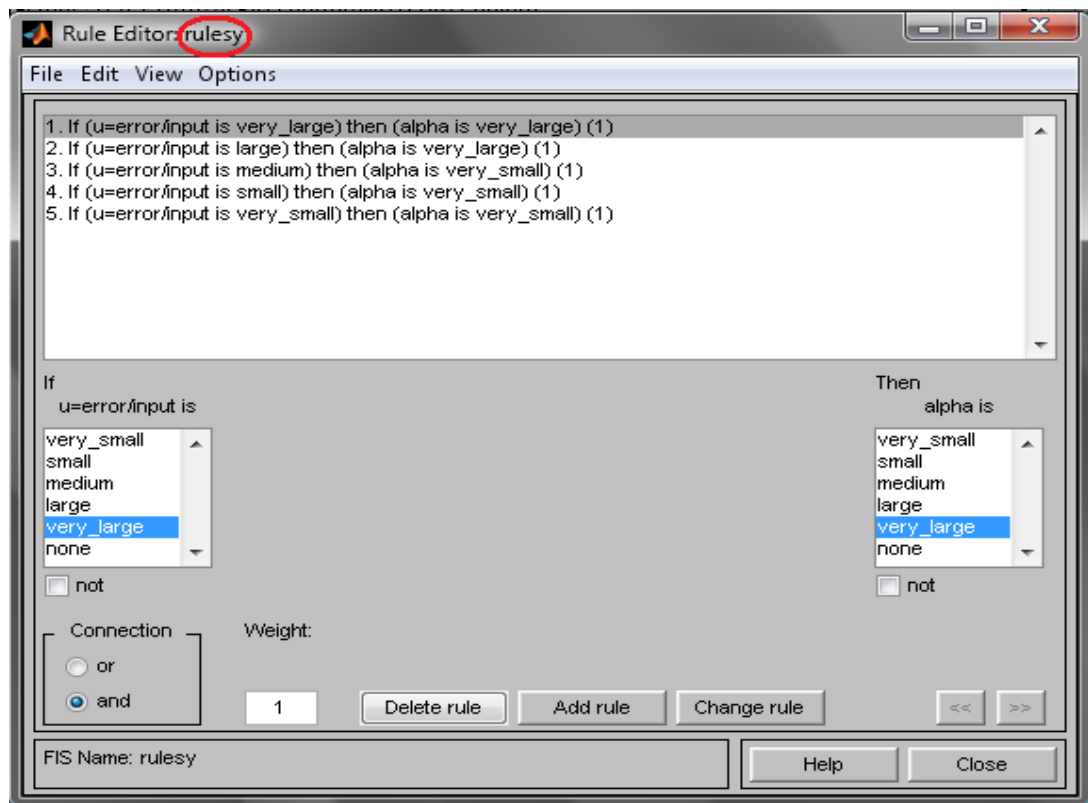


Figure 6.29: Matlab window showing a typical rule base connecting input u with output α . Note that, this rule base is the specific one prepared for section y as name "rulesy" refers to the section name. Rule bases for section x and section z surely have different rule structures.

Integration of a fuzzy tuner in to a typical Fuzzy IMC PID control scheme is also given in Figure 6.30. The concerning control scheme is the one designed to control the primary process model derived from the reboiler of distillation column which was the main interest of studies in very first parts. Figure 6.31 shows comparative graphical representation of step responses generated by both the non-self tuning and the fuzzy tuned, “R data” based self tuning Fuzzy IMC PID controllers.

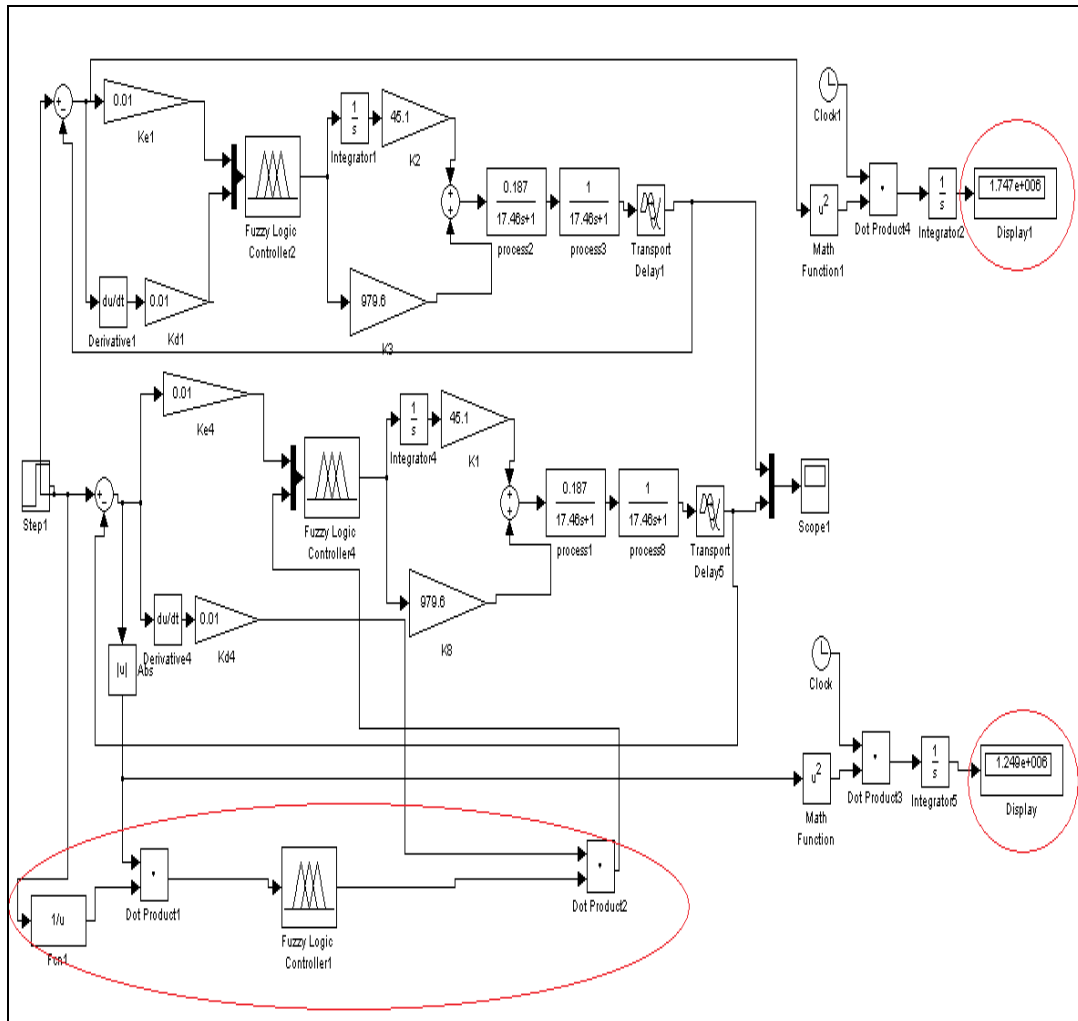


Figure 6.30: Integration of fuzzy tuner into non-self tuning scheme. Simultaneously working non-self tuning and self tuning schemes compared by means of ISTE (integrated time weighted square of error) index.

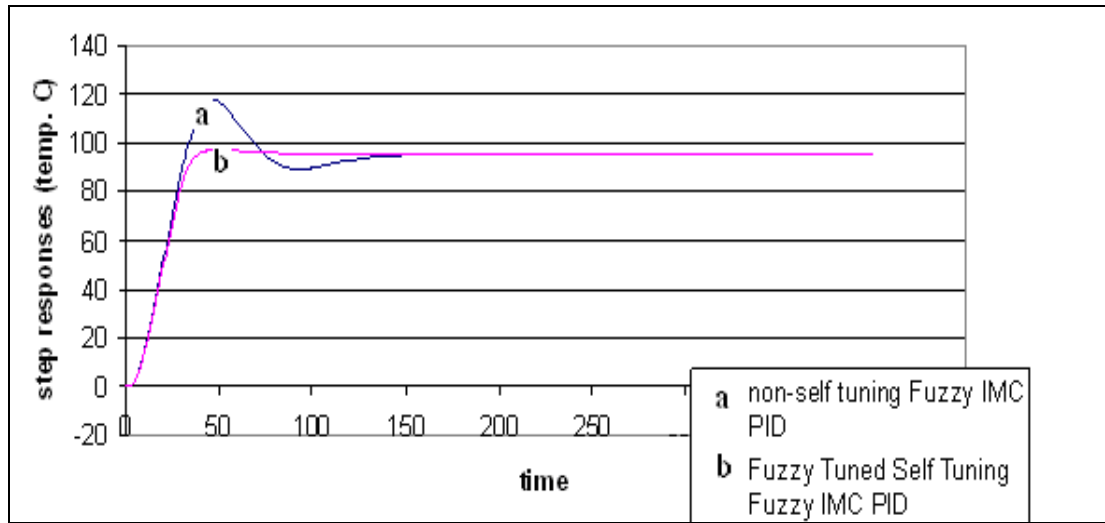


Figure 6.31: Comparative graphical representation of step responses generated by both the non-self tuning and three region fuzzy rule based self tuning Fuzzy IMC PID controllers.

As it can obviously be inferred from graphics above, fuzzy tuned self tuning fuzzy controller strategy improves control performance for primary process model derived from the concerning reboiler by minimizing overshoot while also keeping pace high at transient zone. This provides the system with a much shorter settling time and taking energy input into account which is the case in real systems, proposed scheme promises much cheaper operating conditions.

In following part, some other graphical expressions are given that have the same purpose with the previous one. For a variety of processes that have different “R” ratios, performance of fuzzy tuned self tuning controller is observed. For each of nearly 20 different processes biased equally among whole 0-1 range, self tuning strategy proposed in this part showed enhanced performance over its non self tuning counterpart. For demonstration, few of those results are given in Figures 6.32 – 6.35.

- Simulation 6.23: $P(S) = [3 / (2S + 1)^2] * e^{-0.1s}$

T=3, R=0.0323

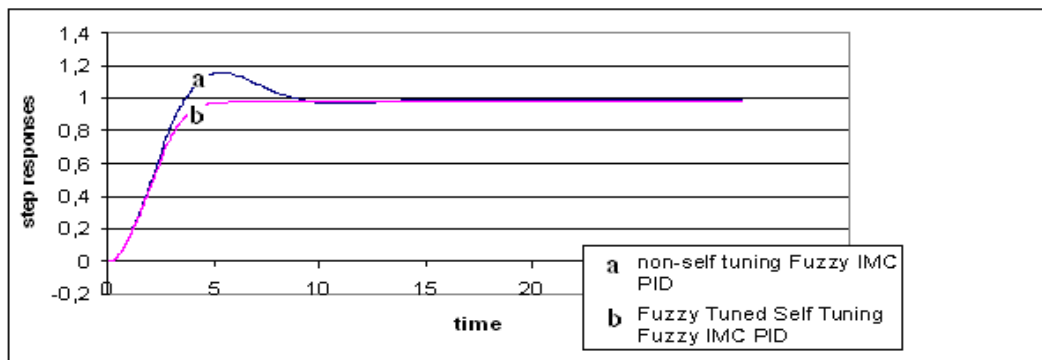


Figure 6.32: Comparative step testing results for simulation 6.23.

- Simulation 6.24: $P(S) = [1 / (25S + 1)^2] * e^{-14s}$

T=38, R=0.269

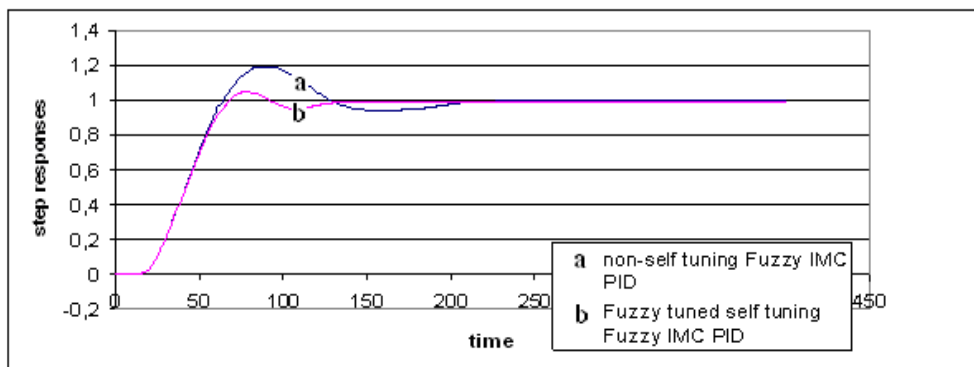


Figure 6.33: Comparative step testing results for simulation 6.24.

- Simulation 6.25: $P(S) = [5 / (10S + 1)^2] * e^{-20s}$

T=16, R=0.556

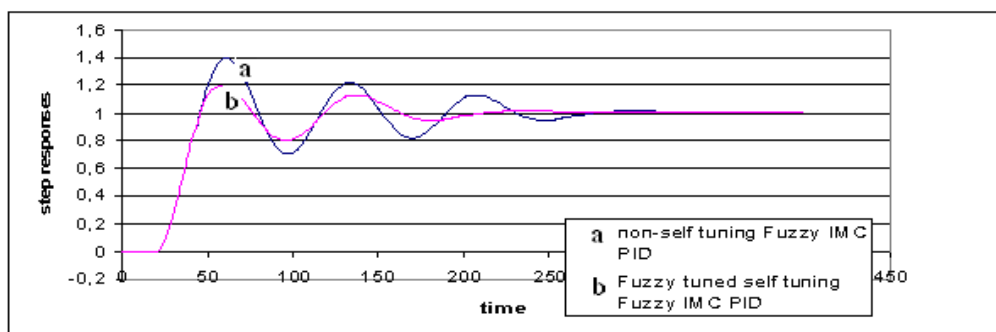


Figure 6.34: Comparative step testing results for simulation 6.25.

- Simulation 6.26: $P(S) = [5 / (3S + 1)^2] * e^{-75s}$
 $T=5, R=0.938$

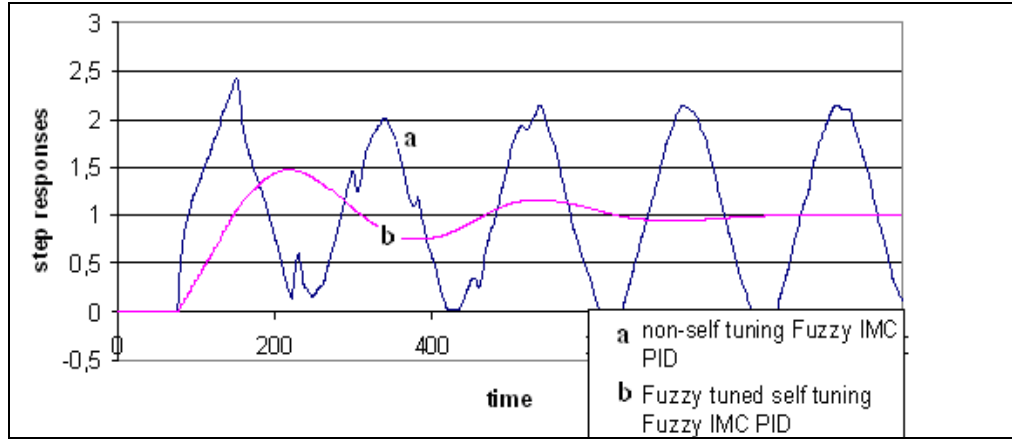


Figure 6.35: Comparative step testing results for simulation 6.26.

The results given in last four figures clearly prove the success of proposed control strategy. According to graphics in Figures 6.31 and 6.32, three region fuzzy rule based self tuning Fuzzy IMC PID controller shows better performance in avoiding overshoot for section x processes whose “R” ratios vary between 0 and 0.33.

According to Figure 6.33, fuzzy self tuning provides the non self tuning controller with a better management ability of reducing overshoots and maintaining shorter settling time.

Figure 6.34 barely shows the difference between performances of classical non-self tuning “minimum alpha - maximum beta” based Fuzzy IMC PID and proposed self tuning Fuzzy IMC PID. The latter introduces necessary damping to the system, while the former causes a chaotic oscillatory behavior.

In Table 6.3, comparative rise time and maximum overshoot ratio results and in Table 6.4, comparative settling time and ITSE (integrated time weighted square of error) results of both the non-self tuning and proposed Multi-Region Self Tuning Fuzzy IMC PID controllers are given for a variety of simulations, whose graphical step response results were presented earlier in this chapter .

Table 6.3: Comparative rise time and maximum overshoot results of non-self tuning and multi-region self tuning Fuzzy IMC PID controllers for various processes.

Simulation No. / Process TF	Rise time (unit time period)		Maximum peak (OS)	
	non-self tuning	multi-reg. sf. tun.	non-self tuning	multi-reg. sf. tun.
6.20 $[1/(25S+1)^2]*(e^{-25S})$	78,2	113,0	23,0 %	1,5 %
6.21 $[6/(15S+1)^2]*(e^{-44S})$	88,6	95,6	48,0 %	25,0 %
6.24 $[1/(25S+1)^2]*(e^{-14S})$	64,0	65,7	19,0 %	9,5 %
6.25 $[5/(10S+1)^2]*(e^{-20S})$	45,1	45,4	40,0 %	19,7 %
6.26 $[5/(3S+1)^2]*(e^{-75S})$	89	148.5	141,5 %	47,6 %

Table 6.4: Comparative settling time and ITSE results of non-self tuning and multi-region self tuning Fuzzy IMC PID controllers for various processes.

Simulation No. / Process TF	Settling time (unit time per.)		ITSE (integrated time weighted square of error)	
	non-self tuning	multi-reg. sf. tun.	non-self tuning	multi-reg. sf. tun.
6.20 $[1/(25S+1)^2]*(e^{-25S})$	325	234	1514	1251
6.21 $[6/(15S+1)^2]*(e^{-44S})$	1934	471	39670	3091
6.24 $[1/(25S+1)^2]*(e^{-14S})$	256	184	784	680
6.25 $[5/(10S+1)^2]*(e^{-20S})$	337	269	1126	681
6.26 $[5/(3S+1)^2]*(e^{-75S})$	no settling	860	$9,8 * 10^5$	$1,2 * 10^4$

7. CONCLUSION AND SUGGESTIONS FOR FUTURE WORK

In this study; firstly, a number of process models were examined in order to investigate their representation performance for the concerning reboiler process reaction curve. Models are generated by using the collected graphical data in specific equations that differ for each kind of model structure. According to comparative results given in related section, it was obvious that 3 term second order plus dead time process model was the best option to define the reboiler reaction curve among all alternatives. After modeling studies were completed, next step was to design a classical IMC PID controller and a Fuzzy IMC PID controller for any given process. Reboiler process transfer function and controller design calculations made for this process were demonstrated as primary model example. Performances of classical and Fuzzy IMC PID controllers were then compared for the primary reboiler process model and also for a few different processes with varying transfer functions. Results have demonstrated the advantage of Fuzzy IMC PID controller over the classical controllers for certain cases. On the other hand, Fuzzy IMC PID controllers exhibited certain drawbacks for highly delay dominant processes.

Next, numerous self tuning strategies were developed for Fuzzy IMC PID controller. The object of developing these strategies was to provide Fuzzy IMC PID controller with a variety of algorithms and rules for controlling all kinds of processes whose time constant and time delay parameters vary in a very large range. On the way going to the resulting rules, first step was examining the necessary self tuning behavior for Fuzzy IMC PID controller to control the primary reboiler process properly with small rise time and minimum overshoot. The next step was to question if the obtained self tuning strategies were general enough to be applied for any given arbitrary process model. This leaded the path of the study in to some series of comparative simulation studies.

The process transfer functions were classified according to the relation between their time constant and delay parameter ($R=L/(L+T)$) and for all class of processes, different rule bases were developed since each class of process needed different approach in order to obtain a system response with small rise time and minimum overshoot. Details were presented accordingly in relevant chapter. The first self tuning rule base table has been obtained by partitioning above mentioned controllability time constant R in to six portions. Later, we have done some simplification on partitioning which led to a new table including only three simple and equal portions which means 0.33 for each in partitioning of 0-1 range. After that, rules in each three sections were replaced with fuzzy “if – then” rules in order to soften the transient zone behaviors along rule boundaries and also along partitioned portion boundaries.

Without exception, the final results showed that proposed multi region self tuning rules improved step response performance of Fuzzy IMC PID controller by providing it with the proper self tuning strategies for each kind of process behavior. According to graphical results and error index performance criteria calculations, self tuning Fuzzy IMC PID controller maintained almost zero overshoot responses for processes with small controllability time constant and provided remarkably improved responses even for processes with very large controllability time constant while non-self tuning Fuzzy IMC PID controller showed chaotic oscillatory response in control of those latter kinds of processes.

As a final conclusion, it can be clearly stated that, Multi Region Self Tuning Fuzzy IMC PID Controller strategies and rule bases that are proposed in this study, enhanced the control ability of Fuzzy IMC PID controllers in great proportions for a variety of processes, whose time constant and time delay parameters vary along a wide range.

For future work, the first step should be the examination of regulatory responses of concerning control loops. Since all simulations conducted in this study deal with servo (step) response performances, detailed investigation is still needed for disturbance effects and responses. Besides that, control simulations for highly non-linear processes have to be conducted in order to amplify the ranges of the concerning self tuning strategies and rule bases.

REFERENCES

- [1] **Duan, X.-G., Li, H.-X., Deng, H.**, 2008, Effective Tuning Method for Fuzzy PID with Internal Model Control, *Ind. Eng. Chem. Res.*, **47**, 8317-8323.
- [2] **Tham, M. T.**, *Distillation: An Introduction*, University of Newcastle upon Tyne, UK. 1997. <http://lorien.ncl.ac.uk/ming/distil/distil0.htm> (Accessed at: 06.04.2010)
- [3] **Luyben, W.L., Yu, C-C.**, 2008, *Reactive Distillation Design and Control*, Wiley, U.S.A.
- [4] **Sundmacher, K., Kienle, A.**, 2003, *Reactive Distillation: Status and Future Directions*, Wiley-VCH, U.S.A.
- [5] **Taylor, R., Krishna, R.**, 2000, Review: Modeling Reactive Distillation, *Chemical Engineering Science* **55**, 5183-5229.
- [6] **Tanrıverdi, H., İ.**, 1996, *Fuzel Alkollerinden Asetat Esterleri Üreten Reaksiyonlu Distilasyon Prosesinin İncelenmesi ve Kontrolü*, Ph.D Thesis, Istanbul Technical University, Institute of Science and Technology, Turkey .
- [7] **Tanrıverdi, H., İ., İskender, H.**, *Çift Eğimli PID Kontrolörü*, Istanbul Technical University, Faculty of Chemistry and Metallurgy, Department of Chemical Engineering, Turkey.
- [8] **İskender, H., Tanrıverdi, H., İ.**, *Karmaşık Bir Kimyasal Prosesin Özyarlamalı Kontrolü*, Istanbul Technical University, Faculty of Chemistry and Metallurgy, Department of Chemical Engineering, Turkey.
- [9] **Cebeci, E.**, 2005, An Investigation on IMC Based Dual Phase PID Controllers, *M.Sc Thesis*, Istanbul Technical University, Institute of Science and Technology, Turkey.
- [10] **Araki M.**, PID Control, in *Control Systems, Robotics and Automation*, **2**.
- [11] **Xue, D., Chen, Y. Q., Atherton, D. P.**, 2007, *Linear Feedback Control: Analysis and Design with MATLAB*, Philadelphia/U.S.A.
- [12] **Seborg, D. E., Edgar, T. F., Mellichamp, D. A.**, 1989, *Process Dynamics and Control*, Wiley, New York /U.S.A.
- [13] **Shinskey, F. G.**, 1994, *Feedback Controllers for the Process Industries*, McGraw-Hill, New York.
- [14] **Perry, R.H., Green, D.W.**, *Perry's Chemical Engineers' Handbook*.

- [15] **Url-1** <<http://www.chem.mtu.edu/~tbco/cm416/zn.html>>, 07.04.2010.
- [16] **Michigan University**, 2009. *Chemical Process Dynamics and Controls Course Lecture Texts*, Michigan/U.S.A.
- [17] **Tham, M. T.**, 2002, Internal Model Control, in *Part of a set of Lecture Notes on Introduction to Robust Control*, Chemical and Process Engineering Department, University of Newcastle Upon Tyne, U.K.
- [18] **Ben Gurion University**, (2010). Chapter 6: PI and PID Parameters from IMC Design, Chemical Engineering Department, Lecture Notes.
http://www.bgu.ac.il/chem_eng/pages/Courses/oren%20courses/Chapter%206%20corrected%2002.pdf, 26.04.2010.
- [19] **Jantzen, J.**, 2007, *Foundations of Fuzzy Control*, Wiley, U.S.A.
- [20] **MATLAB 6.5** Help / Fuzzy Logic Toolbox.
- [21] **Reznik, L.**, 1997, *Fuzzy Controllers*, Oxford, U.K.
- [22] **Erenoğlu, I., Eksin, İ., Yeşil, E., Güzelkaya, M.**, *An Intelligent Hybrid Fuzzy PID Controller*, Istanbul Technical University, Faculty of Electrical and Electronics, Engineering, Control Engineering Department, Istanbul.
- [23] **Woo, Z.-W., Chung, H.-Y., Lin, J.-J.**, 2000, *A PID Type Fuzzy Controller with Self Tuning Scaling Factors*, Fuzzy Sets and Systems, **115**, 321-326.
- [24] **Güzelkaya, M., Eksin, İ., Yeşil, E.**, 2003, *Self Tuning of PID Type Fuzzy Logic Controller Coefficients via Relative Rate Observer*, Engineering Applications of Artificial Intelligence, **16**, 227-236.
- [25] **Karasakal, O., Yeşil, E., Güzelkaya, M., Eksin, İ.**, 2005, *Implementation of a New Self Tuning Fuzzy PID Controller on PLC*, Turk J Elec. Engin., **13**, 2, Tübitak, Turkey.
- [26] **Mudi, R. K., Pal, N. R.**, 1999, *A Robust Self Tuning Scheme for PI and PD Type Fuzzy Controllers*, IEEE Transactions on Fuzzy Systems, **7**, 1.
- [27] **Li, H.-X., Tso, S. K.**, 2000, *Quantitative Design and Analysis of Fuzzy PID Control - A Step Towards Autotuning*, International Journal of Systems Science, **31**, 5, 545-553.

APPENDICES

APPENDIX - A: Further Information and Technical Detail about Reactive Distillation

APPENDIX - B: Studies for Providing First Order Models Representing Second Order Processes

APPENDIX - C: MATLAB – SIMULINK Studies

APPENDIX – A

Further Information and Technical Detail About Reactive Distillation

The development of the chemical industry over the last two centuries has provided modern civilization with a whole host of products that improve the well-being of the human race. The result has been a better quality of life, longer life expectancy, more leisure time, rapid transportation to anywhere in the world (and outer space), healthier food, more comfortable homes, better clothing and so forth [2].

A major factor in this development has been inexpensive energy and inexpensive raw materials. Coal was the major energy source in the 19th century. Petroleum and natural gas were the major sources in the 20th century. Crude oil offers definite advantages over coal in terms of ease of production and transportation from its origins to the points of consumption. Natural gas also has an inherent advantage over coal because of the hydrogen to carbon ratio. Natural gas is mostly methane (CH₄) with an H/C ratio of 4, but coal's H/C ratio is approximately 1. This means that coal produces much more carbon dioxide when these fuels are burned. Therefore, as an energy source, coal contributes more to greenhouse gases and global warming problems. In addition, coal contains sulfur compounds that require expensive stack-gas cleanup facilities [2].

However, the era of inexpensive energy is definitely over because of the rapid growth in demand in developing countries and the increasing difficulty and expense of finding and producing new supplies. It is clear that, our modern society must undergo dramatic and perhaps painful changes in lifestyle that will sharply reduce per capita energy consumption in order to achieve a sustainable supply of energy [2].

The end of the era of cheap energy has had a major impact in the chemical industry. Significant modifications of the processes to produce chemicals have been made to reduce energy consumption. New and innovative processing methods have been developed and commercialized. Extensive use of heat integration has cut energy consumption in some processes by factors of 2 or 3 [2].

Economic and environmental considerations have encouraged industry to focus on technologies based on process “intensification”. This is an area of growing interest that is defined as any chemical engineering development that leads to smaller inventories of chemical materials and higher energy efficiency. Reactive distillation is an excellent example of process intensification. It can provide an economically and environmentally attractive alternative to conventional multiunit flowsheets in some systems [2].

In the chemical process industries, chemical reaction and purification of the desired products by distillation are usually carried out sequentially. In many cases, the performance of this classic chemical process structure can be significantly improved by integration of reaction and distillation in a single multifunctional process unit. This integration concept is called “reactive distillation” (RD); when heterogeneous catalysts are applied the term “catalytic distillation” is often used [3]. The process diagrams for both the conventional configuration and reactive distillation are given in Figure A.1 [4].

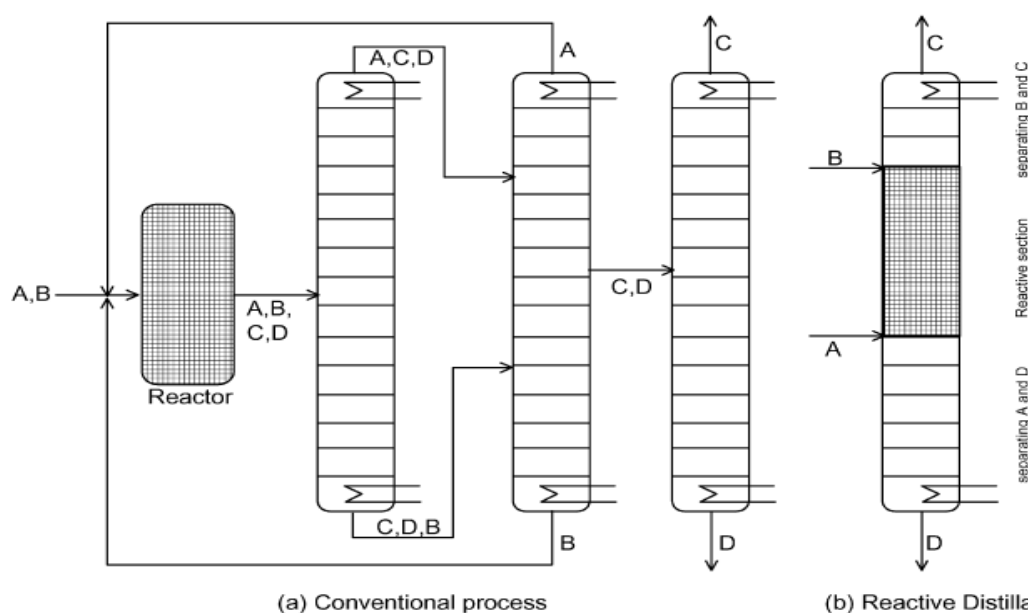


Figure A.1: Processing alternatives for a typical $A + B \rightleftharpoons C + D$ reaction. a) Conventional reactor followed by a separator configuration b) Reactive distillation scheme [4]

As advantages of this integration, chemical equilibrium limitations can be overcome, higher selectivities can be achieved, the heat of reaction can be used in situ for distillation, auxiliary solvents can be avoided and azeotropic or closely boiling mixtures can be more easily separated than in non-RD. Increased process efficiency and reduction of investment and operational costs are the direct results of this approach. Some of these advantages are realized by using reaction to improve separation; others are realized by using separation to improve reaction [3].

Due to the interaction of reaction and distillation in one single apparatus, the steady-state and dynamic operational behavior of RD can be very complex. Therefore, suitable process control strategies have to be developed and applied, ensuring optimal and safe operation. This is another very important area of current and future research and development [3].

Today, RD is discussed as one part of the broader area of reactive separation, which comprises any combination of chemical reaction with separation such as distillation, stripping, absorption, extraction, adsorption, crystallization and membrane separation. In the next decade, unifying approaches to reactive separators should be developed allowing the rigorous selection of the most suitable type of separation to be integrated into a chemical reactor [3].

Despite the fact that the basic idea of combining reaction and distillation is old, there has been an enormously growing interest in the design and operation of RD processes in recent years. Figure A.2 shows the number of journal papers that have appeared on the subject during the last 30 years. It is worth noting that the total number of publications including the papers in conference proceedings and so on is a multiple of the number of publications in scientific journals. In an analogous manner, the industrial interest in applying this attractive process technology has increased continuously. This is reflected by the steadily growing number of patents applied since 1970 [3].

The first patents date back to the 1920s (Backhaus, 1921, 1922, 1923 a,b). Early journal articles are by Keyes (1932), Leyes and Othmer (1945a,b), Schniep, Dunning and Lathrop (1945), Berman, Melnychuk & Othmer (1948b) and Berman et al. (1948a). The first publications deal mainly with homogeneous self-catalysed reactions such as esterifications, trans-esterifications, and hydrolysis. Heterogeneous catalysis in RD is a more recent development and was first described by Spes (1966)

[4]. The concept of combining these two important functions for enhancement of overall performance is not new to the chemical engineering world. The recovery of ammonia in the classic Solvay process for soda ash of the 1860s may be cited as probably the first commercial application of RD, as shown in Figure A.3. Many old processes have made use of this concept. The production of propylene oxide, ethylene dichloride, sodium methoxide and various esters of carboxylic acids are some examples of processes in which RD has found a place in some form or the other, without attracting attention as a different class of operation. It was not until the 1980s, thanks to the enormous demand for MTBE (methyl tert-butyl ether), that the process gained separate status as a promising multifunctional reactor and separator [2]. Figure A.4 shows reactive distillation schemes for MTBE production from methanol and iso-butene and some other processes in which reactive distillation can be used [4].

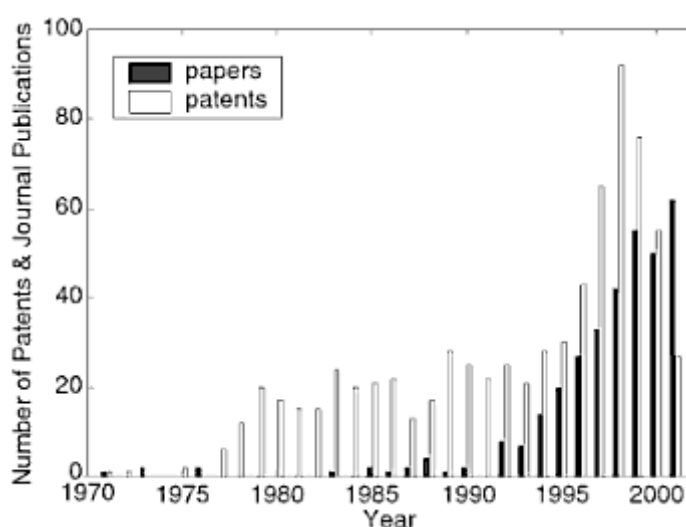


Figure A.2: Journal publications on reactive and catalytic distillation over last three decades according to the Science Citation Index and patents in these fields according to the Deutsches Patent und Markenamt [3]

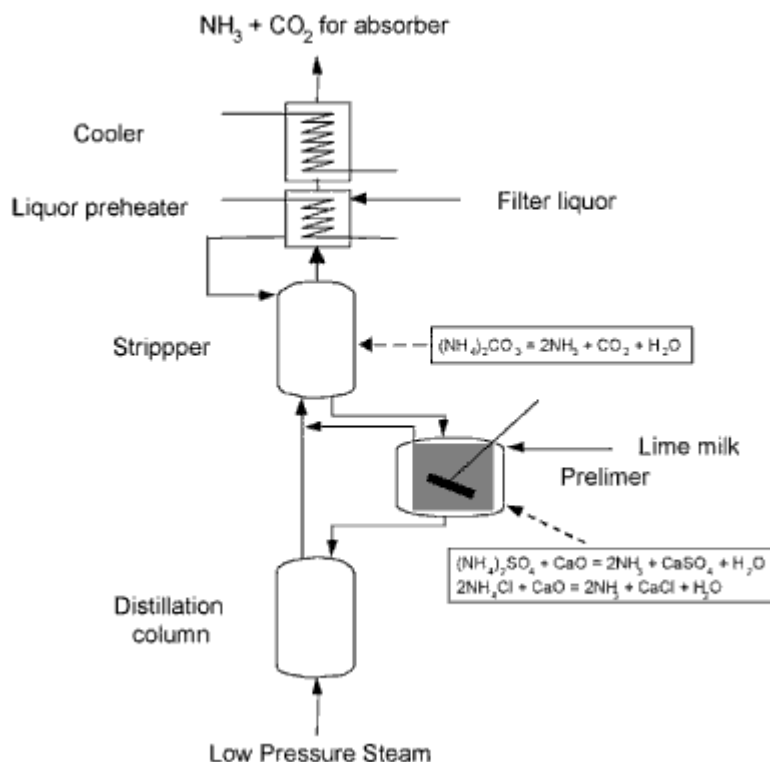


Figure A.3: Ammonia recovery in Solvay process [3]

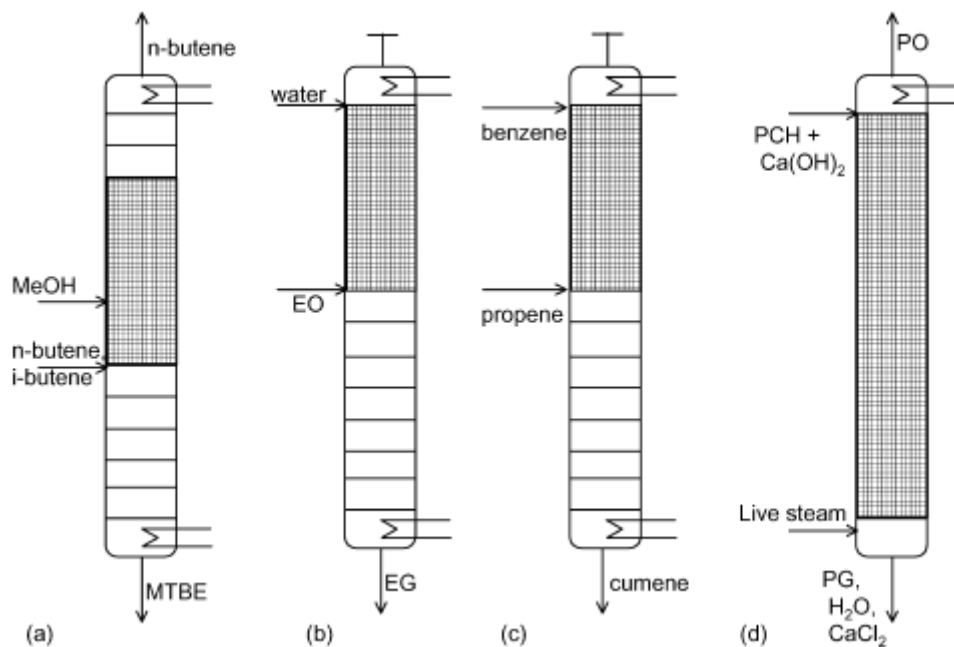


Figure A.4: a) Production of MTBE from MeOH and isobutene b) Production of ethylene glycol by hydration of ethylene oxide c) Cumene production from benzene and propene d) Production of propylene oxide from propylene chlorohydrin and lime [4]

The commercial success of RD for the production of MTBE was immediately followed by another remarkable achievement with the Eastman Kodak process that condensed the whole chemical plant for methyl acetate in a single RD unit that accepts reactants and delivers pure products [3]. The concerning reactive distillation unit is given in Figure A.5 and both the conventional process diagram and reactive distillation diagram for production of methyl acetate are given in Figure A.6.

Since this demonstration of its ability to render cost-effectiveness and compactness to the chemical plant, RD has been explored as a potentially important process for several other chemicals and reactions. Along with esterifications and etherification, other reactions such as acetalization, hydrogenation, alkylation and hydration have been explored. The objectives of existing and potential applications of RD are to: surpass equilibrium limitation, achieve high selectivity towards a desired product, achieve energy integration, and perform difficult separations and so on. One or more of these benefits are offered by the processes in which RD is used [3].

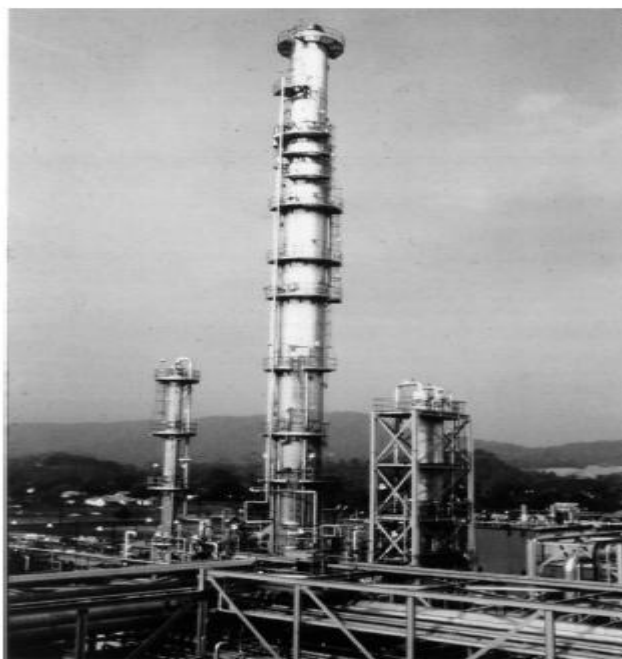


Figure A.5: The Eastman methyl acetate reactive distillation column [2]

Nowadays, many research and development activities are under way to introduce RD into other chemical processes. But despite the convincing success of RD in esterification and etherification applications, it is important to note that RD is not always advantageous. In some cases, it is not even feasible. Therefore, the development of reliable tools for the conceptual design of RD processes is one of the most important fields of current research activities [3].

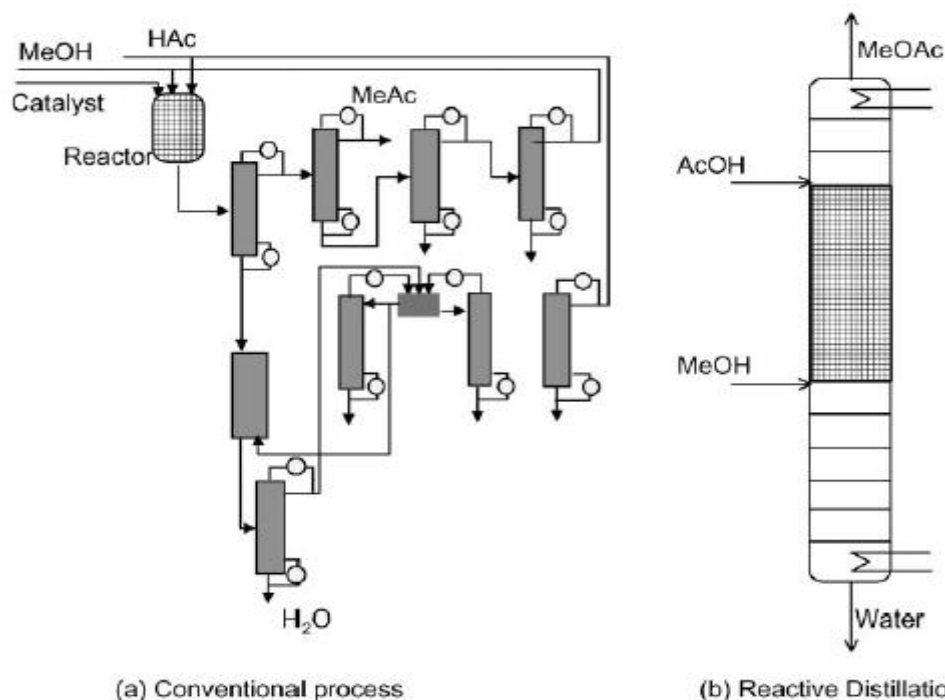


Figure A.6: a) Flow diagram for conventional methyl acetate production process b) Reactive distillation unit proposed to replace the conventional process [4].

Reactive distillation is attractive in those systems where certain chemical and phase equilibrium conditions exist. Because there are many types of reactions, there are many types of reactive distillation columns. Examination of the ideal classical situation can be appropriate to easily outline the basics.

Consider the system in which the chemical reaction involves two reactants producing two products. The reaction takes place in the liquid phase and is reversible [2].



For reactive distillation to work, we should be able to remove the products from the reactants by distillation. This implies that the products should be lighter and/or heavier than the reactants. In terms of the relative volatilities of the four components, an ideal case is when one product is the lightest and the other product is the heaviest, with the reactants being the intermediate boiling components [2].

$$\alpha_C > \alpha_A > \alpha_B > \alpha_D$$

Flowsheet of the concerning ideal reactive distillation column is given in Figure A.7. In this situation, the lighter reactant A is fed into the lower section of the column but not at the very bottom. The heavier reactant B is fed into the upper section of the column but not at the very top. The middle of the column is the reactive section and contains N_{RX} trays. Figure A.8 shows a single reactive tray on which the net reaction rate of the reversible

reaction depends on the forward and backward specific reaction rates (k_F and k_B) and the liquid holdup (or amount of catalyst) on the tray (M_n). The vapor flowrates through the reaction section change from tray to tray because of the heat of the reaction [2].

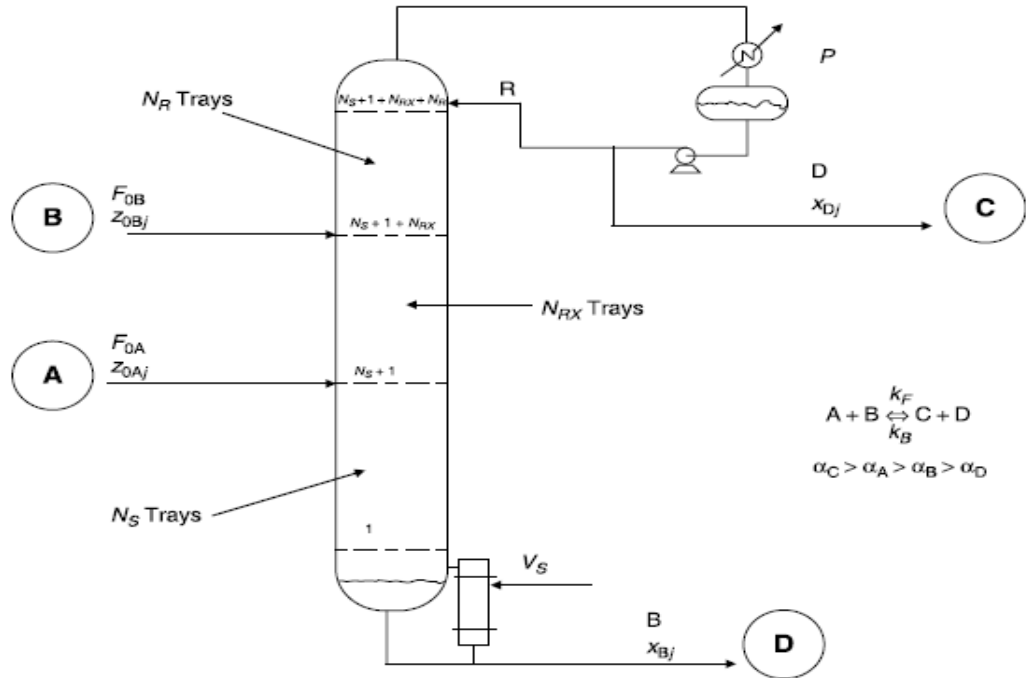


Figure A.7: Ideal reactive distillation column [2]

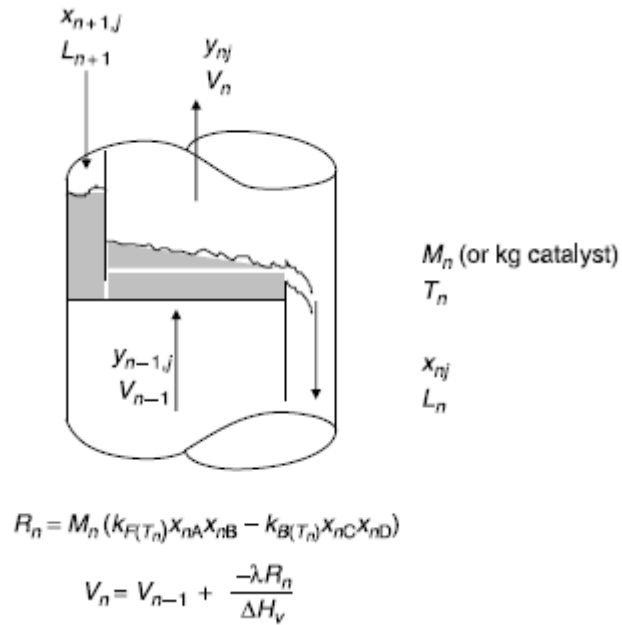


Figure A.8: One reactive tray in detail [2]

As component A flows up the column, it reacts with descending B. Very light product C is quickly removed in the vapor phase from the reaction zone and flows up the column. Likewise, very heavy product D is quickly removed in the liquid phase and flows down the column [2].

The section of the column above where the fresh feed of B is introduced (the rectifying section with N_R trays) separates light product C from all of the heavier components, so a distillate is produced that is fairly pure product C. The section of the column below where the fresh feed of A is introduced (the stripping section with N_S trays) separates heavy product D from all of the lighter components, so a bottom is produced that is fairly pure product D. The reflux flowrate and the reboiler heat input can be manipulated to maintain these products purities. Figure A.9 gives typical composition profiles for this ideal case. The specific numerical case has 30 total trays, consisting of 10 stripping trays, 10 reactive trays and 10 rectifying trays. Trays are numbered from the bottom. Note that the concentrations of the reactants A and B peak at their respective feed trays 11 and 20, respectively. The purities of the two products are both 95 mol%, with B the major impurity in the bottoms and A the major impurity in the distillate [2].

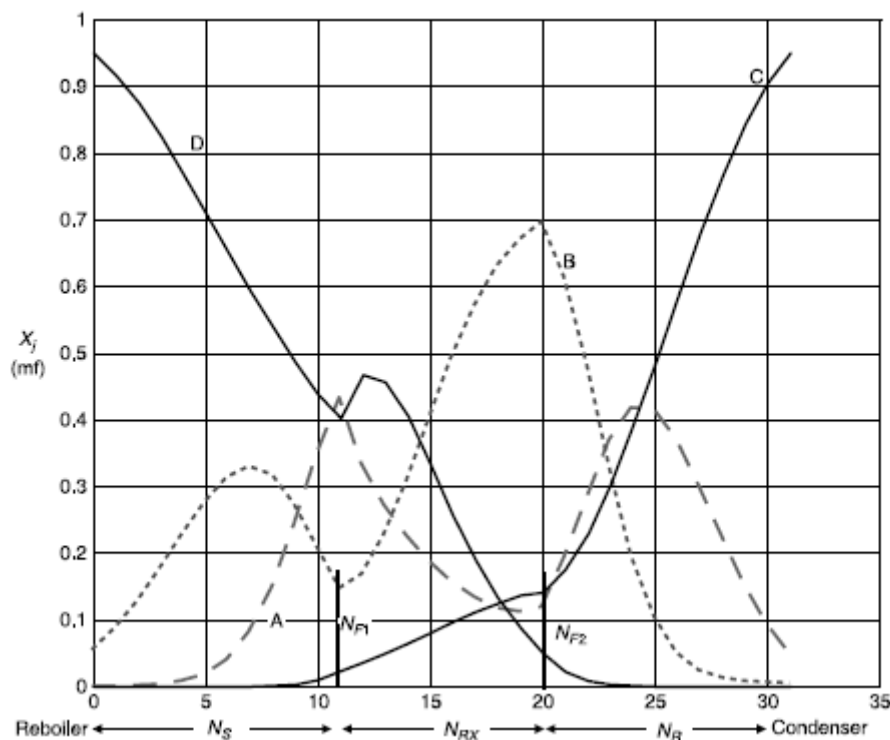


Figure A.9 Base case composition profiles (95% purities) [2]

The benefits of RD can be summarized as follows [4]:

- (a) Simplification or elimination of the separation system can lead to significant capital savings.
- (b) Improved conversion of reactant approaching 100%. This increase in conversion gives a benefit in reduced recycle costs.

- (c) Improved selectivity. Removing one of the products from the reaction mixture or maintaining a low concentration of one of the reagents can lead to reduction of the rates of side reactions and hence improved selectivity for the desired products.
- (d) Significantly reduced catalyst requirement for the same degree of conversion.
- (e) Avoidance of azeotropes. RD is particularly advantageous when the reactor product is a mixture of species that can form several azeotropes with each other. RD conditions can allow the azeotropes to be reacted away in a single vessel.
- (f) Reduced by-product formation.
- (g) Heat integration benefits. If the reaction is exothermic, the heat of reaction can be used to provide the heat of vaporization and reduce the reboiler duty.
- (h) Avoidance of hot spots and runaways using liquid vaporization as thermal fly wheel [4].

Against the above-mentioned advantages of RD, there are several constraints and foreseen difficulties [3]:

- (a) Volatility constraints. The reagents and products must have suitable volatility to maintain high concentrations of reactants and low concentrations of products in the reaction zone.
- (b) Residence time requirement. If the residence time for the reaction is long, a large column size and large tray hold-ups will be needed and it may be more economic to use a reactor-separator arrangement.
- (c) Scale up to large flows. It is difficult to design RD processes for very large flow rates because of liquid distribution problems in packed RD columns.
- (d) Process conditions mismatch. In some processes the optimum conditions of temperature and pressure for distillation may be far from optimal for reaction and vice versa [4].

The design and operation issues for RD systems are considerably more complex than those involved for either conventional reactors or conventional distillation columns. The introduction of an in situ separation function within the reaction zone leads to complex interactions between vapor - liquid equilibrium, vapor - liquid mass transfer, intra-catalyst diffusion (for heterogeneously catalyzed processes) and chemical kinetics. Successful commercialization of RD technology requires careful attention to the modeling aspects, including column dynamics, even at the conceptual design stage. Many of the reactor and distillation paradigms do not translate easily to RD. The potential advantages of RD could be nullified by improper choice of feed stage, reflux, amount of catalyst, boil up rate, etc. Thus, it is possible to decrease conversion by increasing the amount of catalyst under certain circumstances. Increased separation capability could decrease process performance [4].

One of the most important design parameters for reactive distillation is column pressure. Pressure effects are much more pronounced in reactive distillation than in conventional distillation. In normal distillation, the column pressure is selected so that the separation is made easier by means of higher relative volatilities. In most

systems this corresponds to low pressure. However, low pressure implies a low reflux drum temperature and low-temperature coolant. The typical column pressure is set to give a reflux-drum temperature high enough (49°C, 120°F) to be able to use inexpensive cooling water in the condenser and not require the use of much more expensive refrigeration [2].

In reactive distillation, the temperatures in the column affect both the phase equilibrium and chemical kinetics. A low temperature that gives high relative volatilities may give small specific reaction rates that would require very large liquid holdups or amounts of catalyst to achieve the required conversion. In contrast, a high temperature may give a very small chemical equilibrium constant for exothermic reversible reactions, which makes it more difficult to drive the reaction to produce products. High temperatures may also promote undesirable side reactions. Thus, selecting the optimum pressure in a reactive distillation column is very important [2].

Another design aspect of reactive distillation that is different from conventional is tray holdup. Holdup has no effect on the steady-state design of a conventional column. It certainly affects dynamics but not steady-state design. Column diameter is determined from maximum vapor loading correlations after vapor rates that achieve the desired separation have been determined. Typical design specifications are the concentration of the heavy key component in the distillate and the concentration of the light key component in the bottoms. However, holdup is very important in reactive distillation because reaction rates directly depend on holdup or the amount of catalyst on each tray. This means that the holdup must be known before the column can be designed and before the column diameter is known. As a result, the design procedure for reactive distillation is iterative. A tray holdup is assumed and the column is designed to achieve the desired conversion and product purities. The diameter of the column is calculated from maximum vapor loading correlations. Then the required height of liquid on the reactive trays to give the assumed tray holdup is calculated. Liquid heights greater than 10-15 cm (4-6 in.) are undesirable because of hydraulic pressure drop limitations. Thus, if the calculated liquid height is too large, a new and smaller tray holdup is assumed and the design calculations repeated. An alternative, which may be more expensive in terms of capital cost, is to make the column diameter larger than that required by vapor loading [2].

APPENDIX – B

Studies for Providing First Order Models Representing Second Order Processes

Table 4.1 (for recall): First order model time constants representing some second order transfer function time constants.

Second order process time constant	First order model time constant
25,0	38,0
5,0	8,0
2,0	3,0
30,0	49,4
3,0	5,0
10,0	16,0
15,0	24,0
4,0	7,0
17.5	21.7

Graphical results that demonstrate the success of first order models in representing second order processes are given below together with Simulink Block Diagrams made up for each different investigation.

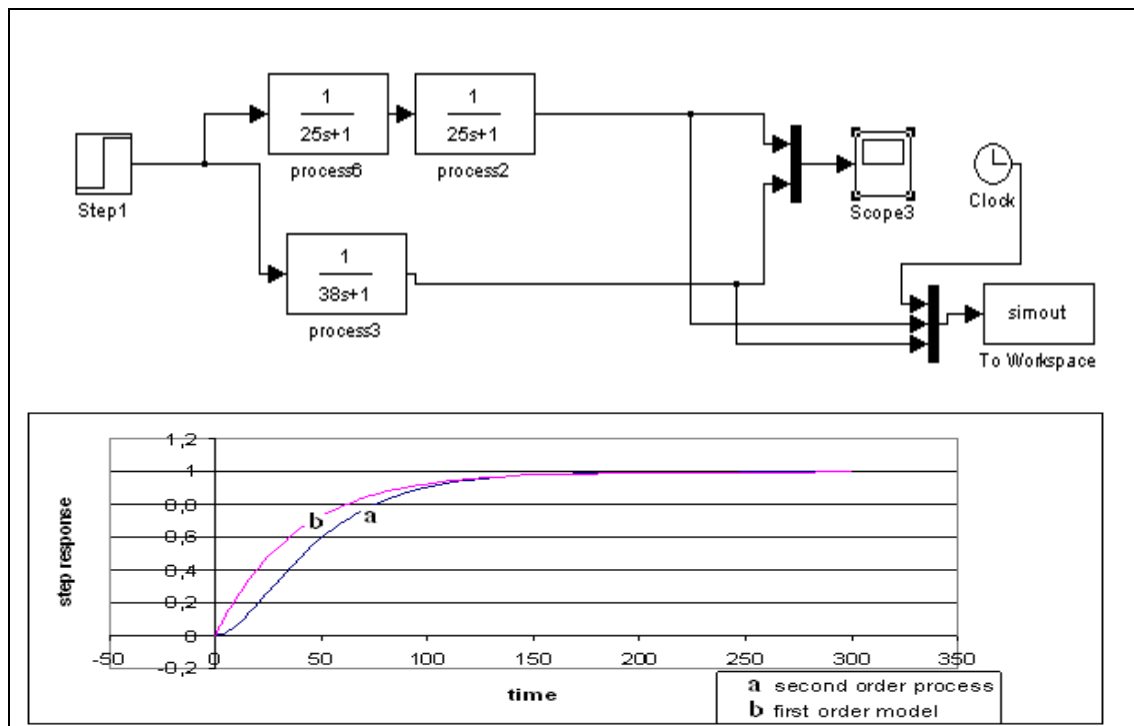


Figure B.1: Block scheme and graphical results for model search B.1.

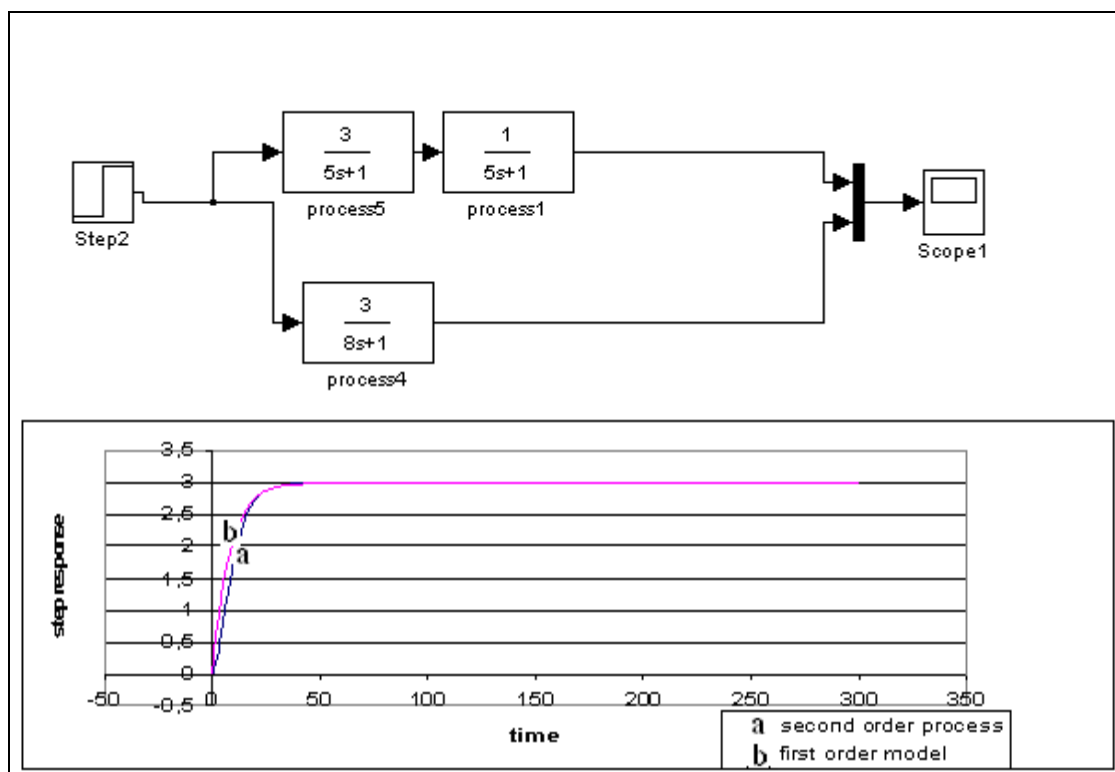


Figure B.2: Block scheme and graphical results for model search B.2.

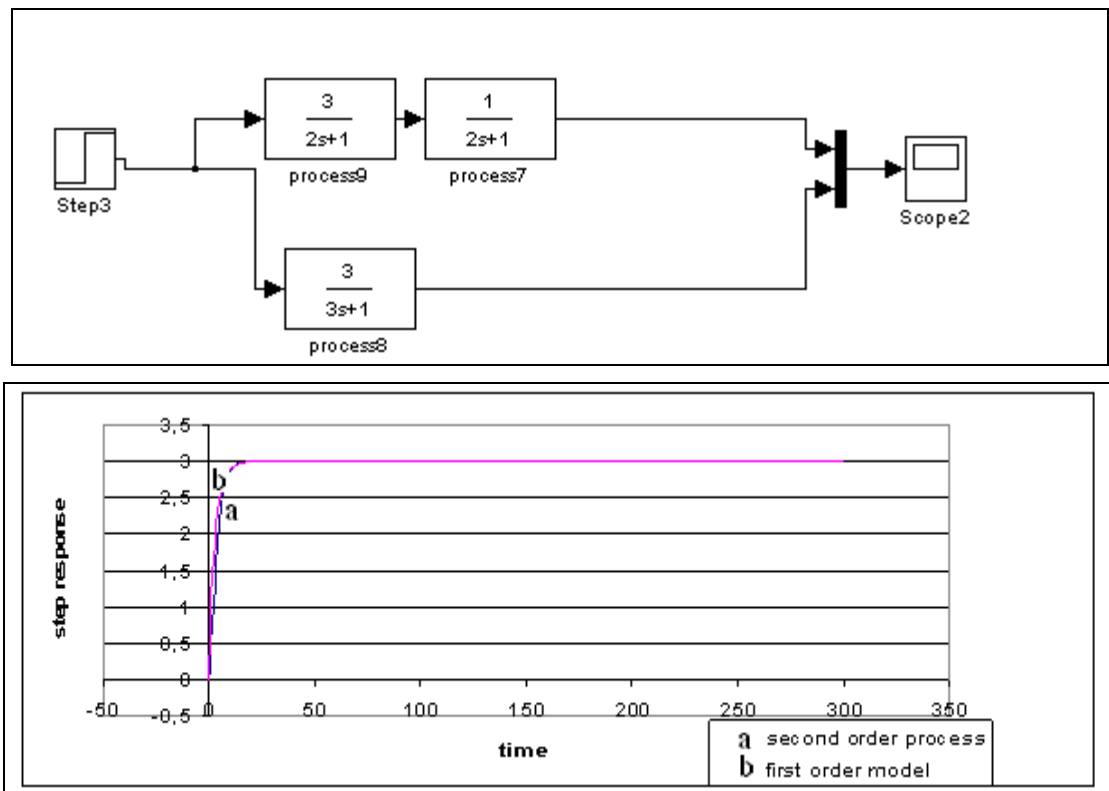


Figure B.3: Block scheme and graphical results for model search B.3.

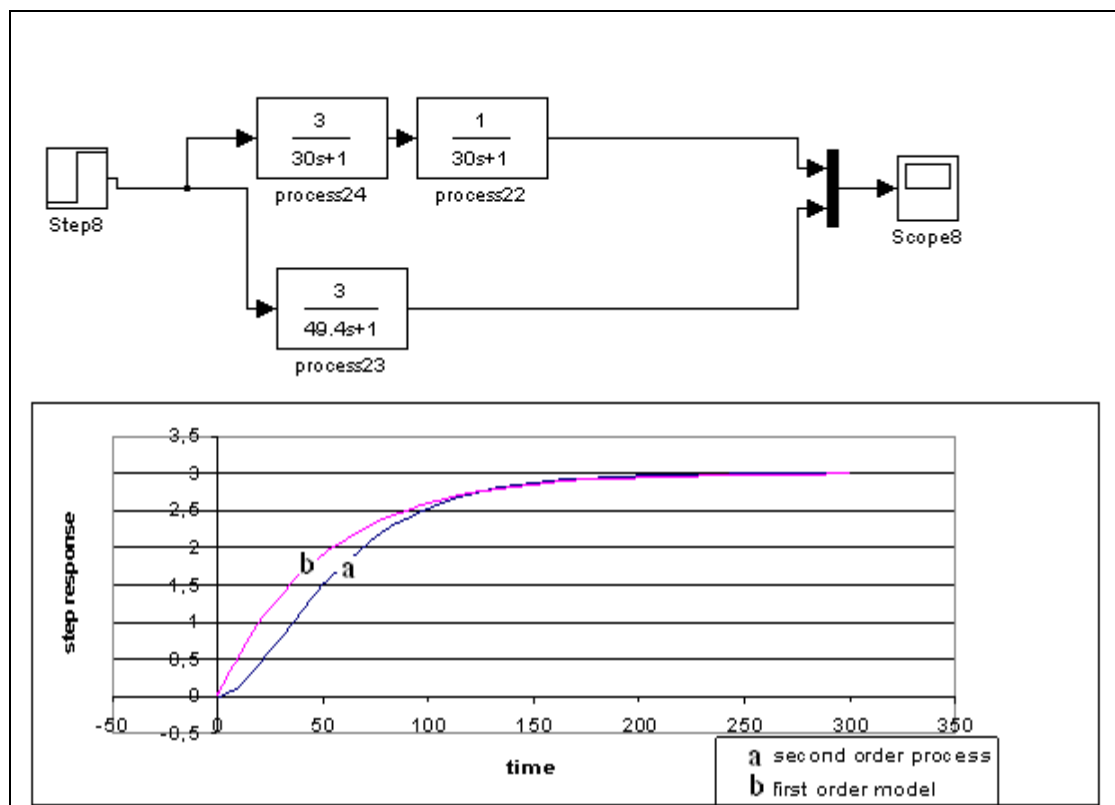


Figure B.4: Block scheme and graphical results for model search B.4.

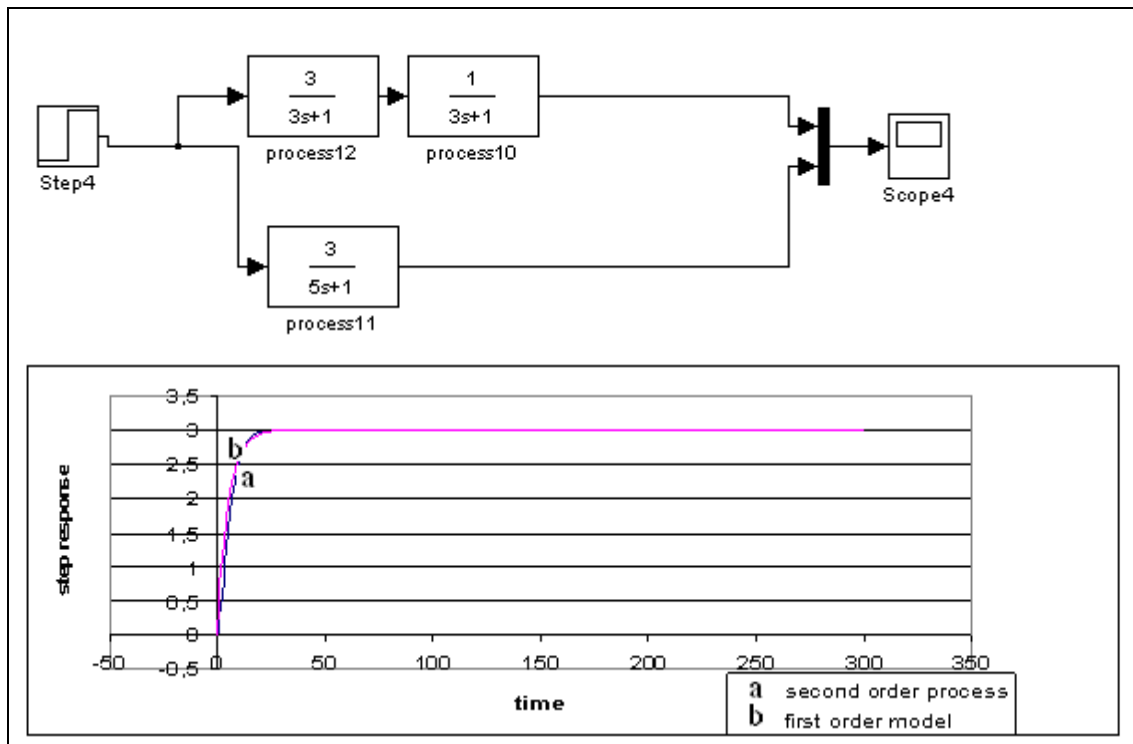


Figure B.5: Block scheme and graphical results for model search B.5.

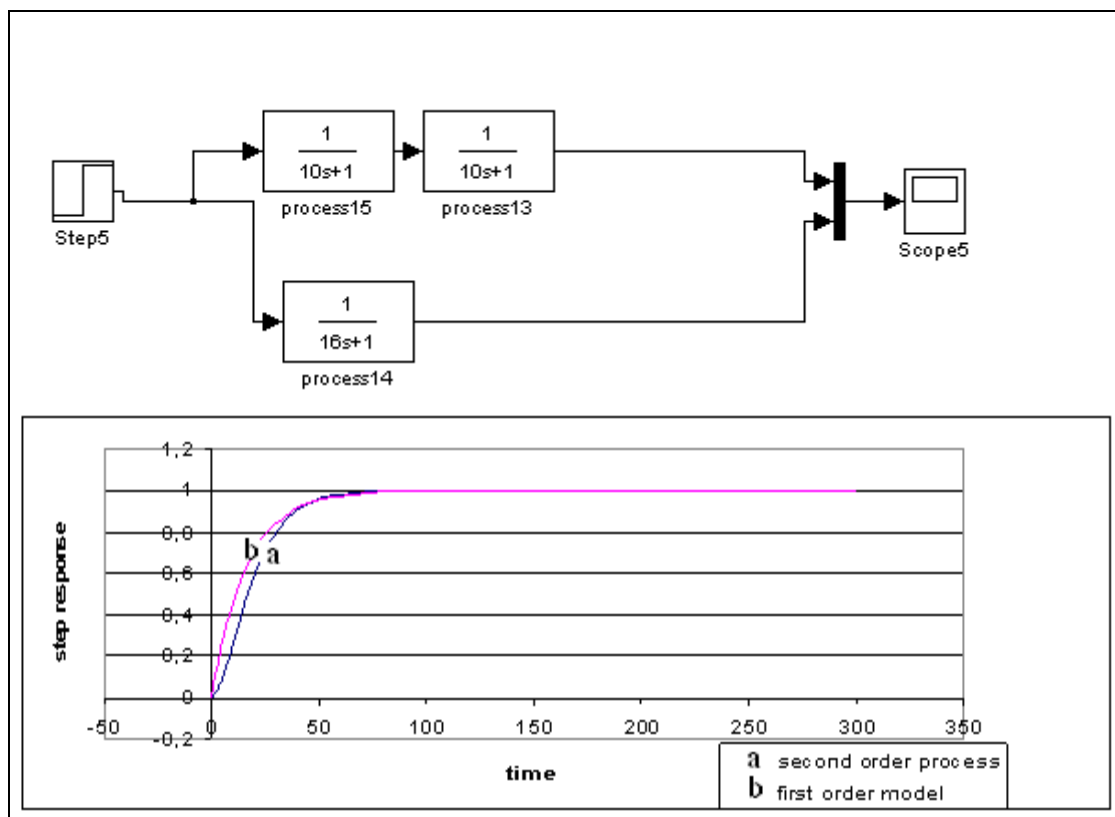


Figure B.6: Block scheme and graphical results for model search B.6.

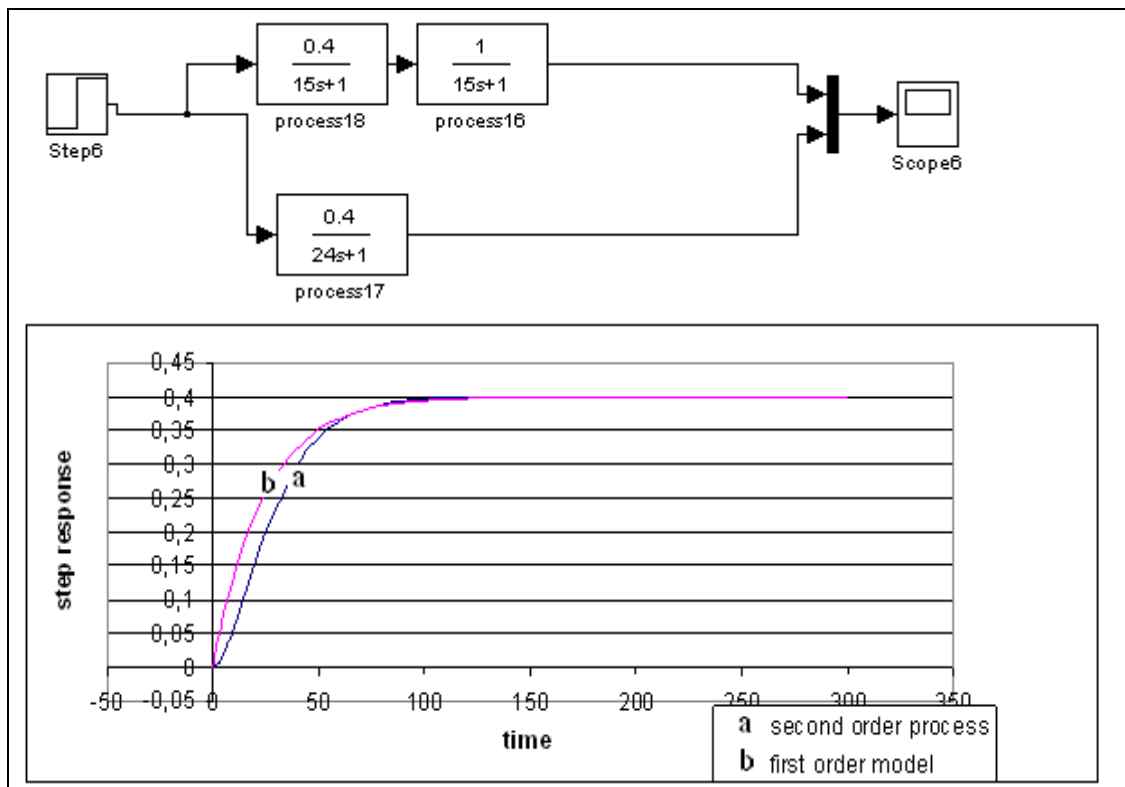


Figure B.7: Block scheme and graphical results for model search B.7.

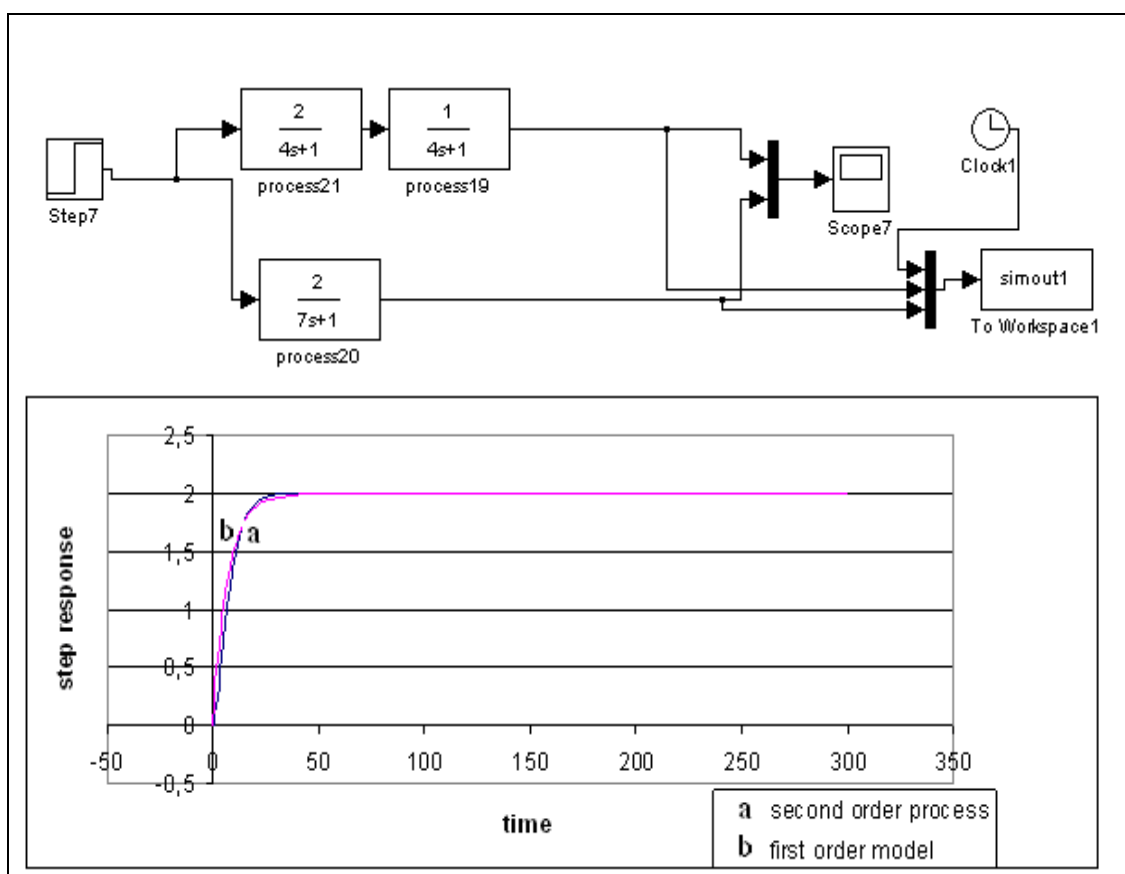


Figure B.8: Block scheme and graphical results for model search B.8.

APPENDIX – C

MATLAB – SIMULINK Studies

- Comparative Simulation Schemes & Calculation of ISTE Error Indexes

Figure C.1 shows the subsystem constructed to calculate integrated time weighted square of error (ISTE) indexes of control schemes that are subject to comparison during this study.

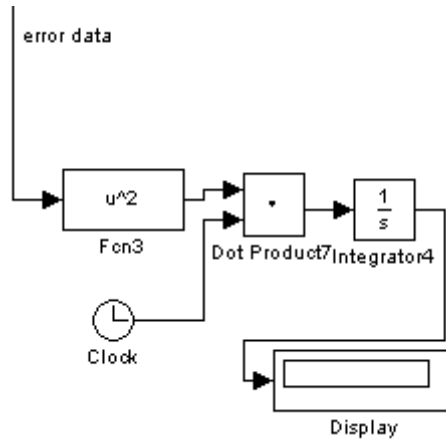


Figure C.1: Block scheme of subsystem made up for calculating integrated time weighted square of error (ISTE) indexes.

This SIMULINK subsystem receives error data from process control scheme, squares it, biases it with time value and integrates the result in order to obtain an integrated time weighted square of error data.

With the help of proposed subsystem, during this study, comparison calculations have been made with high precision and spending little time and effort.

Following block diagrams in Figure C.2 and Figure C.3 show some examples of comparison studies, results of which were used to examine performances of proposed control schemes during whole study.

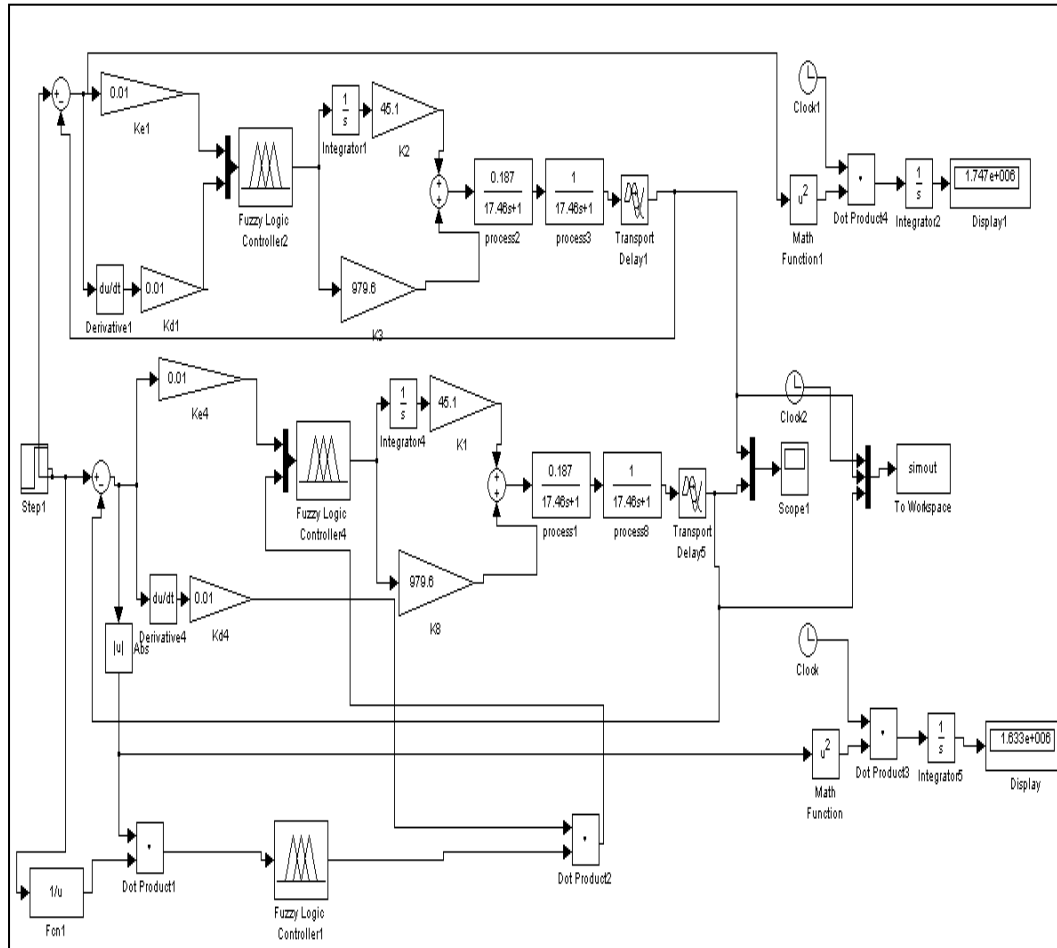


Figure C.2: This scheme is used for comparison of non self tuning Fuzzy PID controller designed for primary reboiler process and its self tuning counterpart. On the rightmost of the scheme, error index calculation subsystems are shown with their numerical displays. The bottom of the scheme contains Fuzzy self tuning system which tunes the alpha coefficient of second control scheme.

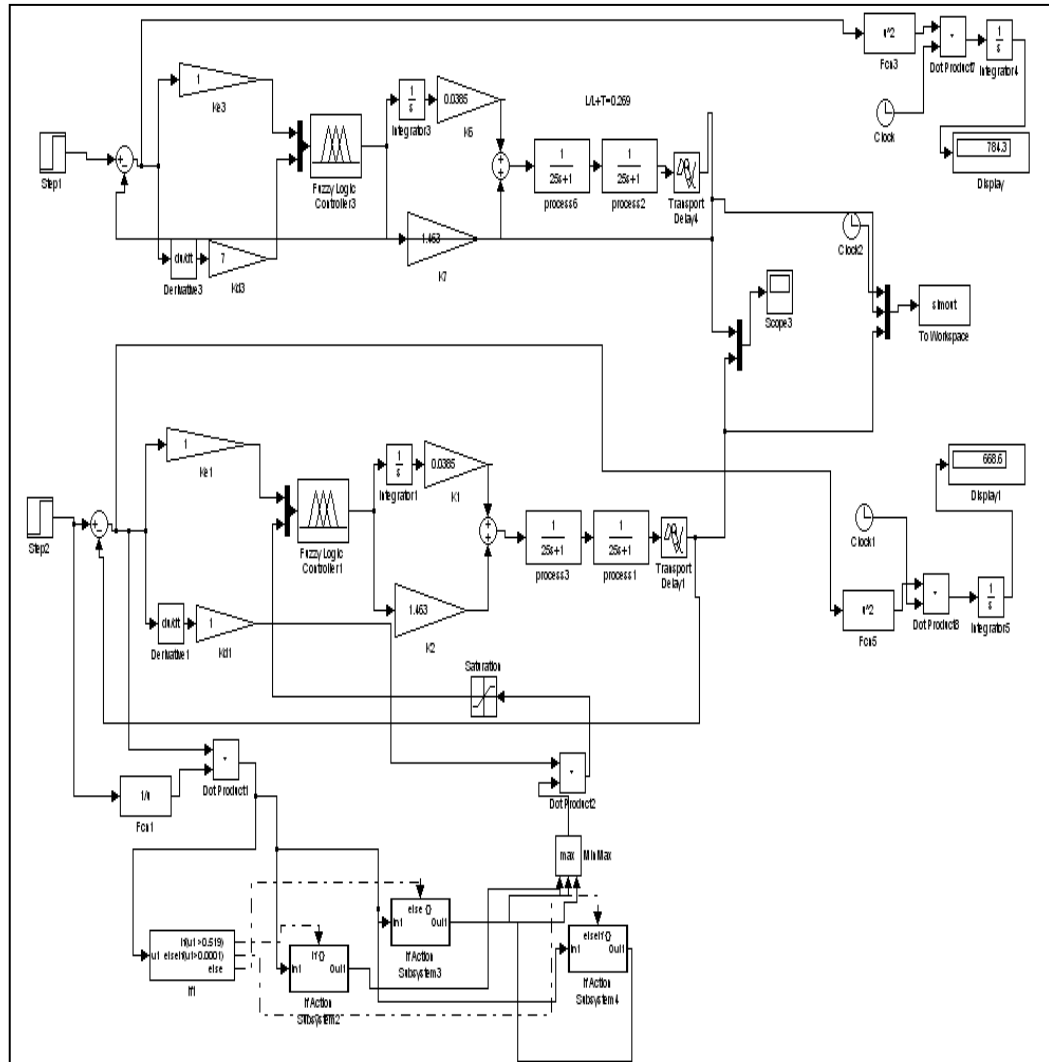


Figure C.3: This scheme is used for comparison study between again a non self tuning Fuzzy IMC PID controller and a self tuning Fuzzy IMC PID controller designed according to the proposed methods in this study. The difference of this self tuning controller is the different self tuning subsystem that it relies on. As it seen on the bottom part of the control scheme, the self tuning device set is not a fuzzy block. It is rather a complex if then action subsystem which has strict decision boundaries. Detailed information about these strategies are given relevant chapters.

- Self Tuning Mechanisms
- Non-fuzzy (Strict Rules) Self Tuning Mechanism

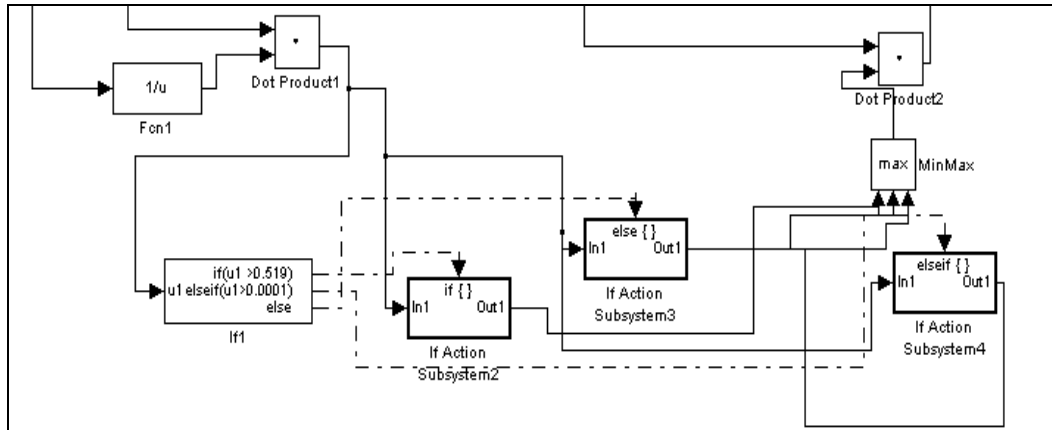


Figure C.4: Non-fuzzy self tuning device set; calculating $u = \text{error}/\text{input}$ ratio and making appropriate decisions according to changing value of “u” ratio.

In following, insight of action subsystems for if, else if and else cases are given.

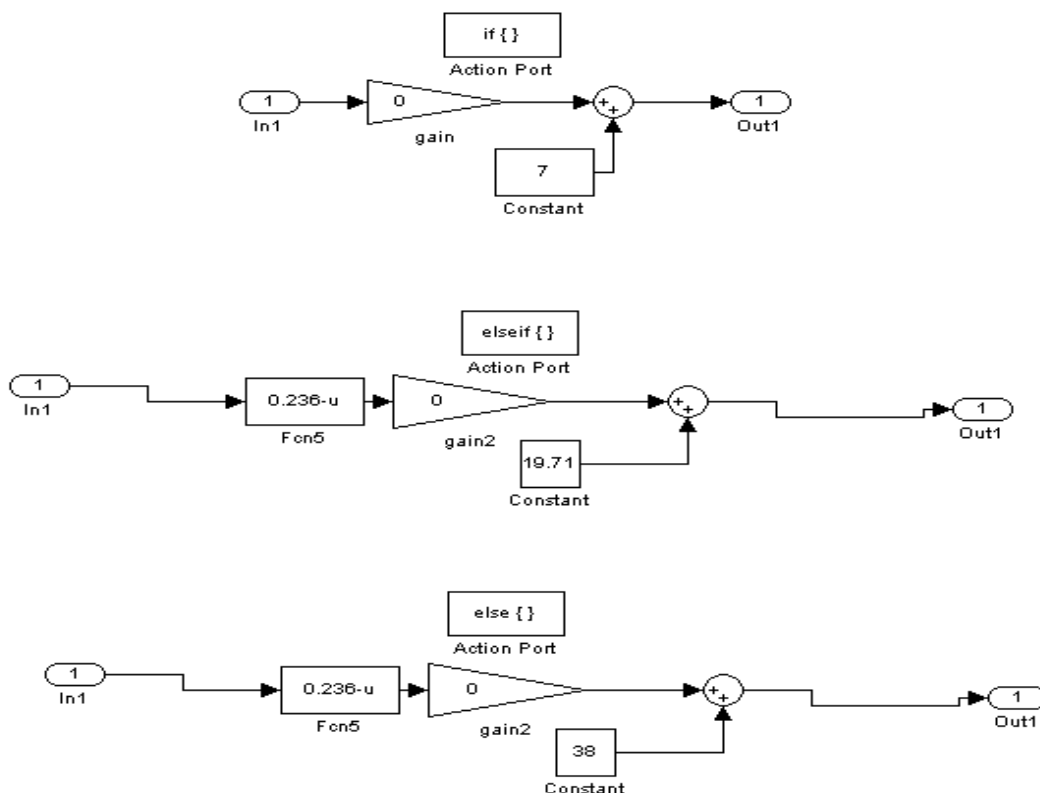


Figure C.5: Insight of action subsystems for if, else if and else cases.

- Fuzzy Self Tuning Mechanism

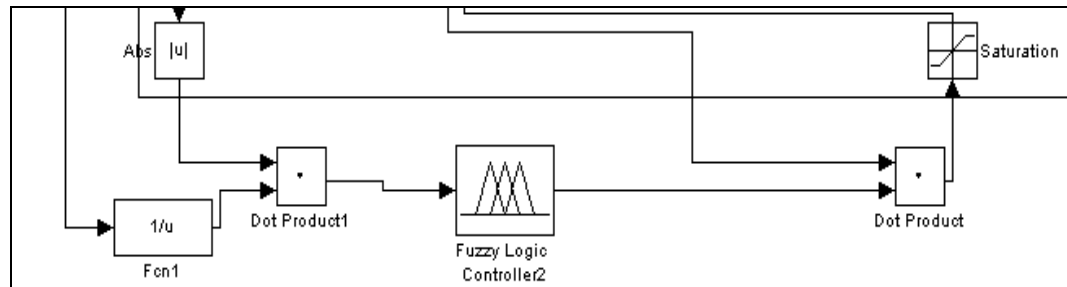


Figure C.6: Fuzzy self tuning device set; calculating $u = \text{error}/\text{input}$ ratio and firing appropriate rules according to changing value of “u” ratio. In following, several rule bases, according to which these fuzzy tuners work, are given schematically.

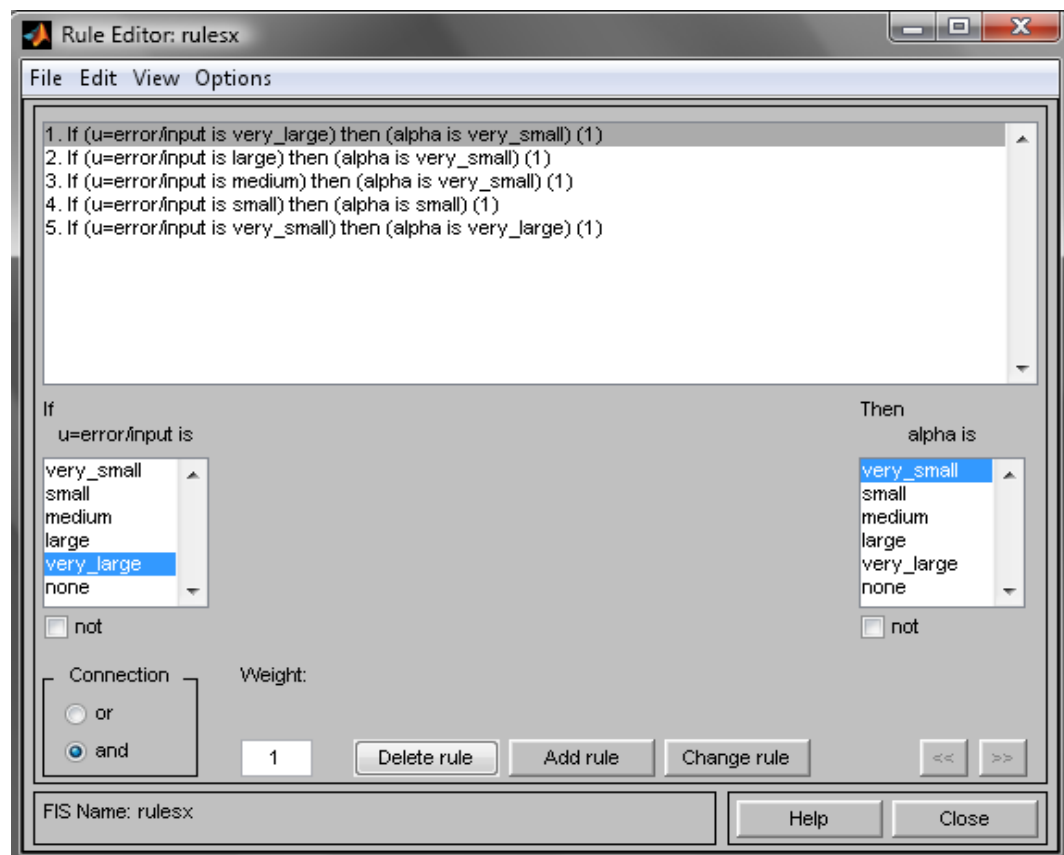


Figure C.7: Rule base editor window for “section x” control systems.

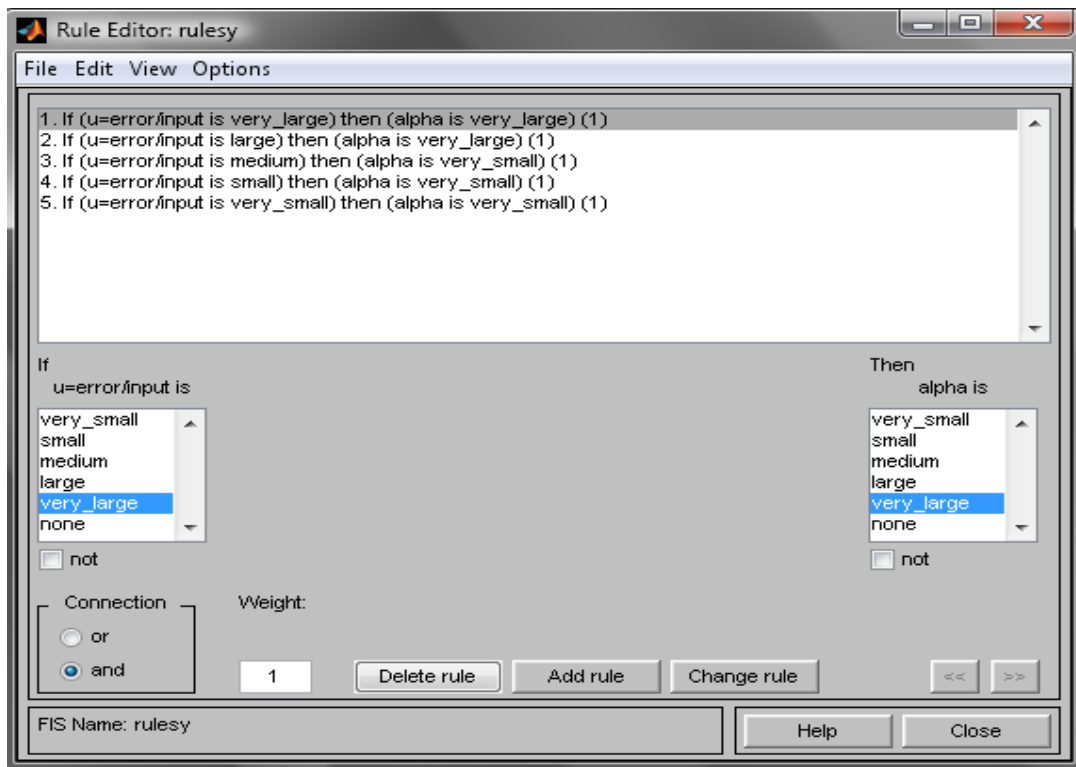


Figure C.8: Rule base editor window for “section y” control systems.

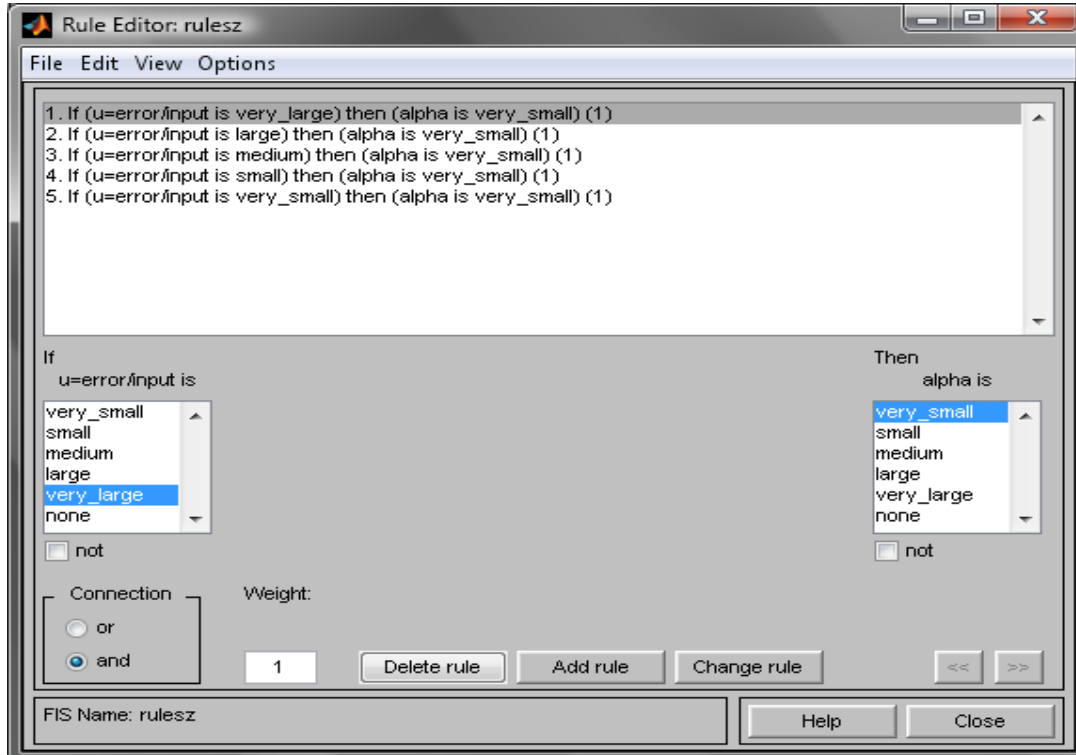


Figure C.9: Rule base editor window for “section z” control systems.

- Fuzzy Inference System for Fuzzy Controller Used in Entire Study
- Fuzzy Inference System

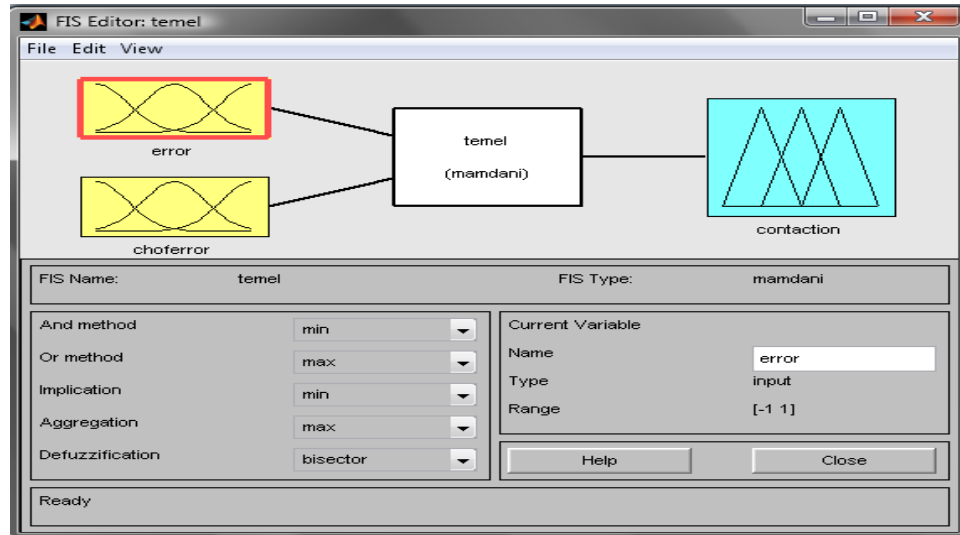


Figure C.10: Fuzzy Inference System editor window for fuzzy controller used in entire study.

- Fuzzy Rule Base

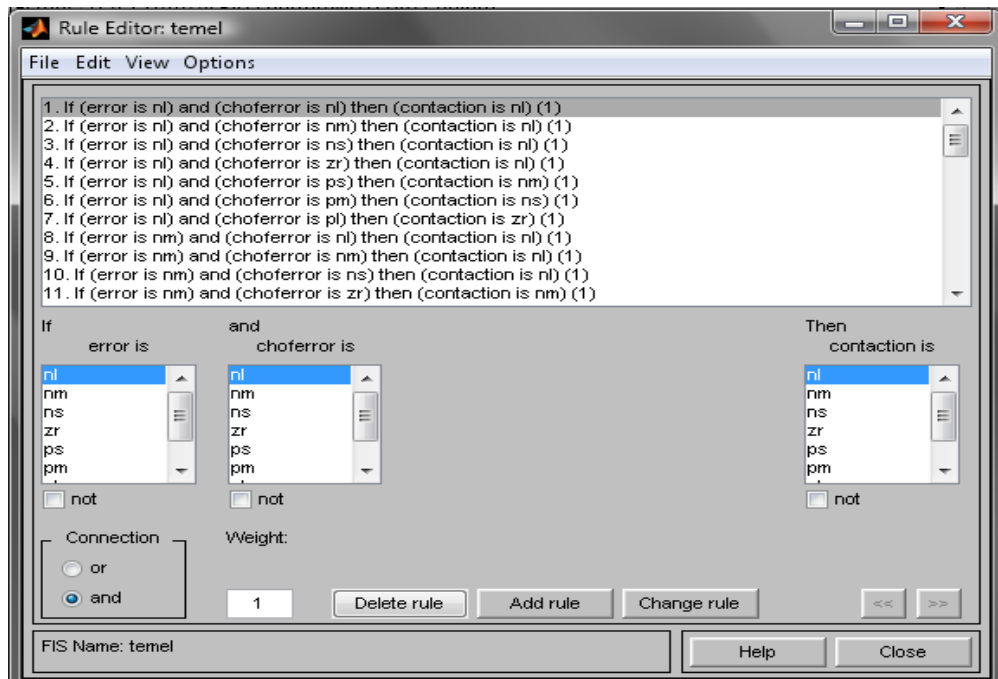


Figure C.11: Rule base editor window for fuzzy controller used in entire study.
(nl:negative large, nm:negative medium, ns:negative small, zr: approximately zero, ps:positive small, pm:positive medium, pl:positive large)

- Fuzzy Membership Functions

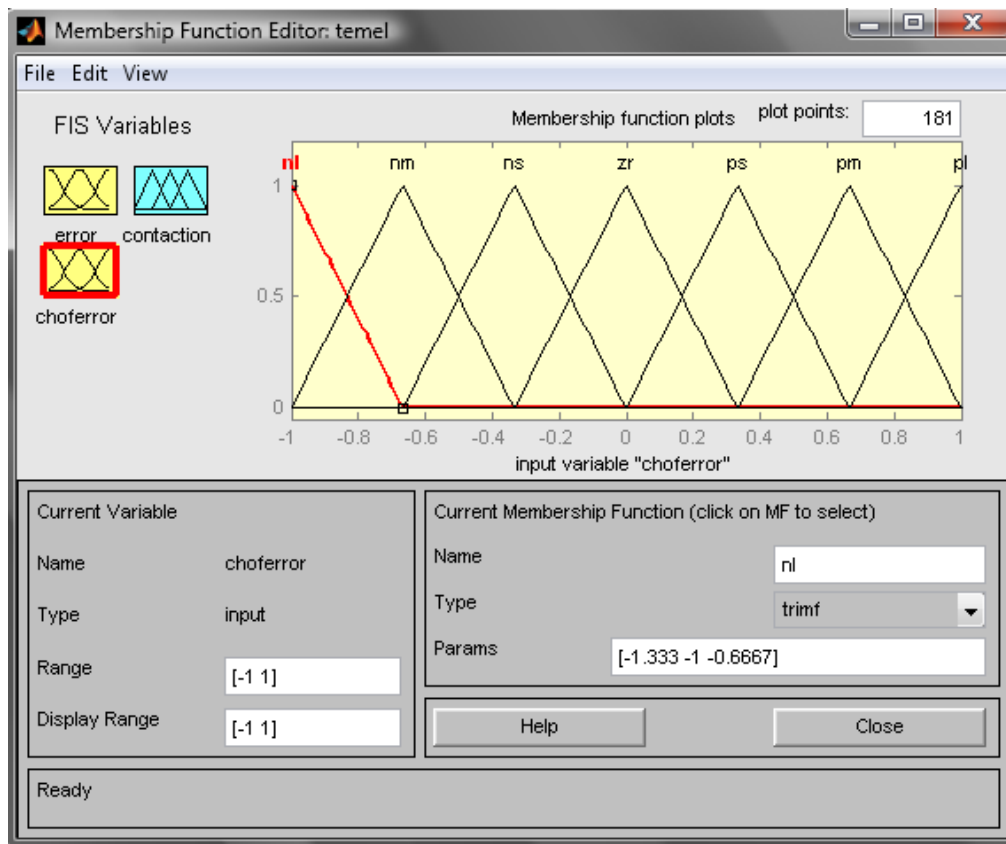


Figure C.12: Membership function editor window for fuzzy controller used in entire study.

The graphical expressions above are snapshots taken from simulation studies conducted using “Fuzzy Logic Toolbox of MATLAB Software Program”. Mentioned membership functions and fuzzy rule base structure were used unchanged as standardized parameters during entire study.

CURRICULUM VITAE



Candidate's full name: Doğan Onur YILMAZ

Place and date of birth: Ankara, 27.09.1986

Permanent Address: Mecidiye Street 48/10, Mecidiyeköy-İSTANBUL

**Universities and
Colleges attended:** İstanbul Technical University (Bachelor) 2004-2008
İstanbul Technical University (Master) 2008-2010